Matthias Engleder BSc

Expression, Purification and Initial Characterization of Novel Hydro-Lyases

MASTER'S THESIS

to achieve the university degree of

Diplom-Ingenieur

Master's degree programme: Biotechnology

submitted to

Graz University of Technology

Supervisor

Ass. Prof. Dipl.-Ing. Dr. techn. Harald Pichler

Institut für Molekulare Biotechnologie, Technische Universität Graz

Mag. Dr. Tamara Wriessnegger

Graz, 2014

AFFIDAVIT

I declare that I have authored this thesis independently, that I have not used other than the declared sources/resources, and that I have explicitly indicated all material which has been quoted either literally or by content from the sources used. The text document uploaded to TUGRAZonline is identical to the present master's thesis dissertation.

16. Dezember 2014
Date

Signature

Danksagung

Ich möchte mich bei folgenden Leuten von ganzem Herzen für die Beteiligung an der Entstehung dieser Arbeit bedanken:

- Der Technischen Universität Graz, dem Austrian Centre of Industrial Biology und unseren Projektpartnern bei DSM für die Möglichkeit, meine Masterarbeit in diesem Projekt durchzuführen
- Tamara Wriessnegger für die herausragende Betreuung meiner Arbeit
- Meinem Arbeitsgruppenleiter Harald Pichler für Motivation, Betreuung und vor allem die viele Zeit und Geduld die er sich immer für Fragen und Diskussionen nahm
- Der Arbeitsgruppe für Strukturbiologie von Professor Karl Gruber am Institut für Molekulare Biowissenschaften der Karl-Franzens-Universität Graz, ohne die der Fortschritt dieses Projekts und meiner Diplomarbeit nicht möglich gewesen wäre
- Professor Peter Macheroux und ganz besonders Silvia Wallner, die durch ihre Expertisen und Anleitungen maßgeblich an vielen Experimenten beteiligt waren
- Professor Helmut Schwab für anregende Diskussionen im Rahmen von Institutsseminaren
- Meinen Arbeitsgruppenkollegen Anita, Miriam, Sabine, Sandra und Tamara für das fantastische Arbeitsklima und ein ständig offenes Ohr bei allen Fragen
- Allen Freuden, die ich während des Studiums kennenlernen durfte
- Mein größter Dank gilt meinen Eltern, ohne die mein Studium nicht möglich gewesen wäre, sowie meinem Bruder, für die stetige Unterstützung und Hilfe in allen Lebenslagen

Table of Contents

1 List of abbreviations

Table 1: List of abbreviations.

Abbreviation	Description
10-HSA	10-Hydroxystearic acid
CD	Circular dichroism
CFE	Cell free extract
CWW	Cell wet weight
ddH_2O	Water, double destilled
DMSO	Dimethyl sulfoxide
EC	Enzyme class
EDTA	Ethylenediaminetetraacetic acid
EtBr	Ethidium bromide
EtOAc	Ethyl acetate
EVC	Empty vector control
FAD	Flavin adenine dinucleotide
GC-MS	Gas chromatography-mass spectrometry
HFA	Hydroxy fatty acid
HTS	High-throughput screening
IMAC	Immobilized metal ion affinity chromatography
IPTG	Isopropyl-β-D-thiogalactopyranosid
ITC	Isothermal titration calorimetry
MCRA	Myosin cross-reactive antigen
NAD(P)	Nicotinamide adenine dinucleotide (phosphate)
OA	Oleic acid
OhyA	Oleate hydratase from *E. meningoseptica*
SDS	Sodium dodecyl sulfate

2 Abstract

The enzymatic addition of water to carbon-carbon double bonds of primary metabolites, catalyzed by hydratases, is a mainstay of life. For example, fumarase plays an essential role in degradation of fatty acids via β-oxidation. However, currently various drawbacks such as narrow substrate range, limited stability and low activity hinder their industrial application. Oleate hydratases are interesting members of this enzyme class because of their ability to catalyze the addition of water to the non-activated cis-9 double bond of oleic acid. The microbial hydration activity that converts oleic acid to 10-hydroxystearic acid has first been reported more than five decades ago. However, it was not until recently that detailed analyses of the enzyme were started. Oleate hydratases are classified in the family of myosin cross-reactive antigen-like proteins which are highly conserved among different bacterial species and are believed to confer a detoxification mechanism of free unsaturated fatty acids in fatty acid-rich environments. In this work, oleate hydratases from several microbial origins were actively expressed in *Escherichia coli* and an assay for reliable *in vitro* quantification of the oleate hydratase activity was developed. Furthermore, the oleate hydratase from *Elizabethkingia meningoseptica* (OhyA) was selected for further analyses after purification from *E. coli*. Biochemical analyses demonstrated that OhyA is a flavoprotein with a non-covalently bound FAD cofactor. To elucidate the role of the flavin cofactor in a non-redox reaction is at the core of ongoing work.

3 Zusammenfassung

Die enzymatische Addition von Wasser an Kohlenstoff-Kohlenstoff Doppelbindungen von Primärmetaboliten, katalysiert durch Hydratasen, ist eine unverzichtbare Stütze des Lebens. Beispielsweise spielt die Fumarase eine zentrale Rolle bei der β-Oxidation von Fettsäuren. Promiskuität, Stabilität und Aktivität von vielen Hydratasen verhindern derzeit jedoch weitestgehend den industriellen Einsatz dieser Enzyme. Oleat-Hydratasen sind interessante Vertreter dieser Enzymklasse da sie in der Lage sind, die Addition von Wasser an die nicht-aktivierte cis-9-Doppelbindung von Ölsäure durchzuführen. Die mikrobielle Synthese von 10-Hydroxystearat wurde vor bereits mehr als fünfzig Jahren nachgewiesen, jedoch wurden gründliche Analysen von Oleat-Hydratasen erst kürzlich in Angriff genommen. Oleat-Hydratasen gehören zur Familie der Myosin Cross Reactive Antigen-like Proteine, die in einer Vielzahl von bakteriellen Spezies hochkonserviert ist. Es wird vermutet, dass die physiologische Funktion von Oleat-Hydratasen für diese Bakterien einen

Entgiftungsmechanismus darstellen könnte, der das Überleben in Milieus mit hohen Konzentrationen an freien, ungesättigten Fettsäuren ermöglicht. In dieser Arbeit wurden Oleat-Hydratasen unterschiedlichen mikrobiellen Ursprungs in *Escherichia coli* überexprimiert und ein *in vitro* Aktivitätsassay zur Quantifizierung der Hydratasereaktion etabliert. Überdies wurde die Oleat-Hydratase von *Elizabethkingia meningoseptica* (OhyA) einer weiterführenden Analyse unterzogen. Alle ausgewählten Oleat Hydratasen konnten erfolgreich als aktive Enzyme exprimiert und aufgereinigt werden. Eine anschließende biochemische Analyse zeigte, dass OhyA ein Flavoprotein mit einem nicht-kovalent gebundenen FAD-Cofaktor ist, der vermutlich in einem äquimolaren Verhältnis an das Protein bindet. Die Aufklärung der Rolle des Flavin-Cofaktors in einer nicht-Redoxreaktion steht im Zentrum laufender Arbeiten.

4 Introduction

The addition of water to isolated or conjugated carbon-carbon double bonds is a common transformation in biological systems. Enzymes that catalyze this reaction are members of the lyase enzyme class (EC), and they are further categorized as hydro-lyases or hydratases in EC 4.2.1[1]. Hydratases can be divided into four groups based on their substrate profile: Enzymes that can catalyze the addition of water to non-activated carbon-carbon double bonds, to partially activated carbon-carbon double bonds by a methylene group, to carbon-carbon double bonds activated by carbonyl groups or to carbon-carbon double bonds activated by acetyl-CoA. The stereospecific enzymatic hydration of non-activated carbon-carbon double bonds of numerous natural substrates has pivotal advantages compared to chemical routes. These include mild transformation conditions, reduced manufacturing costs and high selectivity of the reaction. More precisely, whereas the commonly applied chemical acid catalyzed water addition proceeds without any selectivity, enzymatic addition of water is a highly regio- and stereoselective process. In fact, the lone enantioselective addition of water by synthetic chemistry has only been reported in 2010[2], whereas enzymatic hydration activity has been known for several decades[3]. Until now, only a very limited number of hydratases are used on an industrial scale. Most prominently, the fumarase from *Brevibacterium flavum* is employed for production of L-malate from fumarate on a multi-ton scale[4]. A large number of chemical hydration reactions are impossible with current knowledge. These also include the regioselective hydration of free unsaturated fatty acids by fatty acid hydroxylating enzymes. Hydroxy fatty acids (HFAs) were classified into several groups by Cao and Zhang depending on the hydroxylation site (α-HFAs, β-HFAs, mid-position HFAs, ω-HFAs, di-HFAs and tri-HFAs)[5]. The mid-position HFA 10-Hydroxystearic acid (10-HSA) is produced by regiospecific, reversible hydration of the non-activated carbon-carbon double bond of cis-9 Octadecanoic acid (oleic acid, OA) by oleate hydratase (Figure 1). 10-HSA is a value-added compound compared to its precursor because of its special properties, such as higher viscosity and reactivity, and can be applied as a surfactant, lubricant, additive in food and cosmetics industries and as a starting material in polymer chemistry.

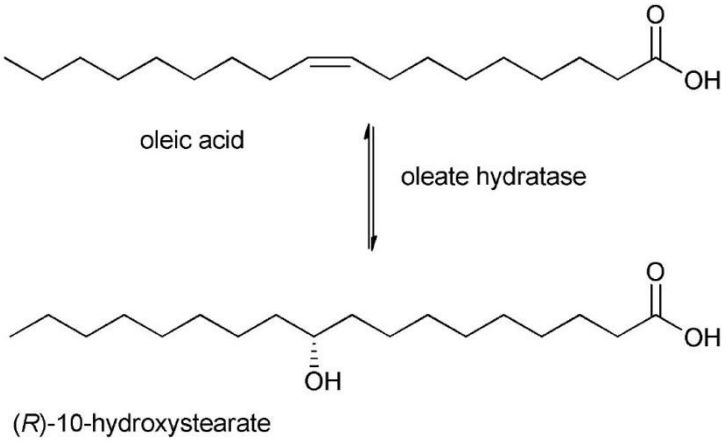

Figure 1: Regio- and enantioselective addition of water to the cis-9 double bond of OA, catalyzed by oleate hydratase. Figure taken from[1].

Although the hydration of OA to 10-HSA was originally reported more than five decades ago[3] and microorganisms capable of OA hydration have been investigated, it was not until recently that more detailed analyses of oleate hydratases from several microbial origins were started. As of now, research has been published on the oleate hydratases from *Elizabethkingia meningoseptica*[6], *Macrococcus caseolyticus*[7], *Bifidobacterium* breve[8], *Lactobacillus acidophilus*[9], *Lysinibacillus fusiformis*[10], *Stenotrophomonas maltophilia*[11] and *Stenotrophomonas nitritireducens*[12]. Oleate hydratases are members of the myosin cross-reactive antigen (MCRA) protein family, which is found in a wide range of both Gram-negative and Gram-positive bacteria. In contrast to chemical hydration, the oleate hydratase reaction is extremely regio- and stereoselective, and oleate hydratases have a very narrow substrate scope: Aside from hydration of the cis-9 double bond of OA, they are only capable of the addition of water to the cis-9 double bonds of Hexadecanoic acid (palmitoleic acid), all-cis-9,12-Octadecadienoic acid (linoleic acid), all-cis-9,12,15-Octadecatrienoic acid (α-Linolenic acid) and all-cis-6,9,12-Octadecatrienoic acid (γ-Linolenic acid) at reasonable rates[13]. Although it has been reported that some members of the MCRA family have fatty acid isomerase or -hydratase activity, the physiological function of MCRA proteins is largely unknown[6,14]. It is, however, assumed that enzymatic formation of hydroxy fatty acids might be the first step in detoxification of unsaturated free fatty acids to allow survival of bacteria in fatty acid–rich environments. This might be of particular importance for pathogens invading habitats such as inflamed tissue or the human skin. The antibacterial activity of unsaturated fatty acids is substantially higher than the effect of their saturated representatives due to their deteriorating effect on the bacterial cell membrane, inhibition of fatty acid synthesis and other targets of action[14–16]. In that regard it has been shown, that MCRA proteins with hydration function form 10-hydroxy or 10,13-dihydroxy fatty acids[10,11,17] and deletion of the hydratase

gene in a mutant strain of *S. pyogenes* caused a 2-fold decrease in the minimum inhibitory concentration of OA.

In this study, nine representatives of the oleate hydratase protein family were selected. Figure 2 shows a phylogenetic tree indicating the evolutionary relations of the different enzymes, together with two other MCRA proteins referred to in this work and the structurally similar fatty acid double bond isomerase from *Propionibacterium acnes*.

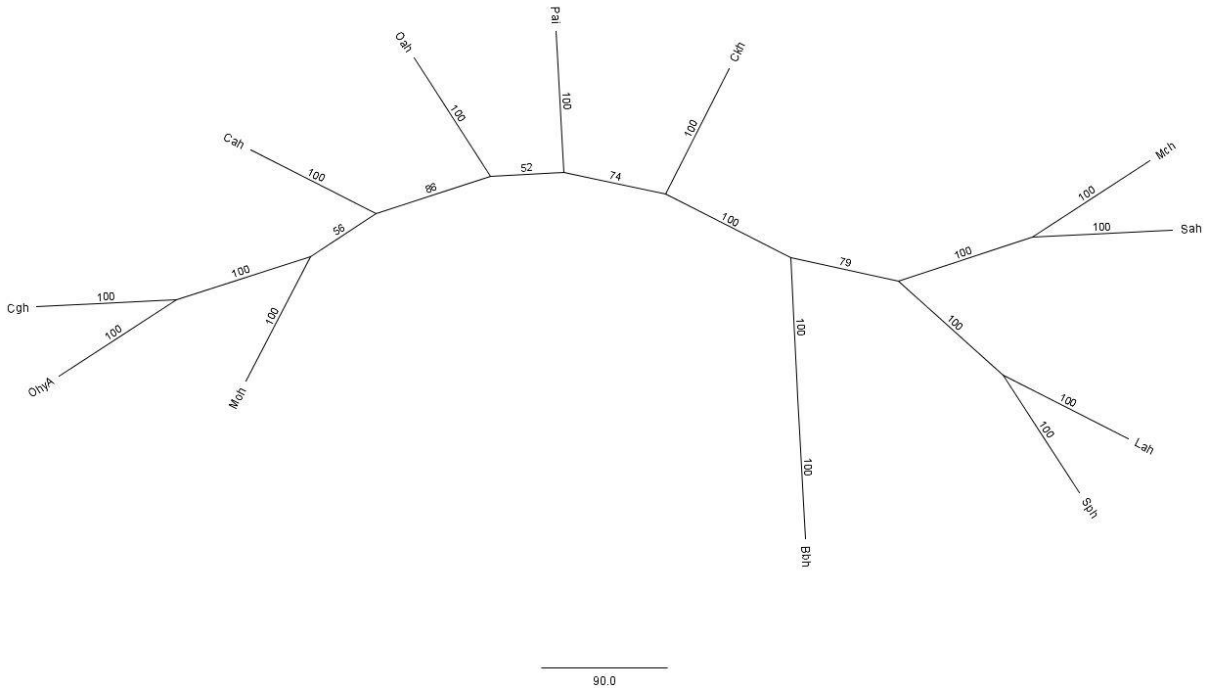

Figure 2: Phylogenetic tree with bootstrap values of selected representatives of the MCRA protein family from different microbial origins (for description of the notations see Table 6), together with the structurally similar fatty acid double bond isomerase from *P. acnes* (Pai).

Alignment of the protein sequences of the oleate hydratases specified in Figure 2 reveals presence of a nucleotide binding motif $GXGXXGX_{21}E/D$, commonly associated with a Rossman fold, in almost all analyzed sequences (Figure 3). In previous studies, this feature has been identified in most other MCRA proteins as the sole sequence similarity to any other known proteins[14]. Thus, many MCRAs and all fatty acid hydratases studied so far contain an FAD cofactor and are, in consequence, flavoproteins.

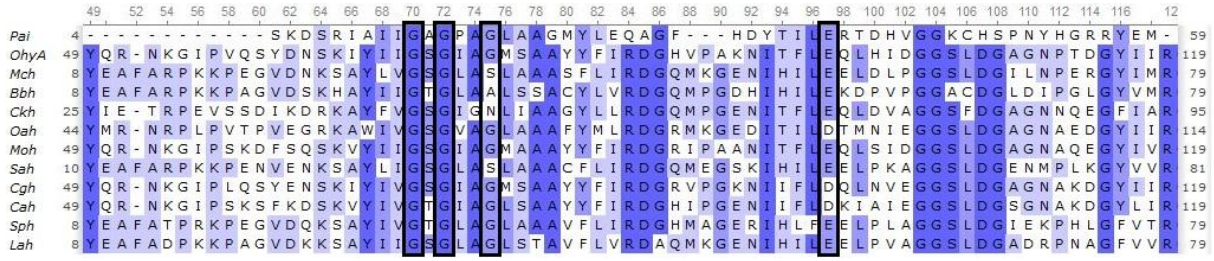

Figure 3: Segment of the multiple sequence alignment of selected representatives of the MCRA protein family, together with the structurally similar fatty acid double bond isomerase from *P. acnes* (Pai). The shading is based on conservation of amino acid residues, with the darkest blue representing 100% conservation among the species. Highlighted are the conserved residues of a predicted nucleotide binding motif, connected with a Rossman fold. For a description of the notations, see Table 6.

The biocatalytic hydroxylation of various substrates with oleate hydratases could provide several advantages compared with other ways to obtain a mono-hydroxylated reaction product. Highly interesting in that regard would be the engineering of a biocatalyst that can readily transform substrates of diverse architectures and properties into value-added, mono-hydroxylated derivatives without supplementation of expensive cofactors or electron supply by a reductase, as required, for instance, in complex cytochrome P450-dependent systems[18]. However, currently oleate hydratases suffer from very low promiscuity, insufficient stability and activity for industrial applications, dependence on the flavin cofactor and limited information on protein structure and mechanistic. Volkov et al. (2013) resolved the crystal structure of the fatty acid double bond hydratase from *L. acidophilus* in a ligand bound form[9]. The homodimeric protein did, however, not retain the flavin cofactor during crystallization. Therefore, the 3D structure was short of a crucial feature for determination of the reaction mode. In summary, more biochemical and structural knowledge on oleate hydratases would be essential for implementation of the oleate hydratase reaction in processes of industrial interest.

In the present work, the nine selected representatives of the oleate hydratase protein family were selected for overexpression in *Escherichia coli* and subsequent purification trials. Furthermore, a suitable activity assay for quantification of the oleate hydratase reaction was developed and the oleate hydratase from *E. meningoseptica* (OhyA), displaying the highest activity among all tested enzymes, was selected for a thorough biochemical analysis and crystallization study. Ultimately, strategies for implementation of a high-throughput screening (HTS)-assay for identification of improved oleate hydratase mutant variants were tested and evaluated.

5 Materials and Methods

The instruments and reagents, as well as bacterial strains and tools for molecular cloning are described in the appendix section.

5.1 General methods

5.1.1 Agarose gel electrophoresis

Agarose gel electrophoresis was performed with 1% agarose gels containing ca. 0.25 µg mL^{-1} of EtBr in TAE buffer. Analytical gels were run at 120 V for approx. 45 min and preparative gels were run at 90 V for approx. 90 min. Sizes and concentrations of separated DNA fragments were checked by comparison to simultaneously separated DNA standards. For all samples, the MassRuler DNA Ladder Mix was used.

5.1.2 DNA gel and PCR purification

All DNA fragments were separated with standard 1% agarose gels at 90 V. Separated DNA and amplified DNA from PCR was purified according to the manual of the Wizard® SV Gel and PCR Clean Up System. 30 µL of ddH_2O were used for final DNA elution.

5.1.3 Preparative DNA restriction

For preparative restriction cuts, the full volume of a single plasmid purification or PCR was mixed with restriction enzyme(s) and appropriate buffer at the recommended concentration. The mixtures were incubated for at least 2 h at 37°C.

5.1.4 Control restriction

For control restriction cuts, 1 µL of purified plasmid was mixed with 1 µL of each restriction enzyme, 1 µL of recommended buffer (10x) and 6 µL of ddH_2O. The reaction was incubated for 1 h at 37°C.

5.1.5 Determination of DNA concentration

DNA concentration was either estimated via agarose gel electrophoresis or by measurement of the absorbance at 260 nm in the NanoDrop 2000 UV-Vis spectrophotometer. For estimation of DNA concentration on an agarose gel, 1 µL of purified DNA fragment was supplied with 8 µL of ddH_2O and 1 µL of 6x loading dye. The whole volume was loaded onto an agarose gel and separated at 120 V. Concentrations were estimated by comparing band intensities to those of 5 µL of the DNA ladder standard loaded on the same gel.

5.1.6 Dephosphorylation

Dephosphorylation of vector backbone was performed using FastAP™ alkaline phosphatase. Therefore, 30 µL of vector DNA were mixed with 1µL of FastAP™ alkaline phosphatase and 3 µL of recommended buffer (10x). The reaction was incubated for 10 min at 37°C and again 1 µl of FastAP™ alkaline phosphatase was added before incubation for another 10 min at 37°C. Afterwards, DNA was purified according to the Wizard® SV Gel and PCR Clean Up System.

5.1.7 DNA ligation

Vector backbone and insert were used at a molar ratio of 1:3 for ligation. One µL of T4-ligase [10 U μL^{-1}], 2 µL of ligase buffer (10x) were added and the total volume was adjusted to 20 µL with ddH_2O. Reactions were performed at 16°C over night or at 22°C for 2 h. Afterwards, mixtures were heated to 65°C for 10 min to inactivate the enzyme, followed by desalting for 30 min on a 0.025 µm Millipore filter floating on ddH_2O. Solutions were transferred to sterile Eppendorf tubes and either immediately used for electrotransformation or stored at -22°C.

5.1.8 Transformation of electrocompetent E. coli cells

For electrotransformation, 80 µL of cells were mixed with 10 µL of plasmid DNA and transferred to pre-chilled electroporation cuvettes. Transformation was performed by application of an electric pulse, EC 2 program, of the MicroPulser electroporator for 5-6 ms at 2.5 kV. Immediately after transformation, 1 mL of SOC-medium was added and the whole broth was incubated in a thermomixer at 650 rpm and 37°C for 1 h. Defined amounts of the regeneration culture were plated on LB supplied with the respective antibiotic and incubated over night at 37°C.

5.1.9 Plasmid isolation

Several transformants were streaked out onto adequate plates and grown over night at 37°C. Plasmids were isolated from single clones using the Gene Jet™ Plasmid Miniprep Kit. Control restrictions were performed with FastDigest™ restriction enzymes. After confirmation of correct cloning, plasmids were stored at -20°C until further use.

5.2 *E. coli* cultivation for recombinant protein expression

5.2.1 Recombinant protein expression in auto induction medium

The pre-culture was prepared by inoculating 20 mL of TB-medium containing the respective antibiotic with a single colony of the respective *E. coli* BL21Star™ (DE3) strain and incubating over night at 28°C and 100 rpm. For preparation of the main culture, 500 mL of

auto induction medium (AIM, terrific broth base including trace elements) supplied with the respective antibiotic were inoculated with the pre-culture to an A_{600} of 0.15 and incubated at 28°C and 100 rpm for approx. 22 h. Afterwards, cells were harvested by centrifuging the cultures for 10 min at 5,000 rpm and 22°C using the Avanti™ centrifuge equipped with the JA-10 rotor. Cultivation medium was decanted and the cell wet weight (CWW) of protein pellets was determined.

5.2.2 Recombinant protein expression in TB-medium

The pre-culture was prepared by inoculation of 10 mL TB-medium containing the respective antibiotic with a single colony of the respective *E. coli* BL21Star™ (DE3) strain and incubated over night at 28°C and 100 rpm. Main cultures were prepared by inoculation of 160 mL (initial expression of recombinant protein) or 500 mL TB-medium, supplied with the respective antibiotic, to an A_{600} of 0.1 and cultures were incubated at 28°C and 100 rpm. At an A_{600} of approx. 0.6-0.8, protein expression was induced by addition of isopropyl-β-D-thiogalactopyranosid (IPTG) to a final concentration of 0.1 mM. Expression was performed for 19 h and 100 rpm. After induction of protein expression, the incubation temperature was reduced to 20°C, except for expression of Oah and Cgh, for which the temperature was maintained at 28°C. Cells were harvested as described above.

5.2.3 Optimization of OhyA expression

For optimization of OhyA expression, *E. coli* BL21Star™ (DE3) [pMS470-HISTEV-OhyA] and *E. coli* BL21Star™ (DE3) [pEHISTEV-OhyA] were cultivated in different media and under different conditions. Main cultures in TB-medium containing respective antibiotics were prepared at 28°C, and at an A_{600} of approx. 0.6-0.8, protein expression was induced by addition of IPTG to a final concentration of 0.1 mM. Expression was performed at 20°C and 100 rpm. Culture samples were taken after 17 h, 24 h, 41 h and 48 h. Main cultures in AIM containing respective antibiotics were prepared at 20°C and 28°C and were incubated for 26 h at 100 rpm. Cells were harvested as described above.

5.2.4 Preparation of CFEs containing recombinantly expressed protein

Cell free extracts (CFEs) were prepared by resuspending harvested cell pellets in either 50 mM potassium phosphate, pH 6.5 (for preparation of aliquots utilized for activity assays), or 50 mM HEPES, pH 7.4, supplied with 10 mM imidazole (for purification of recombinant protein). The cell suspensions were transferred to pulping bottles and sonicated for 2x5 min under 80% duty cycle and output control level 8 with extensive cooling. Whole cell lysates

were immediately put on ice and centrifuged in 50 mL tubes for 40 min at 20,000 rpm and 4°C to pellet cell debris.

5.3 Protein expression analysis

5.3.1 Determination of protein concentration in CFEs

Protein concentrations in CFEs were determined via the Bio-Rad protein assay according to a 96 well plate protocol established by A. El-Heliebi[19]. Therefore, CFEs were diluted with ddH_2O and 10 µL thereof were transferred to the wells of a standard microtiter plate. Ten µL of ddH_2O were used as blank and bovine serum albumin (BSA) was used for calibration at concentrations from 0.05 mg mL^{-1} to 1 mg mL^{-1}. After addition of 200 µL of 1:5 diluted Bio-Rad reagent to each well, the plate was incubated under shaking for 5 min and absorbances were recorded at 595 nm.

5.3.2 SDS-PAGE

SDS-PAGE was performed according to the manual of the NuPage® SDS-PAGE Gel System, Life Technologies. Prior to loading of probes into the wells of a ready-to-use-gel, protein samples were mixed with LDS Sample Buffer (4x), Sample Reducing Agent (10 x) and ddH_2O. The mixture was denatured at 70°C for 10 min. Ten µL of the PageRuler™ Prestained Protein Ladder were applied. The gels were run in MOPS SDS Running Buffer at maximum voltage, maximum power and 110 mA for 50 min. After electrophoresis, gels were placed in a plastic box and covered in Coomassie blue staining solution for 20 min under moderate shaking at 22°C. Gels were destained over night with 10% acetic acid.

5.4 Purification of recombinant protein

The prepared CFE was filtered through a 0.22 µm syringe filter prior to purification. Protein purification was either conducted with self-packed Ni-NTA affinity chromatography columns and a gravity-flow protocol, or with prepacked, ready-to-use columns and the Äkta purifier system using the buffers listed in Table 2. Purification was always either conducted in a cold room at 4°C or with permanent cooling of all aliquots on ice.

Table 2: List of buffers used for purification of recombinant protein. Washing Buffers were only used for gravity-flow purification of His_6-tagged protein.

Buffer	Composition
Binding Buffer	50 mM HEPES, pH 7.4, 300 mM NaCl, 10 mM Imidazole
Washing Buffer 1	50 mM HEPES, pH 7.4, 300 mM NaCl, 20 mM Imidazole
Washing Buffer 2	50 mM HEPES, pH 7.4, 300 mM NaCl, 30 mM Imidazole
Elution Buffer	50 mM HEPES, pH 7.4, 50 mM NaCl, 250 mM Imidazole
Desalting Buffer	50 mM HEPES, pH 7.4, 50 mM NaCl

5.4.1 Gravity-flow purification

For gravity-flow purification of His_6-tagged protein, Ni-NTA affinity chromatography with self-packed columns was performed. Ni-Sepharose beads were prepared and used according to the GE Healthcare Instruction manual (affinity media) for Ni Sepharose™ 6 Fast Flow. Therefore, the slurry containing used beads was transferred to a centrifuge tube and beads were sedimented by centrifugation for 5 min at 4,000 rpm and 22°C in a tabletop centrifuge. Supernatants were discarded and replaced with 5 mL of ddH_2O. Beads were washed by shaking for 3 min and resedimented by centrifugation as above. Washing and centrifugation was repeated once using Binding Buffer. The Ni Sepharose™ 6 Fast Flow was transferred to a measuring cylinder and dispersed in Binding Buffer to a 50% slurry and afterwards, the beads were filled into an empty PD-10 column.

Once packing of the column was completed, the column was washed with 5 column volumes (CV) of Binding Buffer and the filtered CFE was loaded. Afterwards, two different washing protocols were tested. In Washing Protocol 1, the column was washed twice with 5 mL of Washing Buffer 1, whereas Washing Protocol 2 was performed by washing twice with 5 mL of Washing Buffer 1, followed by washing twice with 5 mL of Washing Buffer 2. Protein was eluted from the column with 3 mL of Elution Buffer in each case. During purification, aliquots of the flow through and washing fractions were collected for evaluation of the purification via SDS-PAGE.

After purification, regeneration of the medium was conducted to recharge Ni Sepharose™ 6 Fast Flow. First, residual Ni^{2+} was removed by washing with 5 CV of 20 mM potassium phosphate, pH 7.4, containing 500 mM NaCl and 50 mM EDTA. Residual EDTA was removed by washing with at least 5 CV of Binding Buffer followed by 5 CV of ddH_2O. The column was recharged by loading 0.5 CV of 0.1 mM $NiSO_4$. Recharged beads were washed with 5 CV of ddH_2O followed by 5 CV of Binding Buffer before storage in 20% ethanol.

5.4.2 Purification with ready-to-use columns and Äkta purifier system

To yield recombinant protein on a preparative scale, His_6-tag purification was carried out using either prepacked, ready-to-use HisTrap™ FF crude- or HiTrap™ TALON crude-columns (GE Healthcare, USA) connected to the Äkta purifier chromatography system. To optimize purification, the two column systems were evaluated with different washing and elution protocols (buffers listed in Table 2) regarding yield and purity of obtained recombinant protein. A tabular summary of column specifications and applied elution protocols is shown in Table 3.

Table 3: Columns and elution protocols tested during purification of recombinant protein with ready-to-use columns. CV: Column Volume; EB: Elution Buffer.

	HisTrap™ FF crude	**HiTrap™ TALON crude**
Metal Ion	Ni^{2+}	Co^{2+}
Binding Capacity	Approx. 400 mg of His-tagged protein	Approx. 200 mg of His-tagged protein
CV	10 mL	10 mL
Protocols	*HisTrap 1*: Gradient, 10 CV EB *HisTrap 2*: Steps, 5 CV 30% EB and 5 CV 100% EB *HisTrap 3*: Steps, 5 CV 10% EB and 5 CV 100% EB	*TALON*: Steps, 5 CV 10% EB and 5 CV 100% EB

After equilibration with Binding Buffer, approx. 50 mL of filtered CFE were applied to the chromatography column at a flow rate of 3 mL min^{-1}. The column was washed with 3 CV of Binding Buffer at a flow rate of 2 mL min^{-1} and the bound protein was eluted with the *HisTrap 1*-, *HisTrap 2*-, *HisTrap 3*- or *TALON*-protocol. For the *HisTrap 1* protocol, elution was performed with a linear gradient of 10 mM to 250 mM imidazole over 10 CV with Elution Buffer, for the *HisTrap 2* protocol, a two-step gradient, including a washing step with 75 mM imidazole over 5 CV, and an elution step with 250 mM imidazole over 5 CV was applied and for the *HisTrap 3*-, as well as the *TALON*-protocol, a two step gradient, including a washing step with 25 mM imidazole over 5 CV, and an elution step with 250 mM imidazole over 5 CV was used. All applied protocols were run at a flow rate of 2 mL min^{-1} and A_{280}, as

well as A_{410} and A_{440} were monitored on-line. Eluted protein samples were collected in 2 mL portions and fractions of interest were pooled and immediately desalted.

5.4.3 Desalting of purified protein

For buffer exchange and removal of high imidazole concentrations after purification, proteins were desalted using either PD-10- or HiPrep 26/10 Desalting columns, previously equilibrated with Desalting Buffer, according to the manufacturer's protocols and eluted with Desalting Buffer.

5.4.4 Gel filtration

Gel filtration was performed in a HiLoad 16/600 Superdex 200 column, with a diameter of 16 mm, packed with dextran covalently bound to highly crosslinked agarose (GE Healthcare, USA) using the Äkta purifier chromatography system. The CV was 120 mL and, according to the manufacturer, the separation range was 10–600 kDa for globular proteins. After equilibration with Desalting Buffer, the gel filtration column was loaded with a maximum volume of 2 mL concentrated, His_6-tag purified protein sample. Fractions were eluted at a flow rate of 1 ml min^{-1} in 3 mL portions and A_{280}, as well as A_{410} and A_{440} were monitored on line.

To correlate elution volume of protein fractions to molecular weight we resorted to an available calibration curve based on Aprotinin (6.511 kDa), Ribonuclease A (13.7 kDa), Carbonic anhydrase (29 kDa), Ovalbumin (45 kDa) and Conalbumin (76 kDa) as globular reference proteins. The mass of the eluted target protein was calculated by comparison with the elution volumes of reference proteins.

5.5 Biochemical analysis

5.5.1 UV-Vis spectroscopy

UV-Visible (UV-Vis) absorbance spectra of FAD, OhyA and apoenzyme were recorded from 250 nm to 1,000 nm in semi micro quartz cuvettes using a Specord 205/BU spectrophotometer. Spectral measurements were performed in 50 mM HEPES, pH 7.4.

5.5.2 Deflavination

Two methods were tested regarding their potency in apo-flavoprotein preparation on a preparative scale.

For evaluation of affinity chromatography, His_6-tag purified OhyA in Binding Buffer was applied onto a 1 mL pre-equilibrated HisTrap FF crude column. After loading the protein

solution at a flow rate of approx. 0.5 mL min^{-1}, the column was washed with 5 mL Binding Buffer. Removal of protein-bound FAD was attempted by washing the column with 20 mL of Binding Buffer containing urea and KBr (Deflavination Buffers 1-4 in Table 4) and each flow through was collected separately. Afterwards, 20 mL of Deflavination Buffer 5 (Table 4) were loaded onto the column and the column outlet was connected with the pump inlet, creating a loop to ensure high efficiency of the washing step. After overnight circulation at a flow rate of 0.5 mL min^{-1} and 4°C in the dark, the loop was disconnected and the flow through again collected, whereas the protein was eluted from the column with 5 mL of Elution Buffer, desalted using PD-10 columns and concentrated to a maximal volume of 2 mL by ultrafiltration. The FAD content of the flow though and OhyA fraction was assessed by absorbance spectral analysis.

Table 4: List of buffers used for preparation of apo-OhyA via affinity chromatography.

Buffer	Composition
Deflavination Buffer 1	Binding Buffer + 1 M urea, 1 M KBr
Deflavination Buffer 2	Binding Buffer + 2 M urea, 2 M KBr
Deflavination Buffer 3	Binding Buffer + 3 M urea, 3 M KBr
Deflavination Buffer 4	Binding Buffer + 4 M urea, 4 M KBr
Deflavination Buffer 5	Binding Buffer + 1.5 M Guanidine hydrochloride, 1.5 M KBr

In addition, deflavination was performed by partial unfolding of the purified protein in the presence of a chaotropic agent and halide anions with simultaneous dialysis at physiological pH. Therefore, His_6-tag purified OhyA was diluted to a volume of 10 mL in dialysis buffer (50 mM HEPES, pH 7.4, containing urea and KBr) and dialyzed at 4°C against 1 L dialysis buffer with gentle stirring. Two different conditions were tested regarding their efficiencies and impact on protein integrity. Dialysis buffers and conditions are summarized in Table 5.

Table 5: List of buffers and conditions used for preparation of apo-OhyA via dialysis.

Buffer	Length of dialysis	Composition
Dialysis Buffer 1	7 d	50 mM HEPES, pH 7.4, 4 M urea, 4 M KBr
Dialysis Buffer 2	24 h	50 mM HEPES, pH 7.4, 2 M urea, 2 M KBr

Protein aliquots resulting after dialysis were checked by absorbance spectral analysis, buffer was exchanged via gel filtration using PD-10 columns and samples were finally concentrated to a maximal volume of 2 mL.

5.5.3 Circular dichroism spectroscopy

Circular dichroism (CD) measurements were carried out with a Jasco J-810 spectropolarimeter. Far-UV CD spectra of purified OhyA, apo-OhyA prepared with Dialysis Buffer 1 and apo-OhyA prepared with Dialysis Buffer 2 were collected between 190 nm and 260 nm with a scan speed of 50 nm min^{-1} and protein concentrations ranging from 6.3 µM to 13.4 µM in quartz cells of 5 mm path length. The obtained values were normalized by subtracting the baseline recorded for the corresponding buffer. The data were expressed in mean residue ellipticity [θ] in deg cm^2 $dmol^{-1}$.

5.5.4 Isothermal titration calorimetry

For preparation of isothermal titration calorimetry (ITC)-measurements, concentrations of both apo-OhyA and FAD were determined as accurately as possible by correlating the absorbance at 280 nm for apo-OhyA (ε = 91,445 M^{-1} cm^{-1}) and 450 nm for FAD (ε = 11,300 M^{-1} cm^{-1}) of appropriately diluted samples in Desalting Buffer to the respective concentrations.

ITC experiments were carried out using a VP-ITC MicroCalorimeter (MicroCal, USA). All buffers and solutions were degassed immediately before each titration to eliminate air bubbles. The sample cell was filled with 0.03 mM apo-OhyA in Desalting Buffer, and the titration syringe was filled with 0.25 mM FAD in Desalting Buffer. The system was equilibrated at 25°C prior to titration of the cofactor to the apoenzyme. Afterwards, the protein in the 1.430 mL calorimeter cell was titrated with the FAD solution at 25°C and a stirring speed of 270 rpm after an initial delay of 60 s. For the first injection, 2 µL of FAD solution were titrated to the cell, and after a spacing period of 600 s, 24 successive automatic injections of 7 µL of FAD solution were performed with an interval of 300 s between each injection. Before termination of the experiment, the thermal power was allowed to return to the level matching the original baseline, indicating complete reaction.

The thermodynamic parameters N (stoichiometry), K_a (association constant) and ΔH (enthalpy change) were obtained by nonlinear least-square fitting of experimental data using a two sequential sites model of the Origin software package (version 7.0) provided with the instrument. The affinity of the cofactor to its binding partner was expressed as the dissociation constant (K_d; $K_d = K_a^{-1}$).

Individual ITC-measurements were carried out with apo-OhyA prepared via dialysis under the two different conditions listed in Table 5.

5.6 Determination of oleate hydratase activity

5.6.1 In vitro activity assay

An *in vitro* activity assays method was developed for reliable and robust quantitation of the fatty acid composition after enzymatic reactions. Therefore, substrate solutions were prepared by adding 20 µL of OA in ethanol (96%, v/v) to 480 µL of 50 mM potassium phosphate, pH 6.5 (assays performed with all oleate hydratases) or pH 6.0 (assays performed with OhyA). Enzyme solutions were prepared by dilution of either CFE containing recombinantly expressed protein or purified protein to the respective concentrations in a final volume of 500 µL of 50 mM potassium phosphate of specific pH values. For assays evaluating the effect of addition of FAD on enzyme activity, enzyme solutions were supplemented with a molar excess of free FAD and incubated on ice for 30 min. All reagents were warmed to the reaction temperature by incubation for 10 min at 25°C prior to the reaction. To start the reaction, equal volumes of substrate and enzyme solutions were mixed. The standard *in vitro* activity assay was performed in a total volume of 1 mL in PYREX® reaction tubes at 25°C and 150 rpm for 10 min in a Multitron Standard shaker. To stop the reaction, the solution was acidified to pH 2.0 with 0.12 M HCl and fatty acids were extracted with 2 mL of ethyl acetate (EtOAc) on a Vibrax VXR basic for 1 h. The mixture was centrifuged for 10 min at 1000 rpm and 22°C. Afterwards, 1.5 mL of the organic phase containing extracted fatty acids were transferred to a clean PYREX® tube and the solvent was removed under a N_2 stream. The obtained fatty acids were derivatized by incubating with 10 µL of pyridine and 10 µL of N,O-Bis(trimethylsilyl)trifluoroacetamide for 10 min at 22°C. Finally, the volume was adjusted to 150 µL with EtOAc and the solution was transferred into vials for GC-MS analysis. For the analysis of fatty acid content, at least technical replicates were carried out with each enzyme sample.

Quantitation of fatty acid composition after the enzymatic reaction was based on internal standardization. n-Pentadecanoic acid and 16-Hydroxypalmitic acid were selected as internal standards for OA and 10-HSA, respectively. Internal standard calibration curves with increasing concentrations of analyte from 0.05 mM to 0.225 mM were prepared. Ethanol (96%, v/v) was used as the solvent for all fatty acids. Sample preparation for subsequent GC-MS analysis was performed as described for the *in vitro* activity assays and calibration curves were derived by plotting the ratio of the analyte peak area to the internal standard peak area as a function of the analyte concentration. Mean values of three individual experiments were taken for the calibration curves. For quantitative *in vitro* activity assays, a modified protocol

was applied in which the substrate solution was prepared by addition of 20 µL OA/internal standard-mix to 480 µL of 50 mM potassium phosphate. The enzymatic reaction and sample preparation for GC-MS analysis were carried out as described above.

5.6.2 GC-MS analysis

Gas chromatography-mass spectrometry (GC-MS) measurements were performed in cooperation with Professor Erich Leitner and the Institute of Analytical Chemistry and Food Chemistry, Graz University of Technology. Therefore, a HP-5 column (crosslinked 5% Ph-Me Siloxane; 30 m, 0.25 mm in diameter and 0.25 µm film thickness) on a Hewlett-Packard 6890 Series II GC equipped with a mass selective detector was used. Sample aliquots of 1 µL were injected in split mode (split ratio 30:1) at 240°C injector temperature and 290°C detector temperature with N_2 as carrier at a flow rate set to 36 cm s^{-1} in constant flow mode. The oven temperature program was as follows: 100°C for 1 min and a ramp to 300°C at 15°C min^{-1} for 13.33 min. The total run time was 19.33 min. The mass selective detector was operated in a mass range of 50-400 amu at an electron multiplier voltage of 1765 V. GC-MS results were evaluated with the GC-MS Data Analysis software of Agilent Technologies.

5.7 Resting cells assay

For *in vivo* assays with resting cells, pre-cultures of the *E. coli* strains to be tested were prepared in 20 mL of TB-Amp and incubated over night at 28°C and 100 rpm. For preparation of the main culture, 40 mL of AIM-Amp were inoculated with the pre-culture to an A_{600} of 0.15 and incubated at 28°C and 100 rpm for approx. 22 h in baffled flasks for recombinant protein expression.

Afterwards, A_{600} values were determined and culture aliquots corresponding to 8.9 A_{600} units (roughly 5 g L^{-1} CWW) were transferred into the wells of a 24-deep well plate. Cell pellets were harvested by centrifugation for 10 min at 4,000 rpm and 22°C.

Afterwards, the supernatants were removed and pellets were carefully resuspended in 1 mL of 50 mM potassium phosphate, pH 6.5, containing 10 mM OA dispersed in 0.5 mg mL^{-1} of Triton X-100. Bioconversions were carried out for 45 min at 35°C and 320 rpm. The reactions were then stopped by centrifugation of cultures for 10 min at 4,000 rpm and 22°C and cautious transfer of the entire supernatant into clean PYREX® reaction tubes. Fatty acids in the supernatants were extracted by acidification to pH 2.0 with 0.12 M HCl, subsequent addition of 2 mL EtOAc and shaking on a Vibrax VXR basic for 1 h. The mixture was centrifuged for 10 min at 1000 rpm and 22°C. Afterwards, 1.5 mL of the organic phase were

transferred to a clean PYREX® tube and the solvent was removed under a N_2 stream. The obtained fatty acids were derivatized by incubation with 10 µL of pyridine and 10 µL of N,O-Bis(trimethylsilyl)trifluoroacetamide for 10 min and finally adjusted to a volume of 150 µL with EtOAc to be transferred into vials for GC-MS analysis. Simultaneously, fatty acids associated with the cell pellets were extracted as well. Therefore, pellets were resuspended in 1 mL of 50 mM potassium phosphate, pH 6.5, and transferred into Eppendorf tubes. Cell pellets were washed twice with 1 mL of washing buffer, either composed of 50 mM potassium phosphate, pH 6.5, or 50 mM Tris-HCl, pH 9.0, both with and without addition of 0.5 mg mL^{-1} of fatty acid free BSA. Washing fractions were collected in clean PYREX® tubes for extraction of fatty acids as described for the supernatant. Fatty acids from the remaining cell pellets were extracted by resuspending pellets in 1 mL of potassium phosphate, pH 6.5, and transfer into clean PYREX® tubes. After addition of glass beads corresponding to a volume of approx. 200 µL, extraction was performed as described for the supernatant.

At least four individual experiments, i.e. technical replicates, were carried out with each cell sample in all resting cells assays.

5.8 Effect of OA on the growth of *E. coli* and *Bacillus subtilis*

Growth of *E. coli* BL21Star™ (DE3) [pMS470-HISTEV] was assessed in cultivation medium containing OA. Twenty mL of LB-medium supplied with 1% Triton X-100 and 20 mL of LB-medium supplied with 1% Triton X-100 and 30 mM OA were inoculated with a pre-culture to an A_{600} of 0.01 and incubated at 37°C and 100 rpm. Samples of 1 mL were aliquoted after 300 min, 345 min, 400 min, 450 min and 480 min and harvested by centrifugation for 10 min at 13,200 rpm and 22°C. The supernatants were removed and cell pellets were washed with 500 µL of a 5 mg mL^{-1} solution of fatty acid free BSA. Afterwards, A_{600} was measured by resuspension of the washed cell pellets in ddH_2O. For each data point, biological triplicates were evaluated.

The inhibitory effect of OA on the growth of a *B. subtilis* wild type strain was determined in a 96 well plate format. Growth media were prepared by addition of OA, dissolved in DMSO (5% v/v), to LB-medium. OA concentrations were 0 mM, 1 mM, 1.5 mM, 2 mM, 2.5 mM, 3 mM and 5 mM. Afterwards, 200 µL of each growth medium were transferred to a 96 well plate and the wells were inoculated with 10 µL of a *B. subtilis* pre-culture. Plates were incubated at 37°C and 750 rpm and the A_{600} of cultures were assessed after 80 min, 165 min and 300 min in a plate reader. For each OA concentration, 12 individual experiments were conducted.

6 Results

6.1 *In vitro* assay for detection of oleate hydratase activity

The GC-MS method for robust and efficient separation, as well as identification of free fatty acids was developed in cooperation with Professor Erich Leitner and the Institute of Analytical Chemistry and Food Chemistry at Graz University of Technology. OA and 10-HSA were used as reference standards at concentrations of 0.2 mM. Unequivocal identification of OA and 10-HSA was accomplished by evaluation of the resulting mass fragmentation patterns (Figure 4).

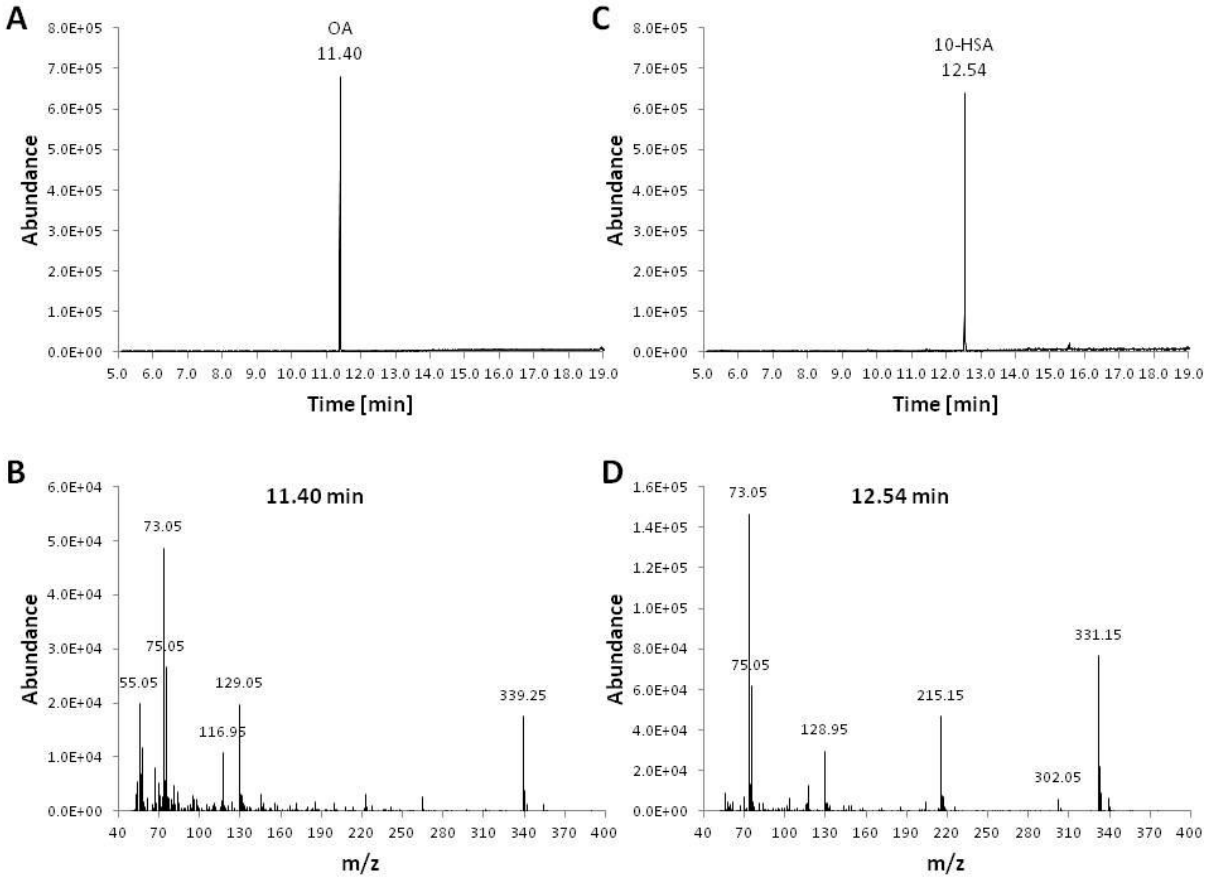

Figure 4: GC chromatogram and mass fragmentation pattern of authentic OA (A, B) and 10-HSA standards (C, D).

The chromatogram of each silylated standard compound showed one distinct peak. For OA, the peak maximum was located at 11.40 min, and for 10-HSA, a peak at 12.54 min was detected (Figure 4 A and 4 C). OA was unambiguously identified by comparison of the fragmentation pattern of the peak maximum at 11.40 min (Figure 4 C) with the NIST 08 Mass Spectral Library, whereas detection of 10-HSA was confirmed by analysis of the fragmentation pattern (Figure 4 D). The silylated derivative of 10-HSA gave a distinct

fragmentation, with the two main ions at m/z 215.15 and m/z 331.15 formed by cleavage on both sides adjacent to the carbon carrying the trimethylsilyl group. The peak at m/z 215.15 was formed by the cleavage of $C_{12}H_{25}O_2Si$, and the peak at m/z 331.15 resulted from the loss of $C_{12}H_{27}OSi$ and C_8H_{17}, respectively. Therefore, it could be verified that the analyzed free fatty acid was 10-HSA.

Since the developed GC-MS method proved to be successful for separation and identification of the fatty acids, its suitability for the detection of substrate and product formed during *in vitro* conversions was tested. The enzymatic conversions were performed with 0.25 mg mL^{-1} of OhyA-CFE, provided by DSM, and an empty vector control (EVC)-CFE of the same concentration, prepared under identical conditions. OA concentrations were 0.5 mM each and reactions were carried out at pH 6.5 and standard conditions (Figure 5).

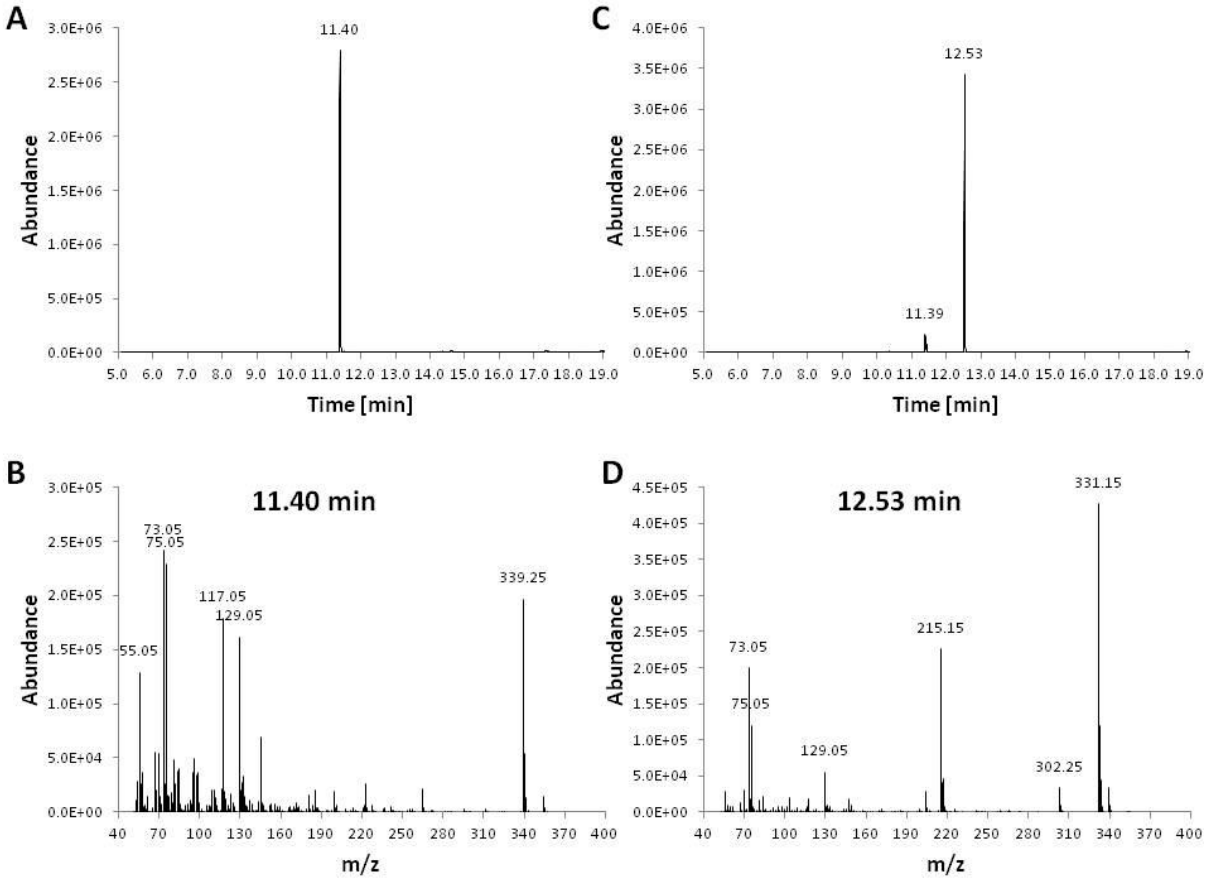

Figure 5: GC chromatogram and mass fragmentation pattern of fatty acids obtained after *in vitro* conversion of 0.5 mM OA using 0.25 mg mL^{-1} of EVC-CFE (A, B) and 0.25 mg mL^{-1} of OhyA-CFE (C, D).

In vitro conversion of OA applying EVC-CFE gave one distinct peak at 11.40 min (Figure 5 A), which was classified as OA by evaluation of its mass fragmentation pattern (Figure 5 B), while conversion with OhyA-CFE gave two peaks at 11.39 min and 12.53 min, respectively

(Figure 5 C). Since the peak at 12.53 min evolved from the formation of 10-HSA as determined by its mass fragmentation pattern (Figure 5 D), *in vitro* hydroxylation of OA due to oleate hydratase activity was confirmed as the EVC-CFE gave no signal for 10-HSA.

Quantitation of OA and 10-HSA was initially attempted by plotting peak areas against the concentrations of 10-HSA standard solutions, but no linear correlation was derived. Considering the necessity of extensive sample preparation before injection of the samples onto the GC column, this procedure was viewed as most likely responsible for insufficient correlation of the data. To circumvent stark variations caused by sample preparation, especially solvent extraction and derivatization, internal standards for quantitation of OA and 10-HSA were added to the substrate prior to the *in vitro* reactions. Calibration curves for OA and 10-HSA with n-Pentadecanoic acid and 16-Hydroxypalmitic acid are depicted in Figure 6 and Figure 7.

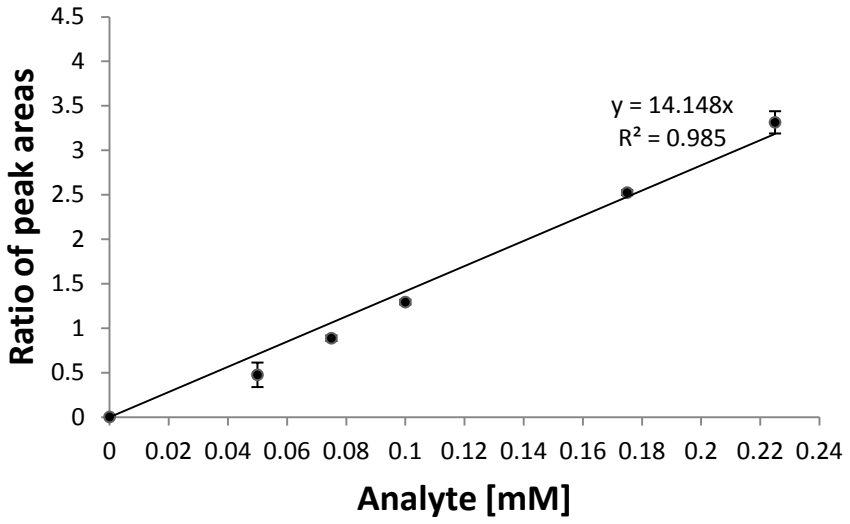

Figure 6: Internal standard calibration curve for quantitation of OA. n-Pentadecanoic acid was the internal standard compound. Mean values and standard deviations of three individual experiments are given.

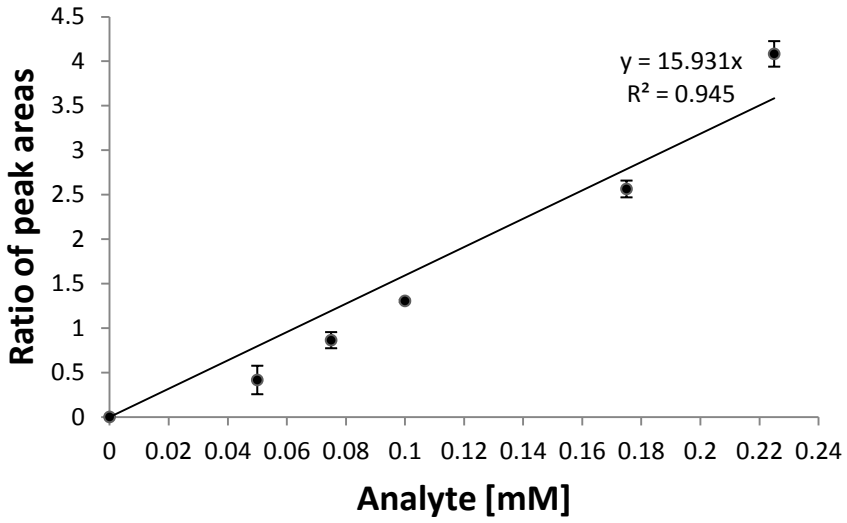

Figure 7: Internal standard calibration curve for quantitation of 10-HSA. 16-Hydroxypalmitic acid was the internal standard compound. Mean values and standard deviations of three individual experiments are given.

After linear regression of the plotted data, resulting in R^2 values of 0.985 and 0.945 for the calibration curves of OA and 10-HSA (Figure 6 and Figure 7, respectively), the quantitative *in vitro* activity assay was evaluated by conversion of 0.15 mM OA to 10-HSA at pH 6.5 and standard conditions with 0.01 mg mL^{-1} of OhyA-CFE and 0.2 mg mL^{-1} of EVC-CFE. 0.1 mM internal standards were added prior to the reactions. Chromatograms and mass fragmentation patterns after GC-MS were evaluated to identify the substrate and product, as well as the internal standard compounds (Figure 8, Figure 9).

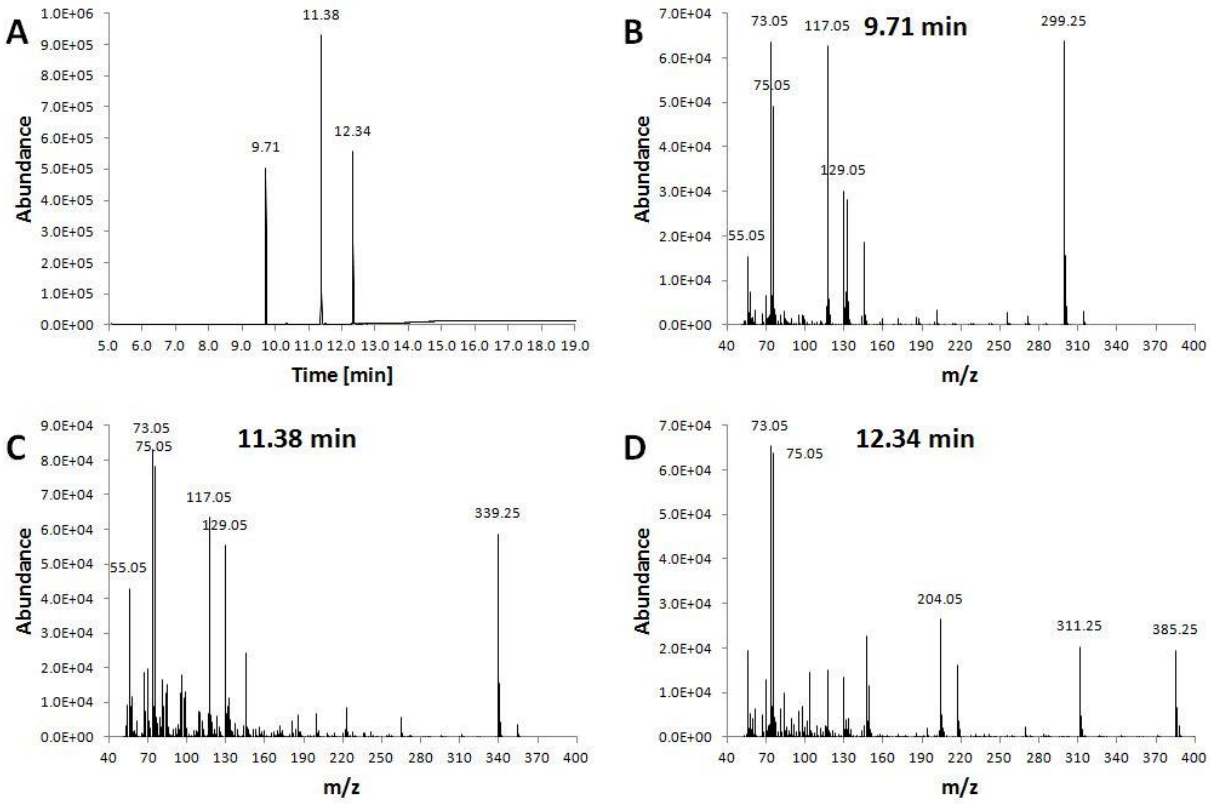

Figure 8: Representative GC-MS analysis of fatty acids obtained after quantitative *in vitro* conversion of 0.15 mM OA with internal standards using 0.2 mg mL^{-1} of EVC-CFE. (A) Chromatogram. (B) Mass fragmentation pattern of the peak maximum at 9.71 min, corresponding to n-Pentadecanoic acid. (C) Mass fragmentation pattern of the peak maximum at 11.38 min, corresponding to OA. (D) Mass fragmentation pattern of the peak maximum at 12.34 min, corresponding to 16-Hydroxypalmitic acid.

Three peaks were identified after analysis of the quantitative *in vitro* assay performed with EVC-CFE in Figure 8 (A). The mass fragmentation pattern of the peak maximum at 9.71 min in (B) was characteristic for the trimethylsilyl ester of n-Pentadecanoic acid, the peak at 11.38 min in (C) had been previously identified as OA and the mass fragmentation pattern of the peak maximum at 12.34 min in (D) was determined as 16-Hydroxypalmitic acid, since the peak at m/z 385.25 resulted from the loss of a methoxyl function from the molecular ion.

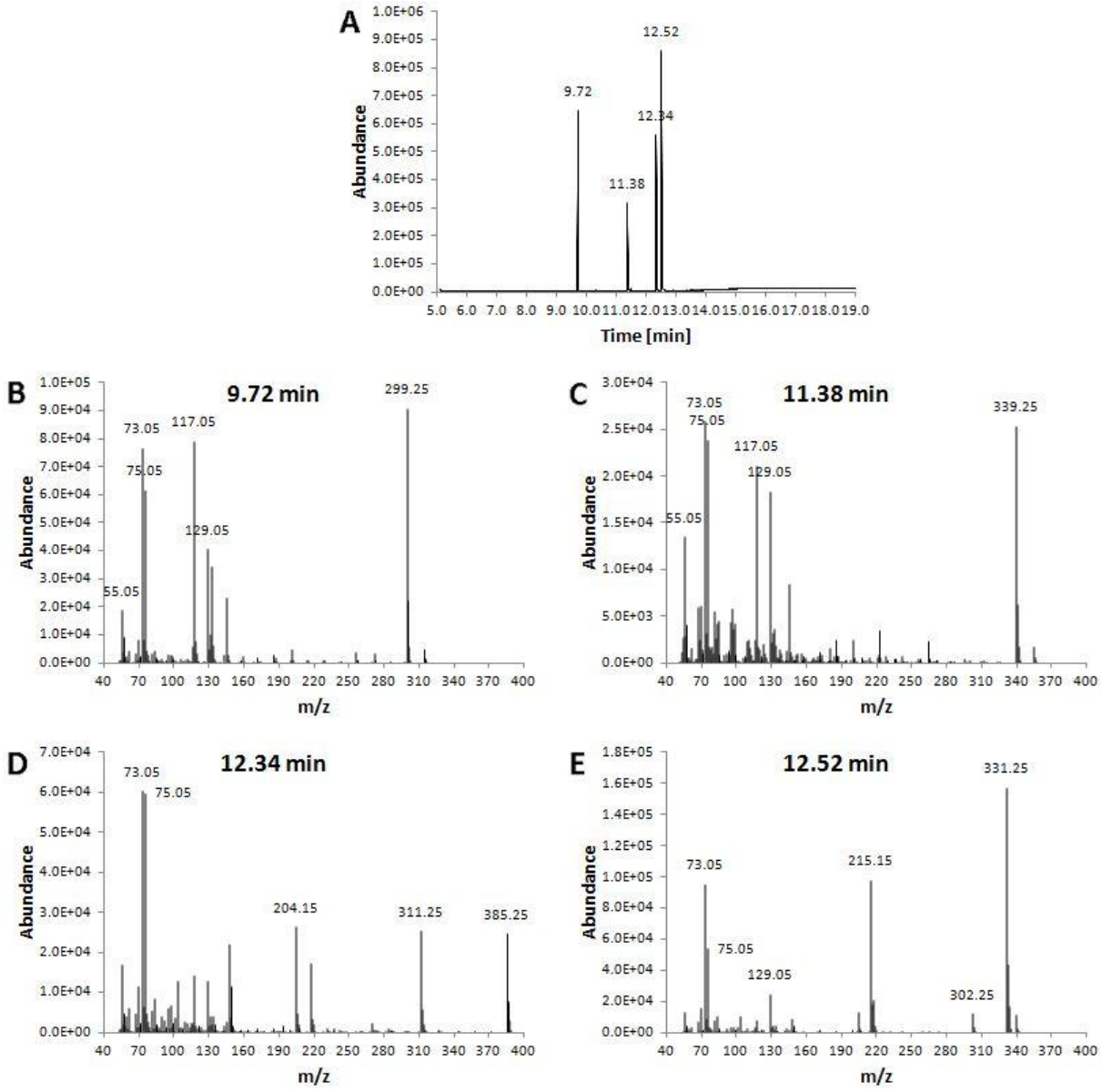

Figure 9: Representative GC-MS analysis of fatty acids obtained after quantitative *in vitro* conversion of 0.15 mM OA with internal standards using 0.01 mg mL^{-1} of EVC-CFE. (A) Chromatogram. (B) Mass fragmentation pattern of the peak maximum at 9.72 min, corresponding to n-Pentadecanoic acid. (C) Mass fragmentation pattern of the peak maximum at 11.38 min, corresponding to OA. (D) Mass fragmentation pattern of the peak maximum at 12.34 min, corresponding to 16-Hydroxypalmitic acid. (E) Mass fragmentation pattern of the peak maximum at 12.52 min, corresponding to 10-HSA.

GC-MS analysis of the quantitative *in vitro* assay with OhyA-CFE gave an additional peak at 12.52 min compared to the assay using EVC-CFE (Figure 9). Mass fragmentation patterns allowed unambiguous identification of the compounds as n-Pentadecanoic acid, OA, 16-Hydroxypalmitic acid and the desired product 10-HSA.

Quantitation was conducted by integration of peak areas and subsequent calculation of free fatty acid concentrations referred to the internal standard curves (Figure 10).

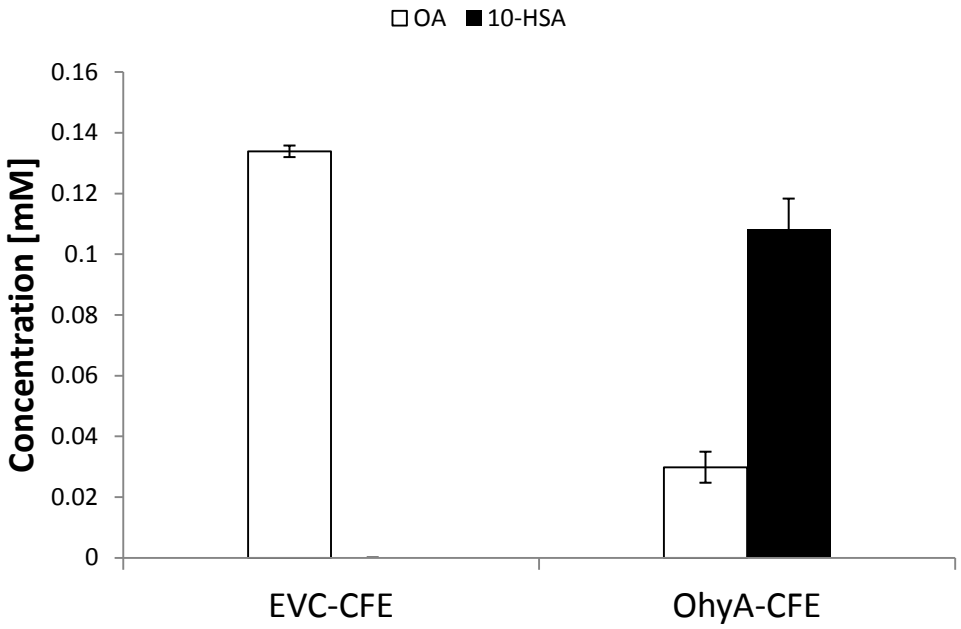

Figure 10: ***In vitro*** **conversion of OA to 10-HSA with EVC-CFE and OhyA-CFE using internal standards for quantitation. Substrate concentration was 0.15 mM and CFE concentrations were 0.2 mg mL^{1} for EVC-CFE and 0.01 mg mL^{-1} for OhyA-CFE, respectively. Reactions were carried out at pH 6.5 and the standard conditions described in the text. Mean values, ranges and standard deviations of two (EVC-CFE) and four (OhyA-CFE) biological replicates are given.**

No 10-HSA was formed by incubation of the EVC-CFE with OA, whereas conversion of the substrate with OhyA-CFE resulted in generation of 0.11 mM 10-HSA, while 0.03 mM OA remained unconverted after a reaction time of 10 min (Figure 10). Considering the acceptable standard deviations, as well as very similar total fatty acid concentrations calculated from the individual experiments, quantitation of the *in vitro* activity assay was regarded as successful and analysis of the oleate hydratase reaction was possible.

6.2 Expression of oleate hydratases in *E. coli*

All genes used in this work were provided by DSM Innovative Synthesis BV (Geleen, the Netherlands) in codon optimized form for expression in *E. coli*. The nine cloned and expressed oleate hydratase genes, as well as their notations, are listed in Table 6.

Table 6: Summary of oleate hydratase genes used in this work. Identities of protein sequences were determined via the Protein-BLAST algorithm.

Gene	Organism	Sequence identity to OhyA [%]	Protein size [kDa]	Accession number
ohyA	*Elizabethkingia meningoseptica*	-	73.5	ACT54545
mch	*Macrococcus caseolyticus*	40	67.3	YP_002559479
bbh	*Bifidobacterium breve*	36	70.5	ADY18551
ckh	*Corynebacterium kroppenstedtii*	44	67	YP_002907233
oah	*Ochrobactrum anthropi*	58	74.2	YP_001373221
moh	*Myroides odoratus*	74	73.5	ZP_09674164
sah	*Staphylococcus aureus*	40	67.8	ZP_06925789
cgh	*Chryseobacterium gleum*	82	73.3	ZP_07086592
cah	*Cellulophaga algicola*	72	73.2	YP_004165724

Genes were amplified via PCR using primers containing restriction sites for cloning into the two different His_6-tagging vectors (Figure 11).

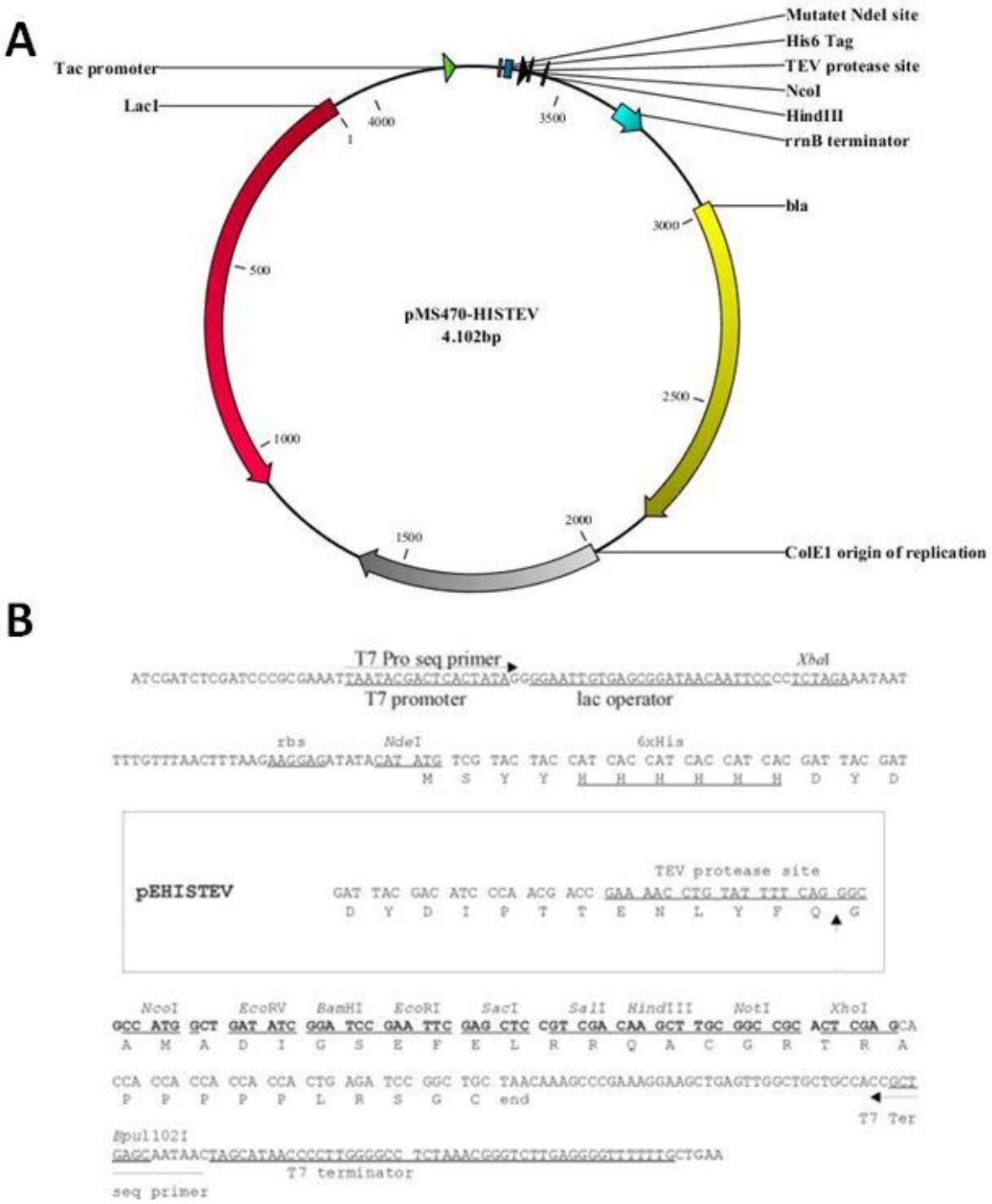

Figure 11: Expression vectors used in this work. (A) Vector map of pMS470-HISTEV. (B) Multiple cloning site of pEHISTEV. Modified figure taken from[20].

Protein expression from both vectors was induced by IPTG, and selection was driven by ampicillin (pMS470-HISTEV) or kanamycin (pEHISTEV, Figure 11). Furthermore, both vectors allowed expression of N-terminally His_6-tagged protein, as well as optional posttranslational removal of the His_6-tag at the TEV protease cleavage site.

Each of the nine oleate hydratase genes, except for *cgh*, was cloned into pMS470-HISTEV via its *Nco*I- and *Hin*dIII-restriction sites, as well as into pEHISTEV via its *Eco*RI- and *Hin*dIII-sites (*cgh*) and *Nco*I- and *Hin*dIII-sites (other genes), respectively. *Cgh* was only cloned into pEHISTEV via its *Eco*RI- and *Hin*dIII-sites, because *Nco*I cuts in the *cgh* gene sequence, and pMS470-HISTEV features two restriction sites for *Eco*RI. After ligation of digested vector backbones and inserts, the resulting plasmids were used for transformation of electrocompetent *E. coli* Top10F' cells for plasmid amplification and supercoiling. Plasmids from several clones of each construct were isolated and control cuts with *Nco*I and *Hin*dIII for the genes cloned into pMS470-HISTEV and *Eco*RI and *Hind*III (*cgh*) or *Nco*I and *Hind*III (other genes) for the genes cloned into pEHISTEV were conducted. After confirmation of successful ligation, 2 µL of each supercoiled construct were transformed into electrocompetent *E. coli* BL21 Star™ (DE3) cells to create the strains for heterologous protein expression. Again, plasmids from several clones of each construct were isolated and correct cloning and plasmid configuration was subsequently confirmed by DNA sequencing (LGC Genomics, Berlin, Germany).

For initial recombinant expression and analysis of oleate hydratases, proteins were expressed in TB-medium as described in the methods section. One *E. coli* BL21Star™ (DE3) [pEHISTEV] culture was cultivated simultaneously as a control experiment. Oah and Cgh were only expressed via the pEHISTEV vector system at 28°C. Table 7 summarizes the CWWs after protein expression.

Table 7: CWWs of *E. coli* BL21Star™ (DE3) after expression of recombinant protein via the two different vector systems. Protein expression was carried out for 19 h at 28°C (Oah and Cgh) or 20°C (other proteins), respectively.

Protein	Vector	CWW [g]
OhyA	pMS470-HISTEV	0.94
	pEHISTEV	0.73
Mch	pMS470-HISTEV	4.63
	pEHISTEV	2.94
Bbh	pMS470-HISTEV	5.73
	pEHISTEV	1.62
Ckh	pMS470-HISTEV	4.61
	pEHISTEV	1.21
Oah	pEHISTEV	5.12
Moh	pMS470-HISTEV	2.80
	pEHISTEV	0.91
Sah	pMS470-HISTEV	4.80
	pEHISTEV	1.68
Cgh	pEHISTEV	5.61
Cah	pMS470-HISTEV	4.92
	pEHISTEV	2.03
EVC	pMS470-HISTEV	7.17
	pEHISTEV	6.11

The weights of the cell pellets varied considerably from 0.73 g for *E. coli* BL21 Star™ (DE3) [pEHISTEV-OhyA] to 7.17 g for *E. coli* BL21 Star™ (DE3) [pMS470-HISTEV] (Table 7). Especially the consistently higher CWW of aliquots after expression of recombinant protein via the pMS470-HISTEV vector system was worth noting.

CFEs were prepared and expression yield of soluble recombinant protein was assessed by SDS-PAGE analysis of total cell lysates and CFEs after separation of cell debris (Figure 12).

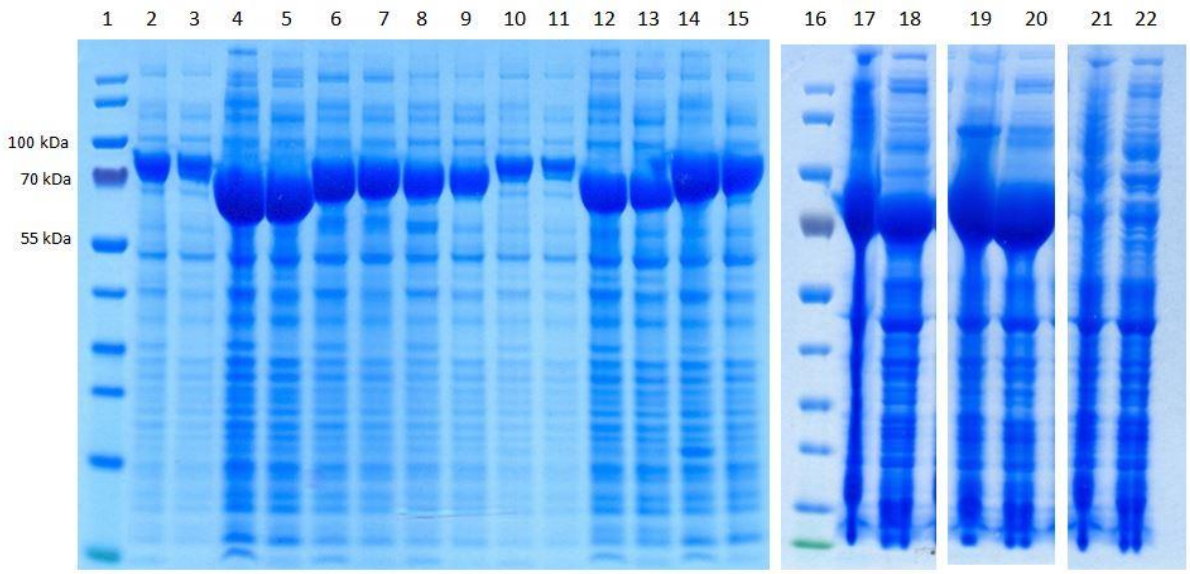

Lane	Protein		µl	Lane	Protein		µl
1	Molecular mass marker	-	5	12	Sah	Total lysate	5
2	OhyA	Total lysate	2	13		CFE	2
3		CFE	2	14	Cah	Total lysate	2
4	Mch	Total lysate	2	15		CFE	2
5		CFE	2	16	Molecular mass marker	-	5
6	Bbh	Total lysate	2	17	Cgh	Total lysate	2
7		CFE	2	18		CFE	2
8	Ckh	Total lysate	2	19	Oah	Total lysate	2
9		CFE	2	20		CFE	2
10	Moh	Total lysate	2	21	EVC	Total lysate	2
11		CFE	2	22		CFE	2

Figure 12: SDS-PAGE analysis of oleate hydratase expression in *E. coli*. Cgh and Oah were expressed at 28°C and other proteins at 20°C. EVC: Empty vector control strain.

All proteins of interest could be readily expressed in *E. coli* as soluble proteins, as indicated by the bands between 65 kDa and 75 kDa in both total lysates and CFEs (Figure 12). No protein was overexpressed with the EVC strain. High expression levels of Oah and Cgh were obtained at 28°C, whereas for soluble expression of other proteins, the cultivation temperature during induction had to be decreased to 20°C (data not shown).

A protocol for gravity-flow purification of N-terminally His_6-tagged oleate hydratases was established and optimized to obtain aliquots for further analyses. First purifications were attempted with Washing Protocol 1 described in Table 2, using buffer containing 20 mM imidazole, to purify Oah and Sah (Figure 13).

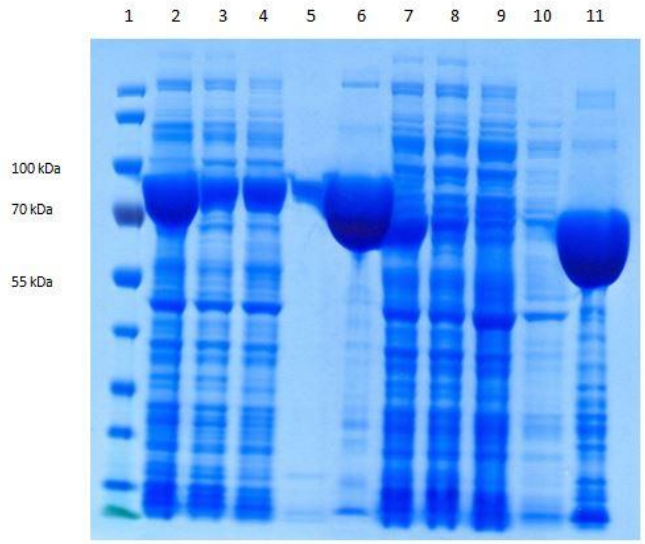

Lane	Protein		µl
1	Molecular mass marker	-	5
2		CFE	2
3		Flow through	2
4	Oah	Washing fraction 1	5
5		Washing fraction 2	5
6		Elution	5
7		CFE	2
8		Flow through	2
9	Sah	Washing fraction 1	5
10		Washing fraction 2	5
11		Elution	5

Figure 13: SDS-PAGE analysis of fractions from purifications of Oah and Sah using Washing Protocol 1.

SDS-PAGE showed that the majority of non-target protein could be removed by washing with 20 mM imidazole (Figure 13). Many small bands were still detected in the elution fractions which indicated that use of more washing steps and application of buffers containing a higher imidazole concentration might be advantageous. Additionally, the substantial amount of overexpressed protein in the flow through and washing fractions, probably caused by inefficient binding of the His_6-tagged protein to the column, were noted. Despite potential for further optimization, good yield and purity of the target proteins was achieved. To increase the efficiency of column washing, the purification protocol was modified by additional washing steps with buffer containing 30 mM imidazole in Washing Protocol 2 (Table 2). The altered protocol was tested with Oah and Sah CFEs (Figure 14).

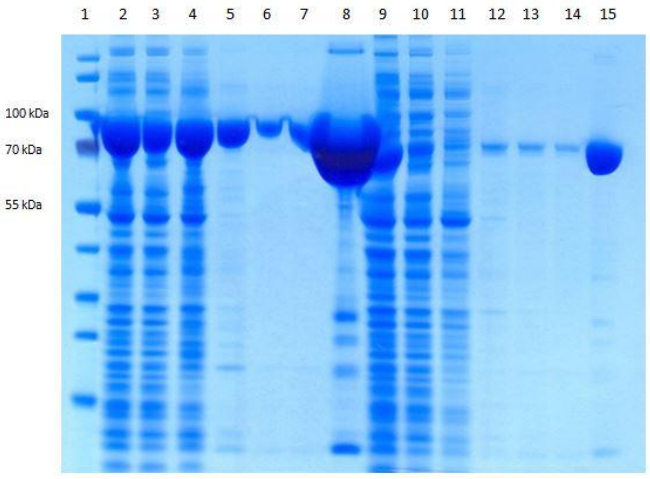

Lane	Protein		µl
1	Molecular mass marker	-	5
2		CFE	2
3		Flow through	2
4		Washing fraction 1	5
5	Oah	Washing fraction 2	5
6		Washing fraction 3	5
7		Washing fraction 4	5
8		Elution	5
9		CFE	2
10		Flow through	2
11		Washing fraction 1	5
12	Sah	Washing fraction 2	5
13		Washing fraction 3	5
14		Washing fraction 4	5
15		Elution	5

Figure 14: SDS-PAGE analysis of fractions from purifications of Oah and Sah using Washing Protocol 2. Buffers for Washing fractions 1 and 2 contained 20 mM imidazole and buffers for Washing fractions 3 and 4 contained 30 mM imidazole.

The number of protein bands and their intensity decreased in the elution fraction as a result of more extensive washing (Figure 14). The issue of target protein loss during column washing however still persisted, especially for Oah.

For purification of the remaining proteins, the conditions of Washing Protocol 2 were maintained. Purified proteins were desalted instantly using PD-10 desalting columns and selected fractions from both purification and desalting were evaluated. SDS-gels of Cgh purification, as well as desalted Oah, Sah and Cgh are depicted in Figure 15 and SDS-gels of OhyA, Mch, Bbh, Ckh, Moh and Cah purification are shown in Figure 16.

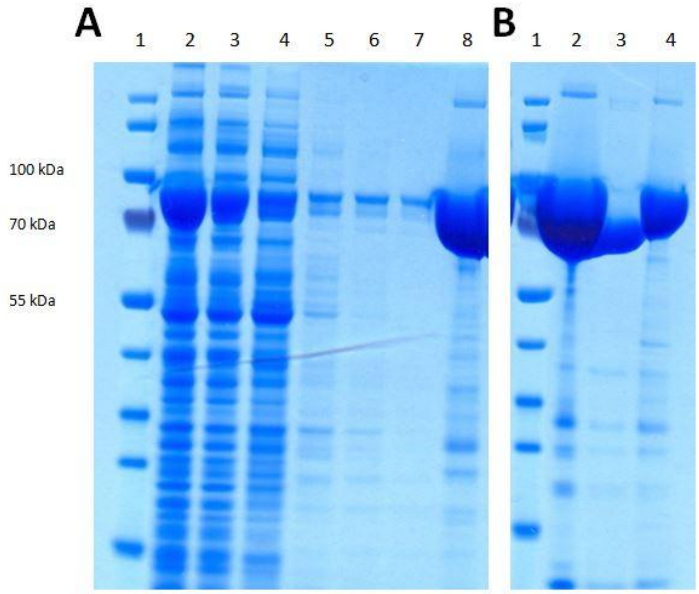

Lane	Protein		µl
A			
1	Molecular mass marker	-	5
2		CFE	2
3		Flow through	2
4		Washing fraction 1	5
5	Cgh	Washing fraction 2	5
6		Washing fraction 3	5
7		Washing fraction 4	5
8		Elution	5
B			
1	Molecular mass marker	-	5
2	Oah	Desalted	5
3	Sah	Desalted	5
4	Cgh	Desalted	5

Figure 15: SDS-PAGE analysis of fractions from purification of Cgh using Washing Protocol 2 and desalted Oah, Sah and Cgh. Buffers for Washing fractions 1 and 2 contained 20 mM imidazole and buffers for Washing fractions 3 and 4 contained 30 mM imidazole. (A) Purification of Cgh. (B) Purified Oah, Sah and Cgh after desalting.

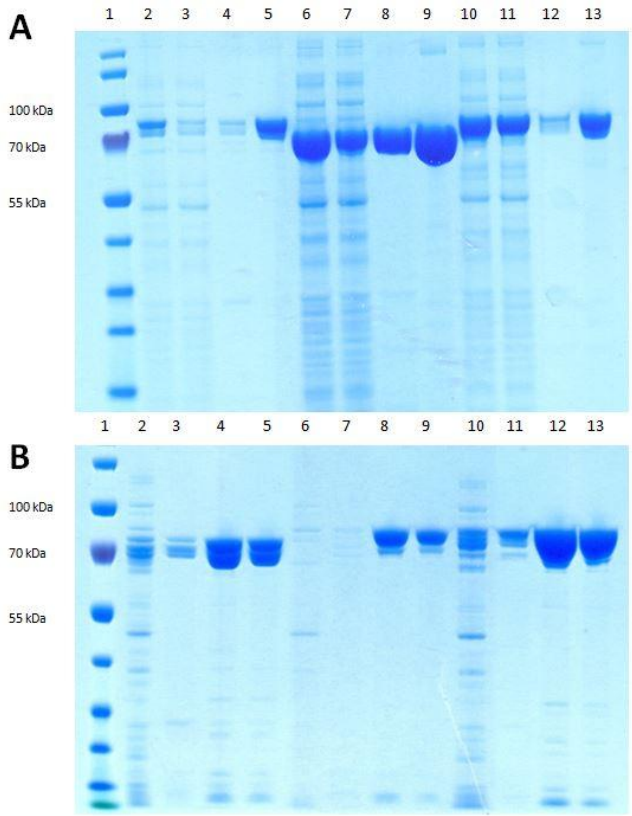

Lane	Protein		µl
1	Molecular mass marker	-	5
2	OhyA	CFE	1
3		Flow through	1
4		Washing fraction 4	5
5		Desalted	1
6	Mch	CFE	1
7		Flow through	1
8		Washing fraction 4	5
9		Desalted	1
10	Bbh	CFE	1
11		Flow through	1
12		Washing fraction 4	5
13		Desalted	1

Lane	Protein		µl
1	Molecular mass marker	-	5
2	Ckh	Flow through	1
3		Washing fraction 4	1
4		Elution	5
5		Desalted	1
6	Moh	Flow through	1
7		Washing fraction 4	1
8		Elution	5
9		Desalted	1
10	Cah	Flow through	1
11		Washing fraction 4	1
12		Elution	5
13		Desalted	1

Figure 16: SDS-PAGE analysis of selected fractions from purification of oleate hydratases using Washing Protocol 2. (A) Analysis of OhyA, Mch and Bbh. (B) Analysis of Ckh, Moh and Cah. The buffer for Washing fraction 4 contained 30 mM imidazole.

Gravity-flow purification and desalting of overexpressed oleate hydratases proved to be successful (Figure 15 and Figure 16). Even after desalting, faint bands of other proteins were observed, and a substantial loss of target protein during washing, congruent with previous purifications, was seen. To facilitate comparison of the different protein fractions, an SDS-gel with all purified oleate hydratases was run (Figure 17).

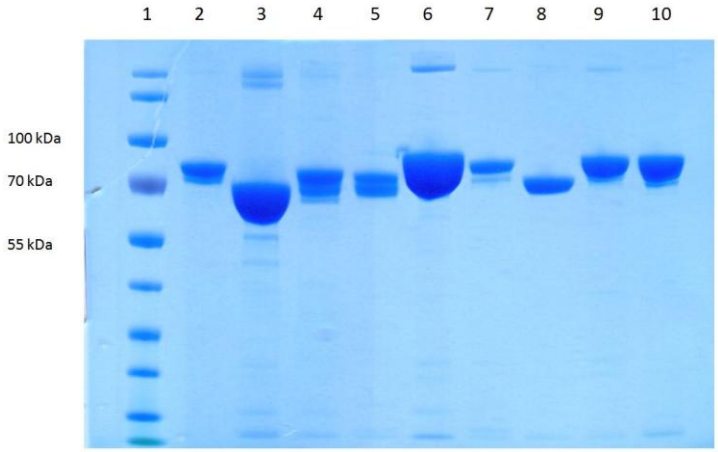

Figure 17: SDS-PAGE analysis of purified and desalted oleate hydratases. Lane 1: Molecular mass marker. Lane 2: OhyA. Lane 3: Mch. Lane 4: Bbh. Lane 5: Ckh. Lane 6: Oah. Lane 7: Moh. Lane 8: Sah. Lane 9: Cgh. Lane 10: Cah. One µL of each protein solution was loaded.

Based on the SDS-gel, the purity of each protein solution was estimated to at least 95% which was considered clearly sufficient for further working steps (Figure 17). The relative concentrations of obtained purified protein solutions could be concluded from the gel. Nonetheless, concentrations were determined with the Bio-Rad protein assay as well (Table 8).

Table 8: Concentrations of purified and desalted protein solutions.

Protein solution	**Concentration [mg mL^{-1}]**
OhyA	1.4
Mch	9.3
Bbh	2.2
Ckh	1.3
Oah	13.0
Moh	0.6
Sah	1.5
Cgh	2.5
Cah	2.8

Concentrations of enzyme solutions ranged from 0.6 mg mL^{-1} (Moh) to 13 mg mL $^{-1}$ (Oah, Table 8), and the results from both the SDS-PAGE and Bio-Rad protein assay were consistent.

6.3 Determination of oleate hydratase activity and characterization of reaction conditions of OhyA and Oah

Purified oleate hydratase samples were examined regarding their ability to catalyze the formation of 10-HSA from OA in the *in vitro* activity assay. For initial activity tests, the quantitative *in vitro* activity assay was not yet available and therefore it could only be monitored whether or not the enzymes converted their natural substrate. In this phase of the project the main aim was, however, mainly to accomplish functional expression of oleate hydratases and therefore, that was considered sufficient. Enzymatic conversions were performed with 2 mM OA at pH 6.5 and standard conditions with 0.01 mg mL^{-1} of purified enzyme solutions, including a negative control without enzyme (Figure 18).

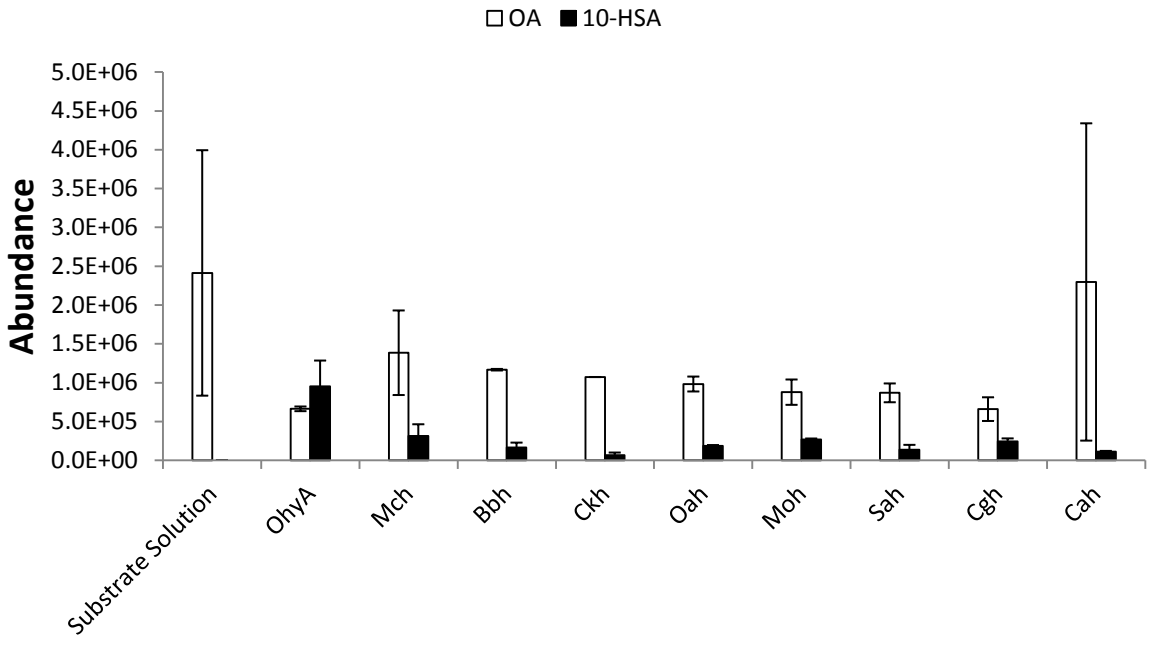

Figure 18: ***In vitro*** **conversion of OA to 10-HSA with purified oleate hydratases. Substrate concentration was 2 mM and enzyme concentrations were 0.01 mg mL^{-1} each. Reactions were carried out at pH 6.5 and the standard conditions described in the text. Mean values and ranges of two individual experiments are given.**

All enzymes were expressed and purified in active forms, since 10-HSA was detected in all analyzed samples without background hydration activity of the cis-9 double bond of OA (Figure 18). The amount of substrate, as well as total fatty acids varied strikingly among the biological duplicates and different enzyme reactions, which emphasized that for any quantitative analysis, incorporation of internal standards was necessary.

Enzymatic reactions were quantitated via *in vitro* reactions using internal standards with freshly prepared CFEs. Total conversions were assessed with two CFE concentrations. The substrate concentration was 0.15 mM and reactions were conducted at pH 6.5 and standard conditions. Concentrations of CFEs were adapted in order to allow formation of reasonable levels of 10-HSA (Figure 19).

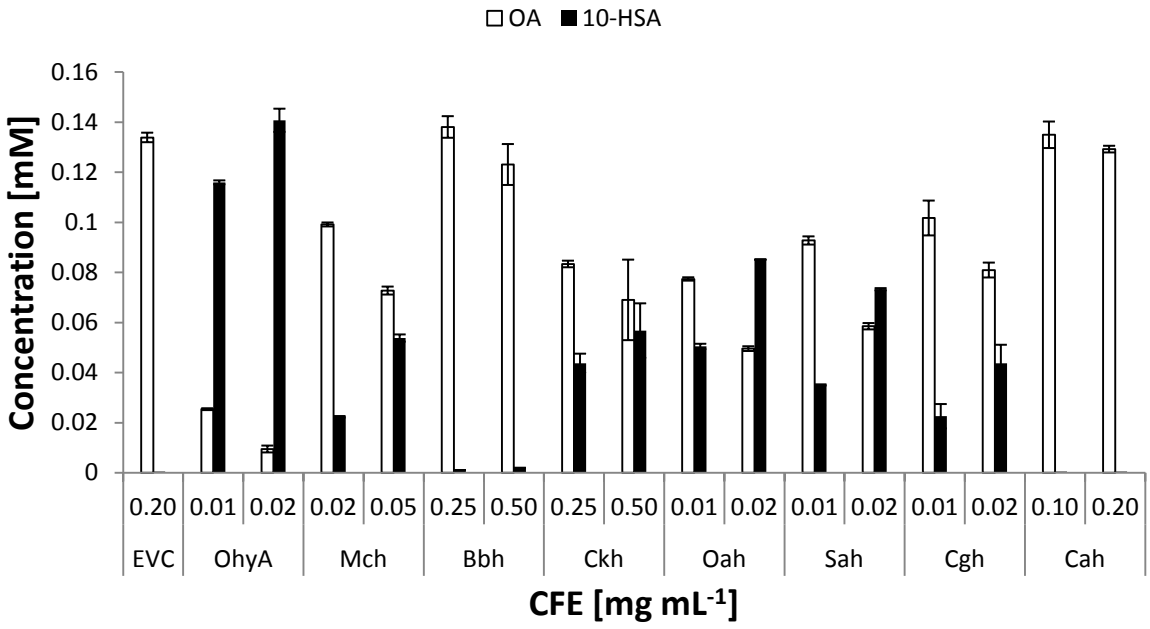

Figure 19: ***In vitro*** **conversions of OA to 10-HSA with CFEs containing recombinantly expressed oleate hydratases using internal standards for quantitation. Substrate concentration was 0.15 mM and total protein concentrations were as stated. Reactions were carried out at pH 6.5 and the standard conditions described in the text. Mean values and ranges of two individual experiments are given.**

As previously observed after *in vitro* conversions with purified oleate hydratases, incubation of OA with the negative control did not result in generation of any 10-HSA (Figure 19). Due to addition of internal standards prior to the reaction, highly reproducible experiments could be performed, as indicated by the total fatty acid concentrations derived from individual experiments and by the short error bars. Albeit no linear dependence of converted OA on enzyme concentration was proven, it was possible to calculate concentrations of OA and 10-HSA after the activity assay. OhyA CFE generated the highest titer of 10-HSA (0.140 mM), followed by Oah (0.085 mM) and Sah CFE (0.073 mM). No relevant 10-HSA titers were detected after *in vitro* assays with Bbh and Cah CFE. Overall, oleate hydratases from different microbial species showed diverse performances. For the five enzymes that produced the highest 10-HSA titers at CFE concentrations lower than 0.1 mg mL^{-1}, specific activities were determined (Figure 20).

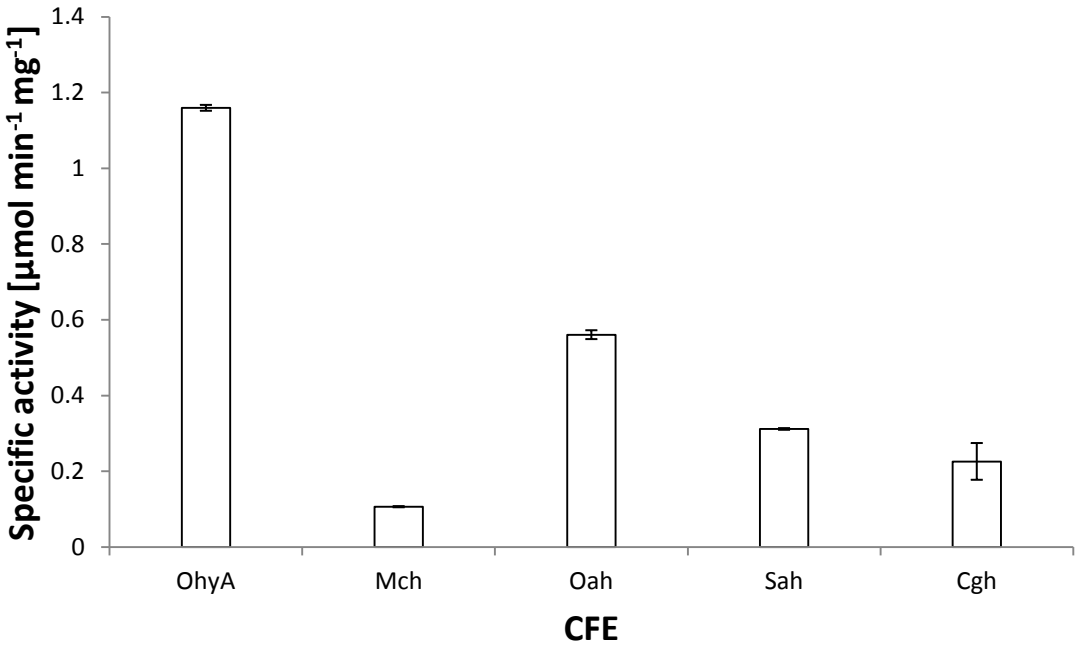

Figure 20: Specific activities of CFEs containing recombinantly expressed oleate hydratases for the conversion of OA to 10-HSA. Substrate concentration was 0.15 mM. Reactions were carried out at pH 6.5 and the standard conditions described in the text. Mean values and ranges of two individual experiments are given.

OhyA CFE displayed the highest specific activity with approx. 1.16 µmol min^{-1} mg^{-1} (Figure 20). Specific activities of Oah-, Sah- and Cgh-CFEs were all one order of magnitude below, whereas for Mch CFE, the lowest specific activity was observed with approx. 0.11 µmol min^{-1} mg^{-1}.

In order to elucidate the effects of reaction conditions on the activity of a limited number of oleate hydratases, temperature and pH profiles of enzymatic reactions with OhyA and Oah CFEs were recorded. The temperature was varied from 15°C to 35°C at pH 6.5, and the effect of pH on enzyme activity was investigated by varying the pH value from pH 5.5 to pH 8.5 at 25°C. The substrate concentration was 0.15 mM and reactions were conducted at standard conditions with 0.01 mg mL^{-1} of CFEs (Figure 21).

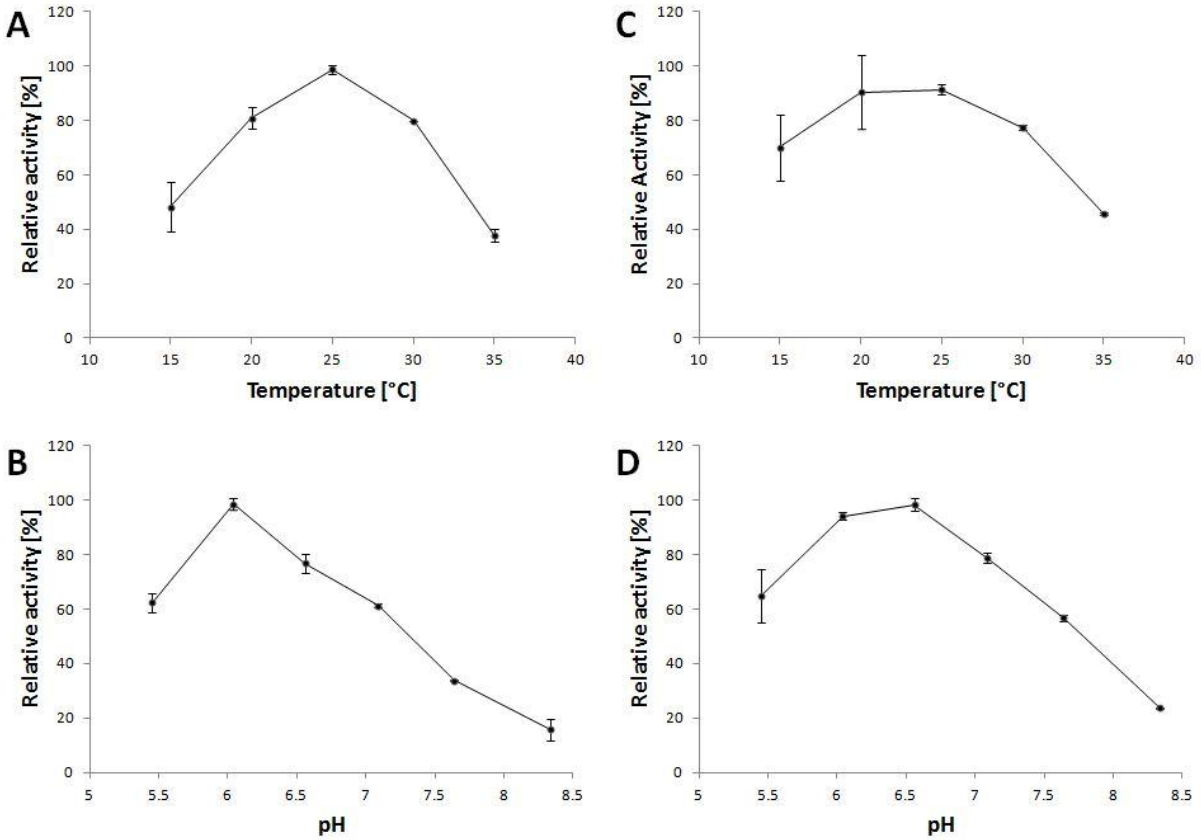

Figure 21: Effect of temperature and pH on the activity of OhyA and Oah as determined in CFEs. (A), (B) Effect of temperature and pH on the activity of OhyA in CFE. (C), (D) Effect of temperature and pH on the activity of Oah in CFE. Substrate concentration was 0.15 mM and CFE concentrations were 0.01 mg mL^{-1} each. Reactions were carried out at the standard conditions described in the text. Mean values and ranges of two individual experiments are given.

The maximum activity of OhyA in CFE was observed at 25°C and pH 6.0, and the activity decreased rapidly and similarly upon in- or decreasing the reaction temperature, indicating a low thermostability (Figure 21). Oah in CFE showed an optimum temperature in the range of 20°C to 25°C, and maximal relative activity was recorded at pH 6.5, but even at pH 6.0 the relative activity decreased only slightly. From these results, a slightly higher thermo- and pH-stability of Oah, compared with OhyA, was deduced.

6.4 Biochemical analysis of OhyA

From the nine oleate hydratases on hand, OhyA displayed by far the highest specific activity and was thus selected for an in depth biochemical analysis. Although expressed as active, soluble proteins, expression levels and growth of expression strains in TB-medium at 20°C where rather low. Incubation of *E. coli* BL21Star™ (DE3) [pMS470-HISTEV-OhyA] and *E. coli* BL21Star™ (DE3) [pEHISTEV-OhyA] in AIM at 28°C resulted in both satisfying growth of the strains and expression level of recombinant protein.

For purification of OhyA after optimization of expression, the Äkta purifier system, equipped with ready-to-use columns for purification of His-tagged protein, was used and optimized regarding yield and purity of target protein by evaluation of a set of protocols (*HisTrap 1*-, *HisTrap 2*-, *HisTrap 3*- and *TALON*-protocol in Table 3). Chromatogram and SDS-PAGE analysis of purification via the *HisTrap 1*-protocol are shown in Figure 22.

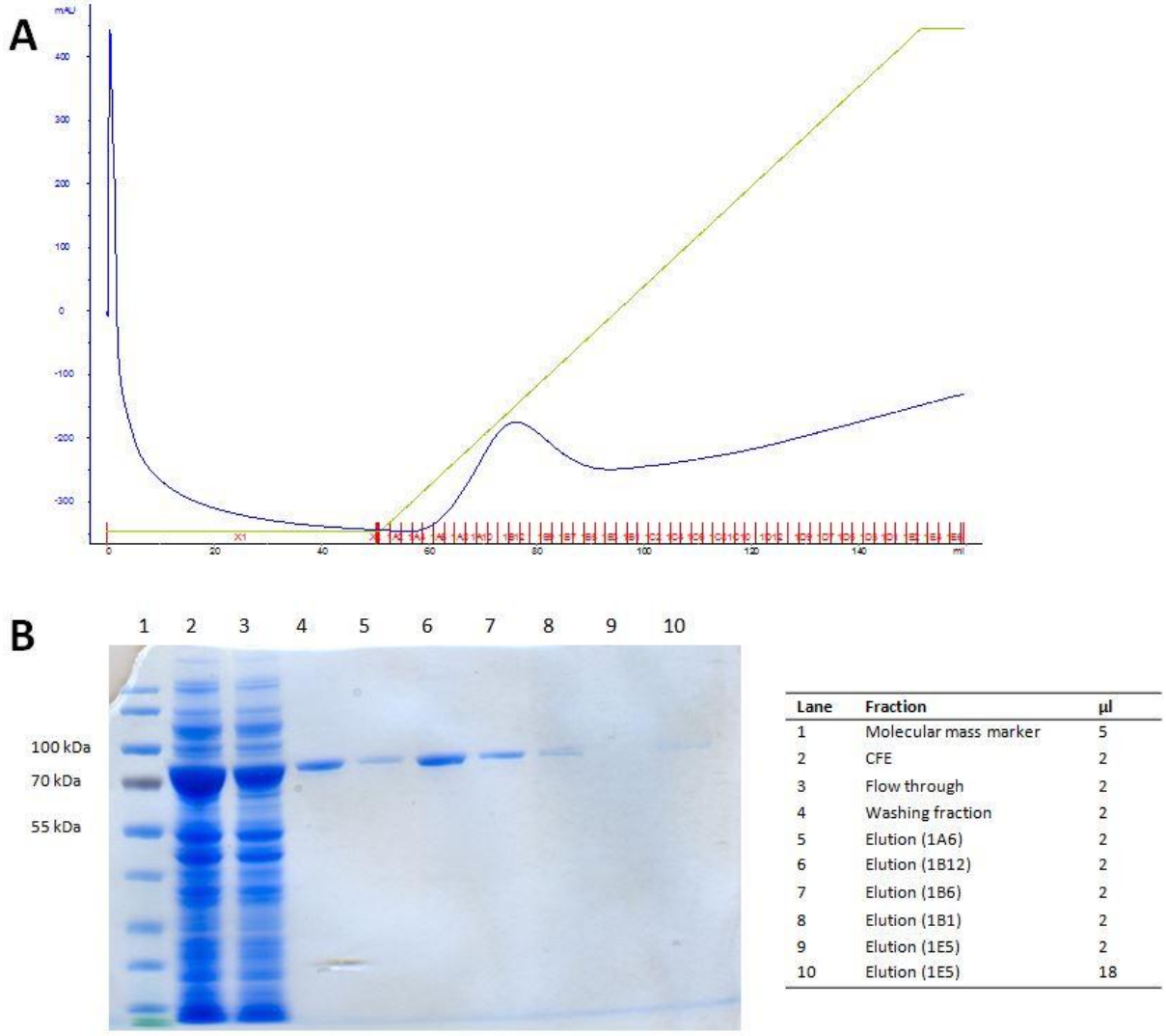

Lane	Fraction	µl
1	Molecular mass marker	5
2	CFE	2
3	Flow through	2
4	Washing fraction	2
5	Elution (1A6)	2
6	Elution (1B12)	2
7	Elution (1B6)	2
8	Elution (1B1)	2
9	Elution (1E5)	2
10	Elution (1E5)	18

Figure 22: Purification of OhyA via *HisTrap 1*-protocol. (A) Chromatogram. Blue line: Absorbance at 280 nm. Green line: Imidazole concentration from 10 mM to 250 mM. (B) SDS-PAGE analysis of selected fractions.

The chromatogram indicated that, overall, a very low A_{280} signal was measured in the elution fractions, including a relatively small protein peak of approx. 200 mAU close to the beginning of the imidazole gradient (Figure 22). During elution, gradually more protein eluted from the column without any distinctive peak. The SDS-gel confirmed elution of the approx. 73.5 kDa OhyA in all examined fractions, with the distinctive peak containing the largest amount of protein. Purification was optimized for a higher yield with the *HisTrap* 2-protocol (Figure 23).

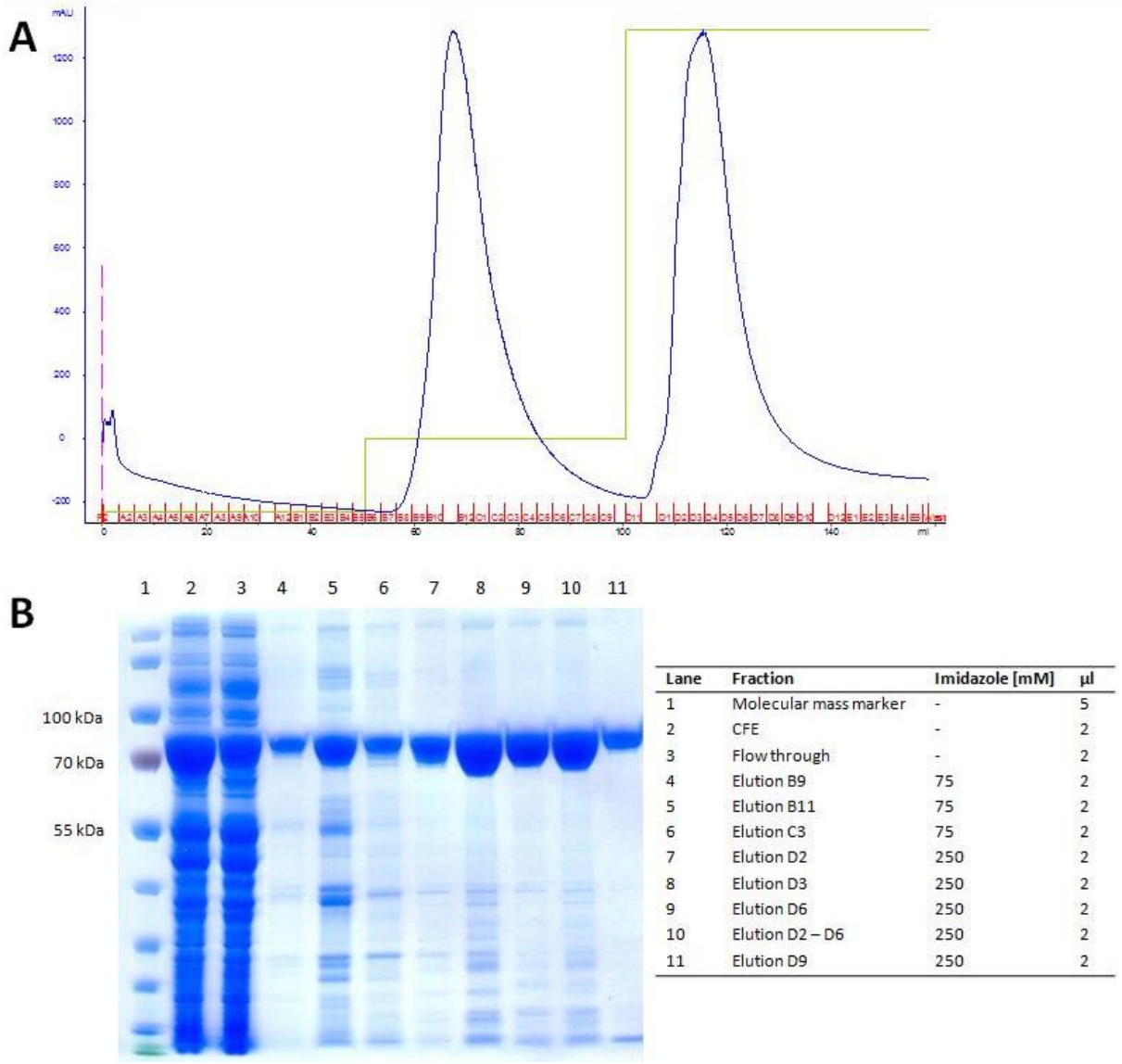

Lane	Fraction	Imidazole [mM]	µl
1	Molecular mass marker	-	5
2	CFE	-	2
3	Flow through	-	2
4	Elution B9	75	2
5	Elution B11	75	2
6	Elution C3	75	2
7	Elution D2	250	2
8	Elution D3	250	2
9	Elution D6	250	2
10	Elution D2 – D6	250	2
11	Elution D9	250	2

Figure 23: Purification of OhyA via *HisTrap 2*-protocol. (A) Chromatogram. Blue line: Absorbance at 280 nm. Green line: Imidazole concentration from 10 to 250 mM. (B) SDS-PAGE analysis of selected fractions.

Application of the *HisTrap* 2-protocol resulted in two distinct peaks of approx. 1500 mAU each after washing of the column with 75 mM and elution with 250 mM imidazole, respectively (Figure 23). As apparent from the corresponding SDS-gel, application of 75 mM imidazole resulted in the elution of notable amounts of OhyA in the washing fraction. Impurities bound to the column could be eliminated as well. In contrast, OhyA is more predominant in the pooled fractions of the second peak, which indicated good purity of the target protein. In order to reduce the loss of OhyA during the washing step, the *HisTrap* 3-protocol was tested (Figure 24).

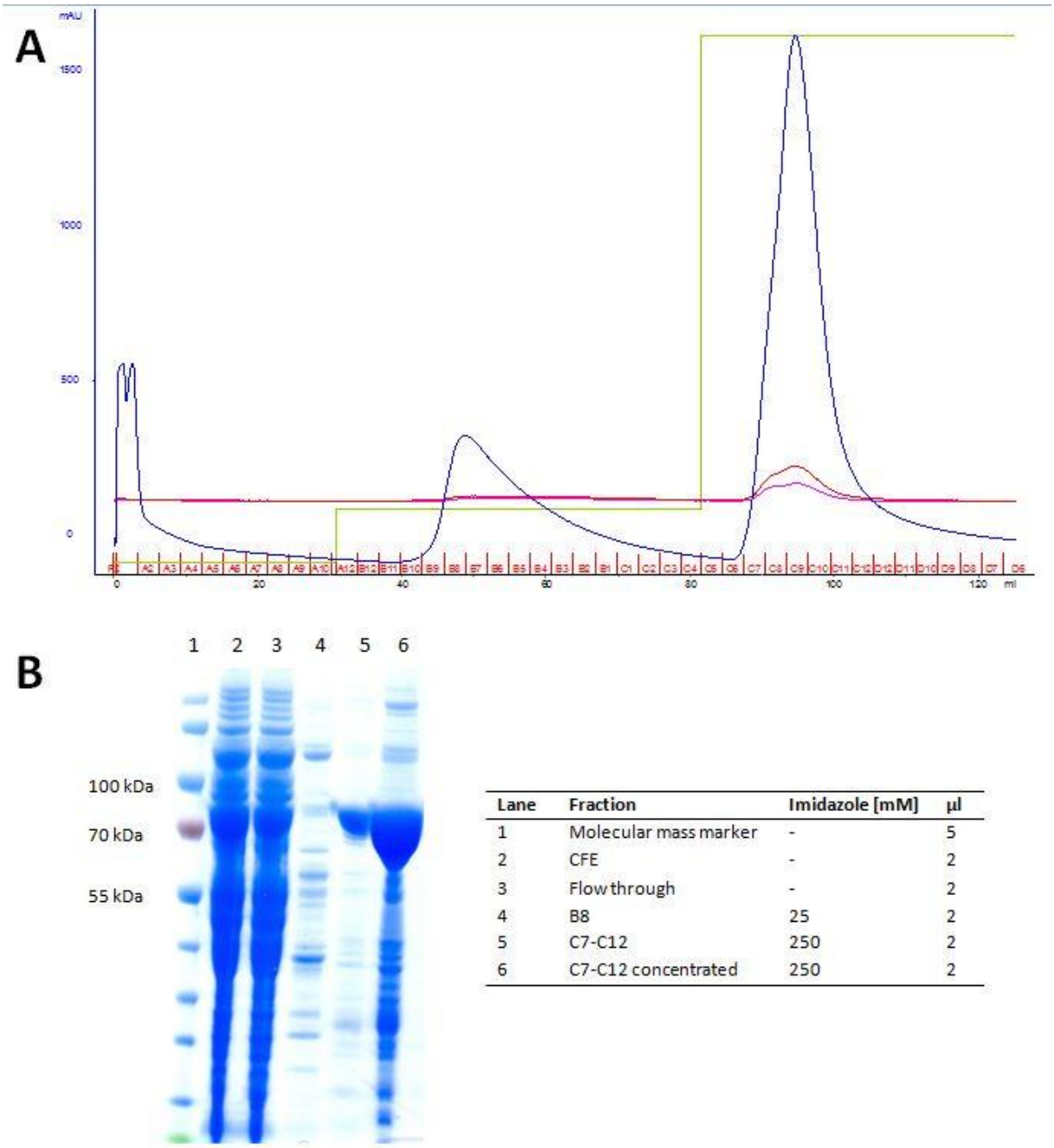

Lane	Fraction	Imidazole [mM]	µl
1	Molecular mass marker	-	5
2	CFE	-	2
3	Flow through	-	2
4	B8	25	2
5	C7-C12	250	2
6	C7-C12 concentrated	250	2

Figure 24: Purification of OhyA via *HisTrap 3*-protocol. (A) Chromatogram. Blue line: Absorbance at 280 nm. Green line: Imidazole concentration from 10 to 250 mM. Red line: Absorbance at 410 nm. Pink line: Absorbance at 440 nm. (B) SDS-PAGE analysis of selected fractions.

The amount of total protein in the washing fraction was reduced compared with the *HisTrap* 2-protocol (Figure 24). Additionally, the second peak was highly prevalent with approx. 1600 mAU, and the flavin-like absorbance at 440 nm suggested the presence of flavin-loaded OhyA. SDS-PAGE confirmed, that elution of the target protein in the washing fraction was largely reduced by decreasing the imidazole concentration from 75 mM to 25 mM, whereas impurities were still removed. Since the abundance of OhyA in the elution fraction with 250 mM imidazole was comparable to the *HisTrap* 2-protocol, purification including a washing

step with 25 mM imidazole was considered an acceptable compromise between yield and purity of His_6-tagged protein. To compare the effect of HisTrap™ FF crude columns to other immobilized metal ion affinity chromatography (IMAC) columns on the purification of OhyA, the *TALON*-protocol was evaluated for purification of target protein as well (Figure 25).

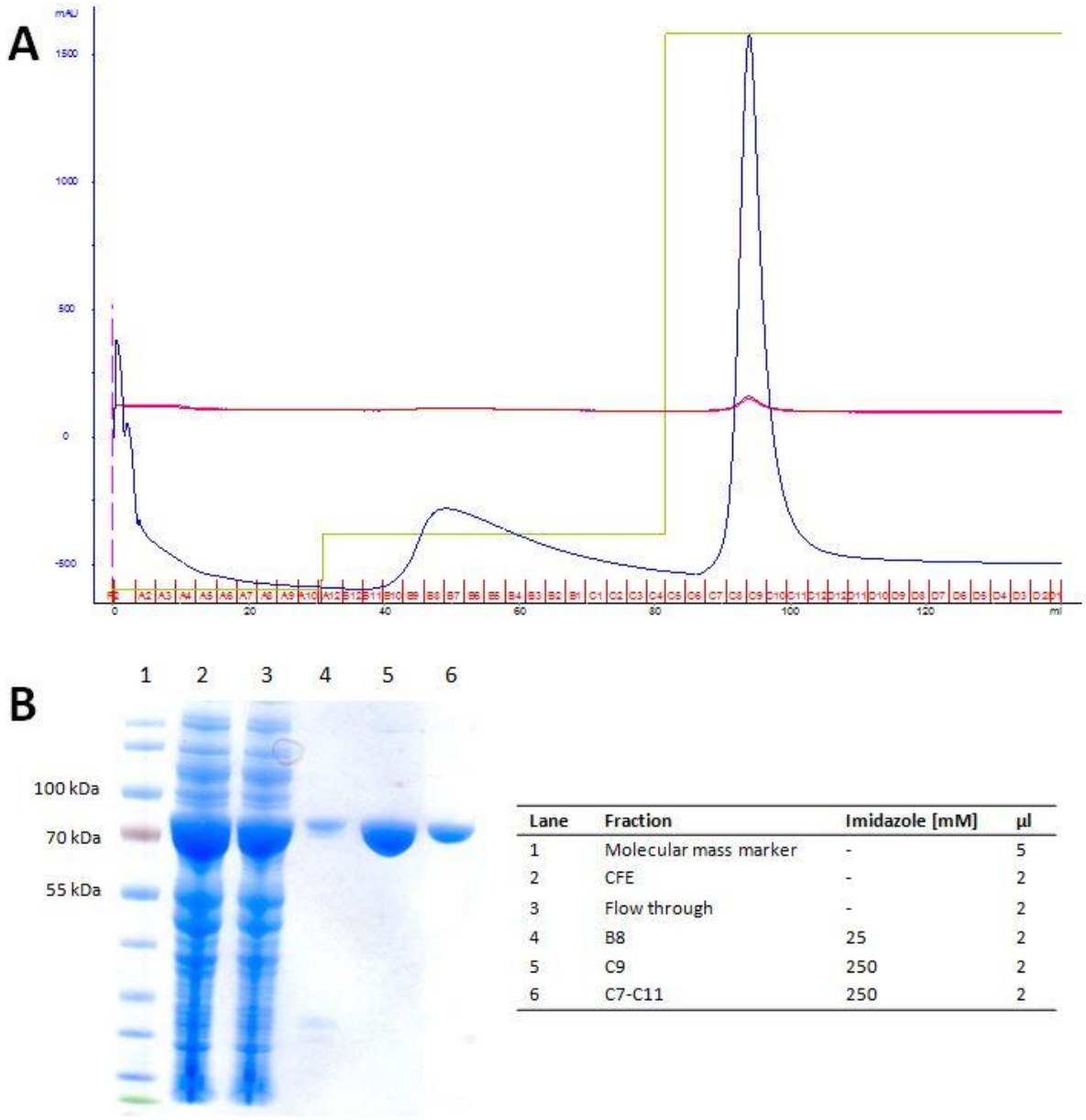

Lane	Fraction	Imidazole [mM]	µl
1	Molecular mass marker	-	5
2	CFE	-	2
3	Flow through	-	2
4	B8	25	2
5	C9	250	2
6	C7-C11	250	2

Figure 25: Purification of OhyA via *TALON*-protocol. (A) Chromatogram. Blue line: Absorbance at 280 nm. Green line: Imidazole concentration from 10 to 250 mM. Red line: Absorbance at 410 nm. Pink line: Absorbance at 440 nm. (B) SDS-PAGE analysis of selected fractions.

Similarly to the *HisTrap* 3-protocol, purification via *TALON*-protocol resulted in considerably more total protein in the elution fraction with 250 mM imidazole than in the washing fraction with 25 mM imidazole, and the absorbance at 440 nm indicated presence of OhyA (Figure 25). SDS-PAGE analysis verified this finding. Furthermore, binding of other proteins in the

cell extract could be reduced, whereas the purity of OhyA was improved by exchanging the IMAC column. In general, OhyA was found in varying abundances in all fractions analyzed via SDS-PAGE, showing that purification always resulted in a substantial loss of target protein regardless of the selected conditions. Even though application of the *TALON*-protocol slightly reduced this effect, inefficient binding of OhyA, as observed previously during gravity-flow purification, was registered. After immediate desalting with a HiPrep 26/10 Desalting column, protein aliquots were incubated on ice at 4°C until further analyses, since storage at -20°C or -80°C led to irreversible denaturation during thawing of the aliquots.

Concentrated, affinity purified OhyA appeared as a yellow protein. The aliquot purified via *HisTrap* 3-protocol was selected first UV-Vis absorbance spectral analysis (Figure 26).

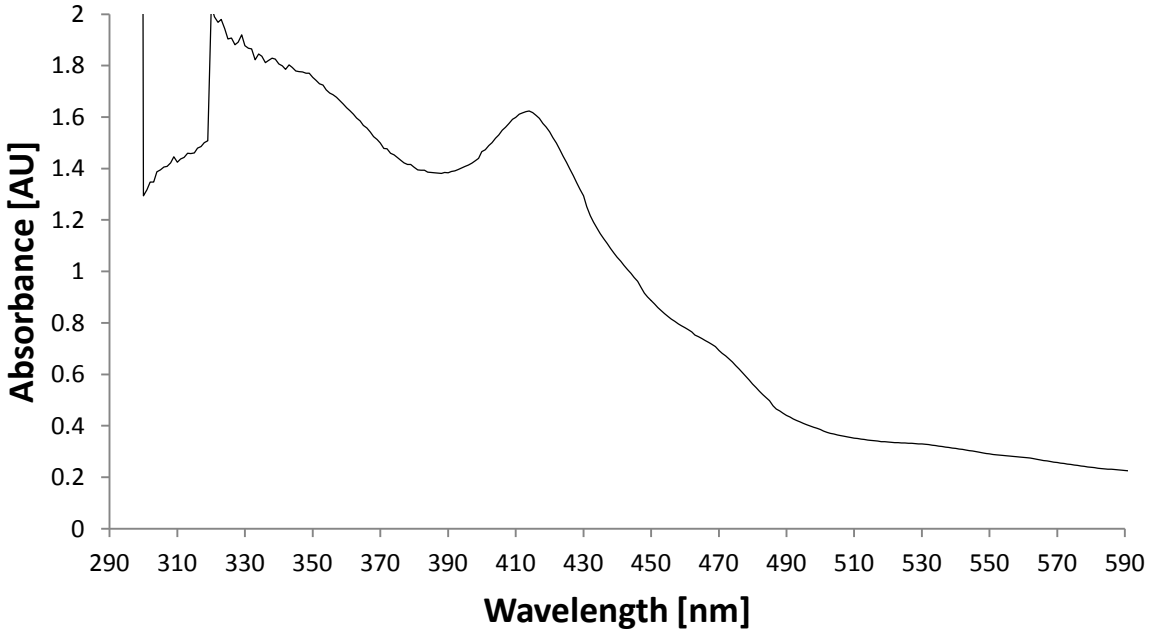

Figure 26: UV-Vis absorbance spectrum of concentrated OhyA after purification with the *HisTrap 3*-protocol.

The UV-Vis spectrum of OhyA after purification with the *HisTrap*3-protocol showed a predominant peak at 410 nm and additional residual absorbances at approx. 440 nm and 465 nm (Figure 26), which suggested that further purification might be necessary to intensify the absorbances between 440 nm and 465 nm. Therefore, an additional purification step via gel filtration was performed (Figure 27).

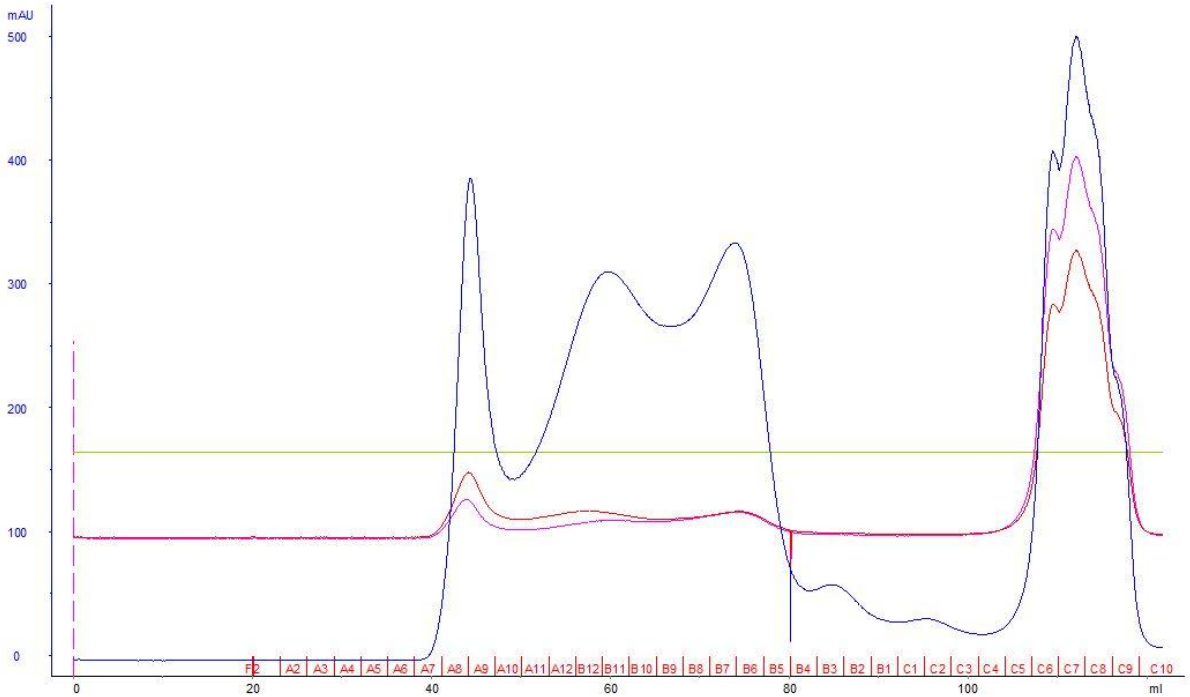

Figure 27: Chromatogram of gel filtration of OhyA, previously purified via *HisTrap 3*-protocol. Blue line: Absorbance at 280 nm. Red line: Absorbance at 410 nm. Pink line: Absorbance at 440 nm.

Three peaks between 40 mL and 80 mL of elution could be distinguished in the gel filtration chromatogram of *HisTrap 3*-protocol purified OhyA (Figure 27). The additional peak at approx. 110 mL was derived from free FAD, since the protein solution was incubated with a molar excess of FAD prior to gel filtration. Monomeric OhyA was determined to elute at 76 mL according to the calibration curve. Thus, the third peak was concentrated for UV-Vis spectral analysis and, furthermore, an SDS-PAGE of selected fractions was conducted (Figure 28).

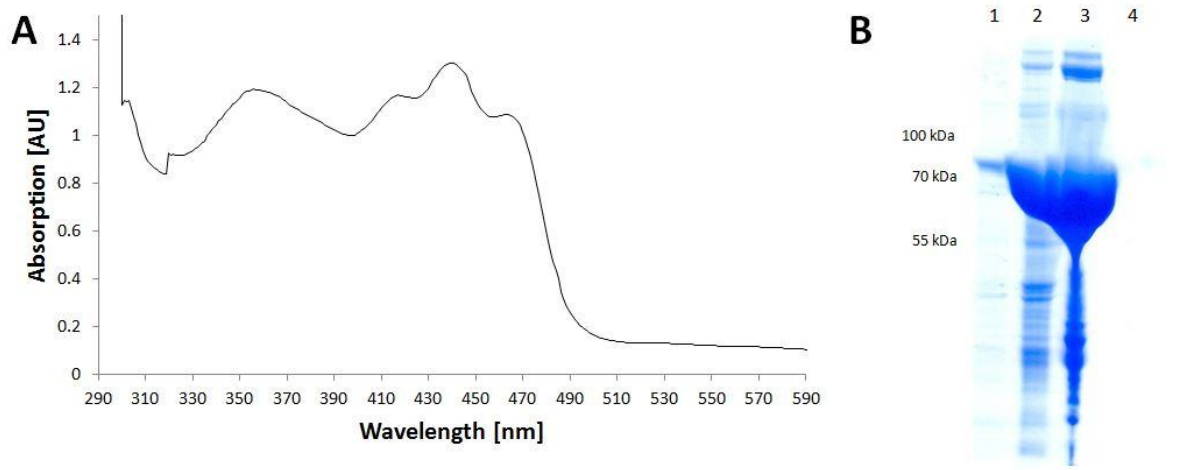

Figure 28: UV-Vis absorbance spectrum and SDS-PAGE analysis of OhyA, purified via *HisTrap 3*-protocol and gel filtration. (A) UV-Vis absorbance spectrum of the concentrated protein aliquot. (B) SDS-PAGE analysis of selected fractions of gel filtration. Lane 1: Fraction A9. Lane 2: Pooled, concentrated fractions A12-B10. Lane 3: Pooled, concentrated fractions B8-B5. Lane 4: Fraction C7.

The UV-Vis absorbance spectrum of OhyA changed essentially after gel filtration (Figure 28). The absorbance ratio 410/440 nm decreased, whilst an additional peak at approx. 360 nm, as well as a shoulder at approx. 465 nm emerged. SDS-PAGE verified elution of monomeric OhyA in the supposed fraction and removal of impurities from the target protein aliquot.

Subsequently, an UV-Vis absorbance spectral analysis was performed with the OhyA aliquot purified via the *TALON*-protocol (Figure 29).

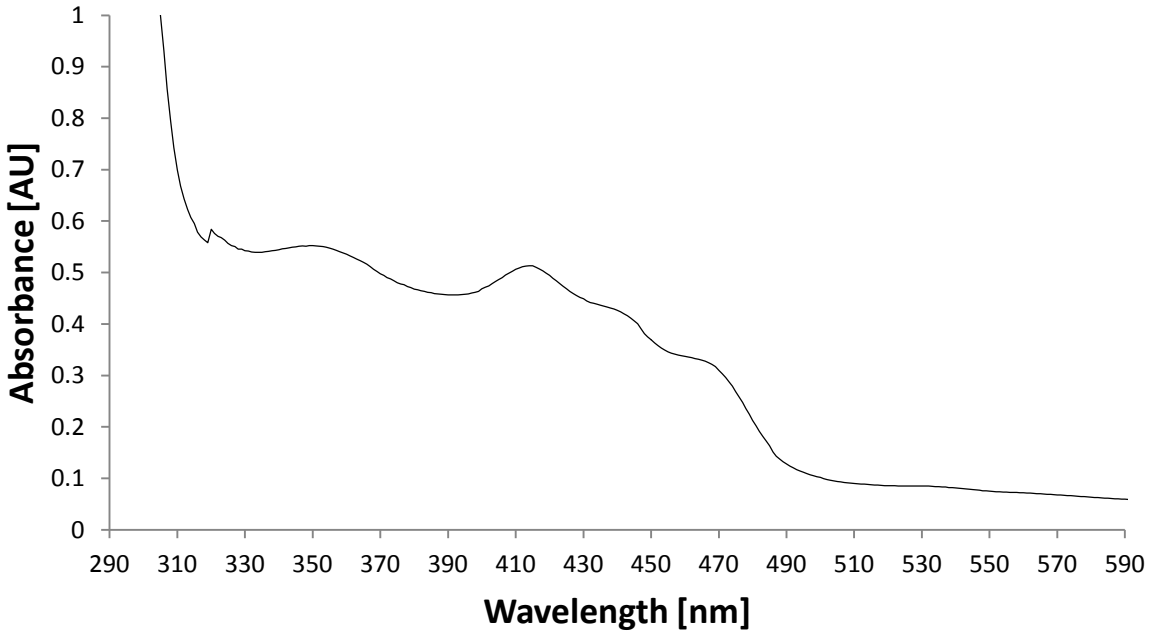

Figure 29: UV-Vis absorbance spectrum of concentrated OhyA after purification with the *TALON*-protocol.

The absorbance spectrum differed from the spectrum obtained after purification via the *HisTrap 3*-protocol (Figure 29). Residual peaks at 440 nm and 465 nm were more distinct, and the peak in the short wavelength range at approx. 360 nm could be spotted. Since the structure absorbing at 410 nm was still most predominant, the protein was further purified by gel filtration (Figure 30).

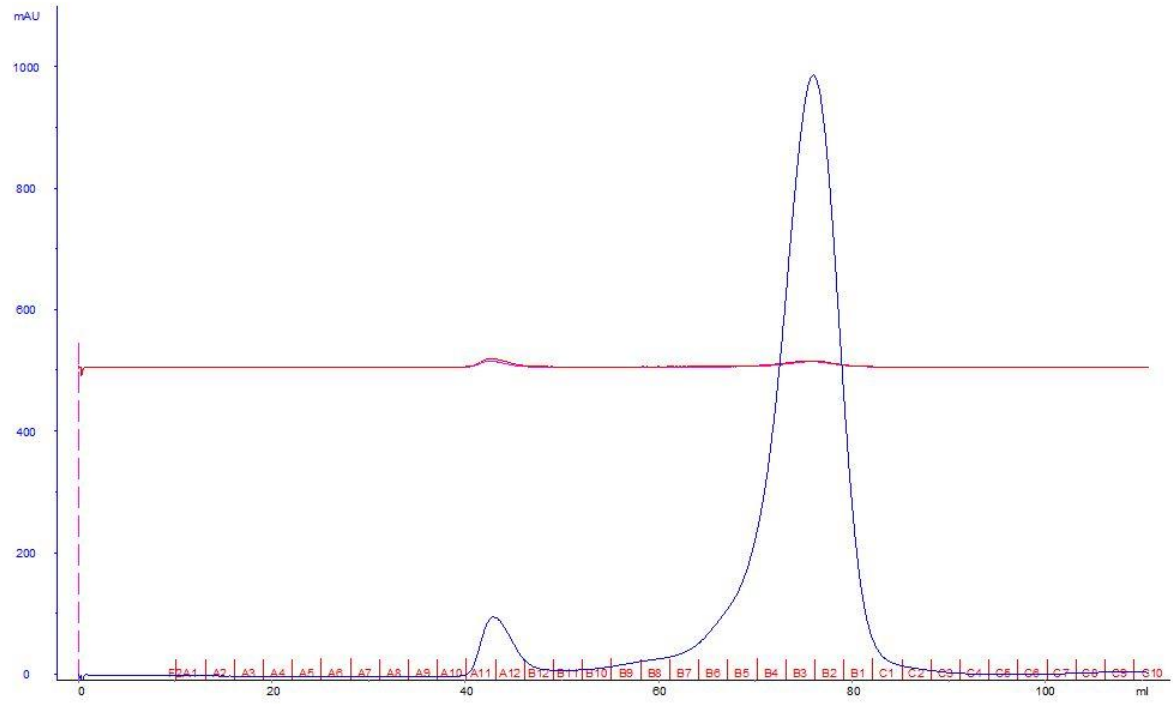

Figure 30: Chromatogram of gel filtration of OhyA, previously purified via *TALON*-protocol. Blue line: Absorbance at 280 nm. Red line: Absorbance at 410 nm. Pink line: Absorbance at 440 nm.

Only two peaks with maxima at approx. 42 mL and approx. 76 mL were identified in the gel filtration chromatogram of the protein aliquot purified via *TALON*-protocol (Figure 30). Fractions from the peak eluting at the size of monomeric OhyA were pooled and concentrated for analysis via UV-Vis absorbance spectroscopy (Figure 31).

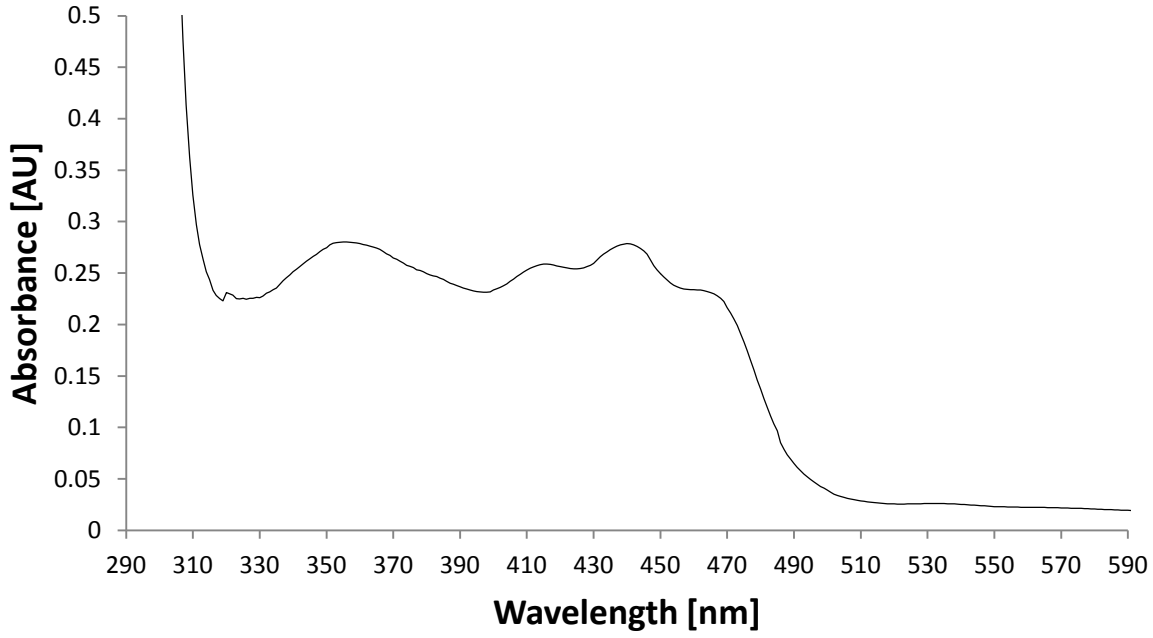

Figure 31: UV-Vis absorbance spectrum of concentrated OhyA, purified via *TALON*-protocol and gel filtration.

Gel filtration of OhyA purified via *TALON*-protocol led to a decrease of the absorbance ratio 410/440 nm, although not as extensively as detected for the aliquot purified via *HisTrap 3*-protocol (Figure 31). Considering the peaks at 360 nm, 410 nm, 440 nm and 465 nm, UV-Vis absorbance spectra of OhyA resembled each other mostly after gel filtration, independent from the IMAC column used in the first purification step. Characteristic absorbance maxima at approx. 360 nm and 440 nm, together with the shoulder at 465 nm and the extra peak at 410 nm underscored, that OhyA was a flavoprotein. OhyA is a protein composed of 646 amino acid residues and has a calculated molecular weight of 73.5 kDa for the monomer. A canonical nucleotide binding motif ($GXGXXGX_{21}E$) was identified by similarity[21]. The protein solution was yellow after His_6-tag purification and the color was retained even after gel filtration. The computed extinction coefficient ε_{280} is 94,115 M^{-1} cm^{-1} according to ProtParam, which allowed determination of the protein concentration based on the A_{280} value of purified protein solutions. Subsequent calculation of protein and flavin concentrations based on the extinction at 280 nm (17.10 AU for OhyA and 0.56 AU for FAD) suggested, that the protein was not saturated with the flavin cofactor despite the yellow color assuming a ratio of 1:1 for FAD/OhyA.

For deflavination experiments with purified OhyA, the protein was partially unfolded with urea and KBr either after immobilization on a HisTrap FF crude chromatography column or during dialysis. On-column removal of the flavin cofactor was not found to be a favorable method for elimination of the flavin because of ineffective binding to the column. Apoprotein was prepared by dialysis (Table 5). UV-Vis spectral analyses of protein aliquots prior to and after dialysis were carried out to evaluate deflavination efficiency (Figure 32).

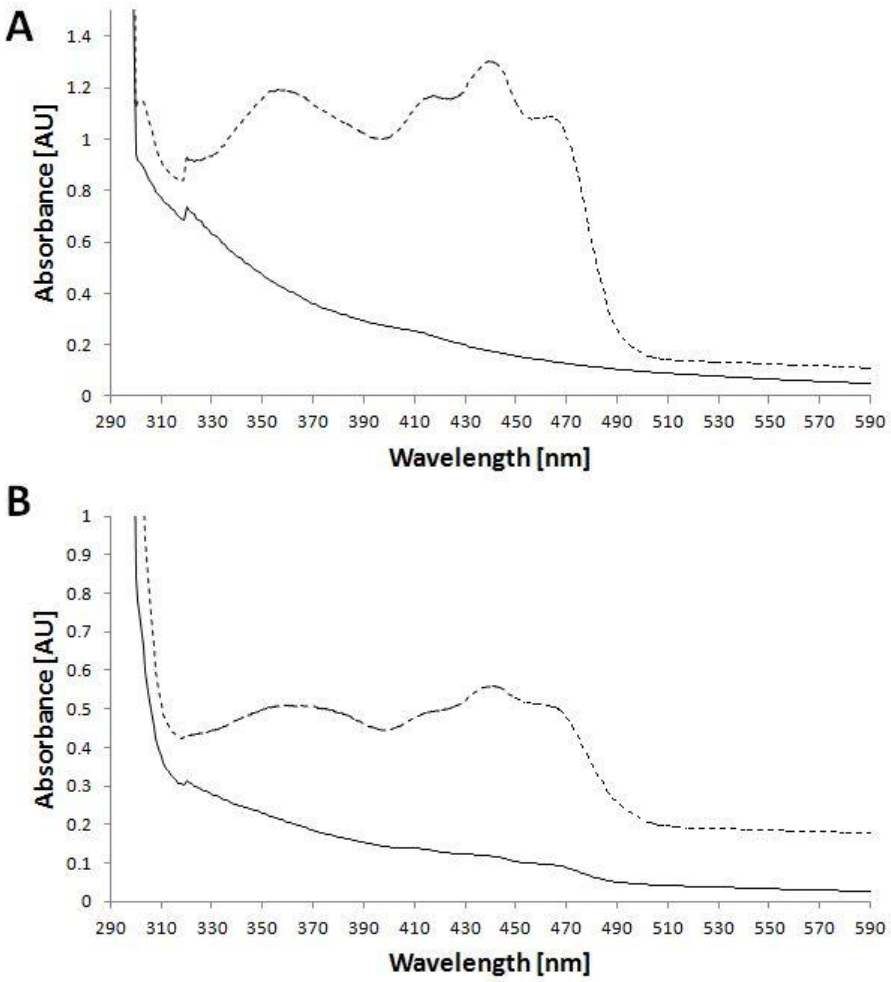

Figure 32: UV-Vis absorbance spectra of OhyA before (dashed line) and after dialysis (solid line) under two different conditions. (A) Deflavination with Dialysis Buffer 1. (B) Deflavination with Dialysis Buffer 2.

Spectral properties of OhyA changed remarkably after dialysis under both tested conditions (Figure 32). Only one clear peak with a maximum at 280 nm remained, whereas almost the entire flavoprotein-like absorbance was eliminated. After application of Dialysis Buffer 1 only minimal residual absorbance at 410 nm remained, while with Dialysis Buffer 2, additional weak absorbances at 440 nm and 465 nm were detected. Effective preparation of apo-OhyA could also be evaluated visually by comparison of concentrated OhyA solutions before and after treatment, as evident from the loss of the characteristic yellow color (Figure 33).

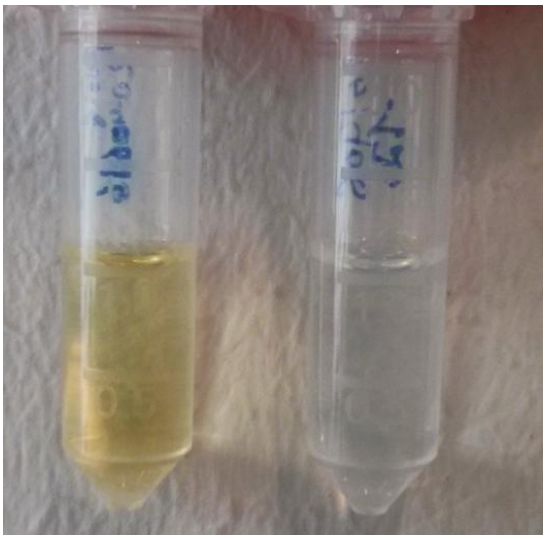

Figure 33: Concentrated OhyA solutions before (left) and after (right) dialysis. Decoloration proved successful deflavination.

Protein fold and secondary structure of OhyA before and after dialysis were analyzed using far-UV CD spectroscopy. For CD measurements, protein aliquots from both deflavination experiments were used (Figure 34).

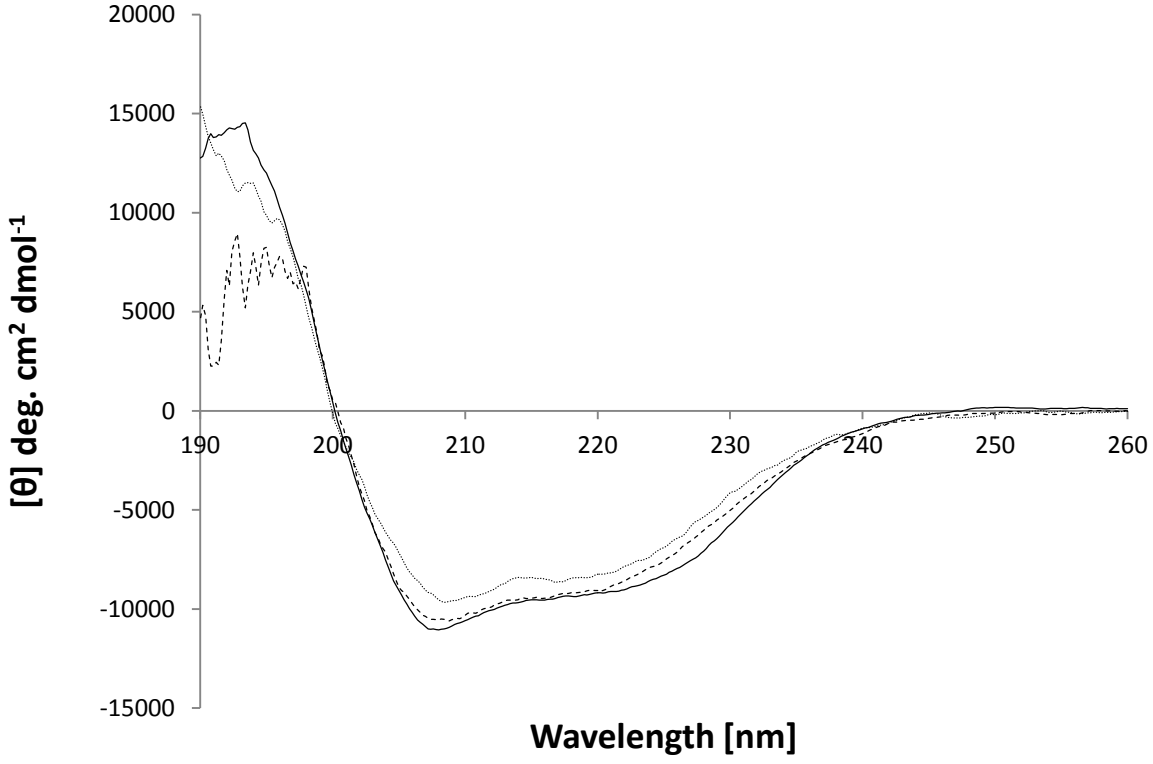

Figure 34: Far-UV CD spectral analysis of OhyA before dialysis and apo-OhyA. Solid line: OhyA before dialysis. Dashed line: Apo-OhyA prepared with Dialysis Buffer 1. Dotted line: Apo-OhyA prepared with Dialysis Buffer 2.

The obtained spectra were typical of folded proteins with a clear α-helix fingerprint with minima at 208 nm and 222 nm and indication of β-sheet fold due to the negative band at 218

nm (Figure 34)[22]. Unstructured curves between 190 nm and 200 nm were the result of strong absorbance of Cl^- ions in the buffer. On the basis of CD spectra, OhyA was an α+β fold protein. Moreover, from the CD spectra it could be concluded that cofactor removal did cause a certain, yet insignificant rearrangement of secondary structure elements.

To elucidate the nature of the interaction between OhyA and the flavin cofactor and to characterize thermodynamic parameters for ligand binding, ITC measurements were conducted by titration of free FAD to the apoprotein aliquots prepared by dialysis (Figure 35).

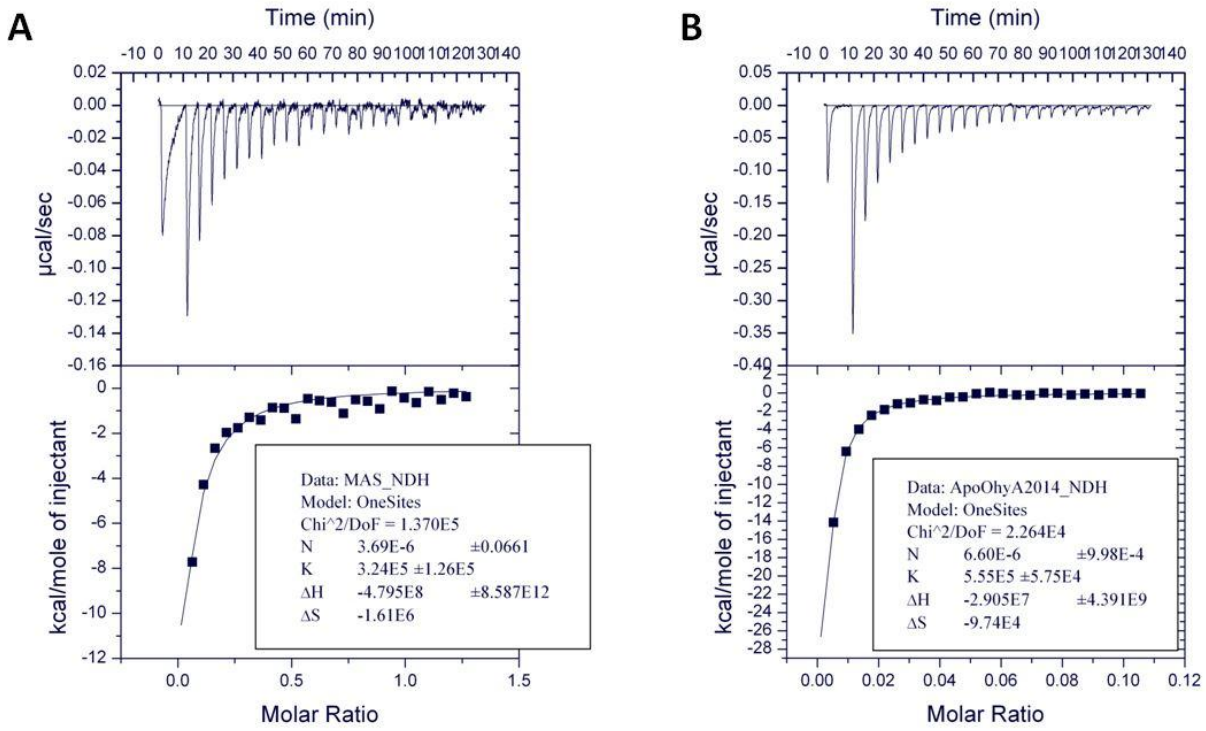

Figure 35: ITC-measurements of FAD binding to apo-OhyA. (A) Binding of FAD to apo-OhyA prepared with Dialysis Buffer 1. (B) Binding of FAD to apo-OhyA prepared with Dialysis Buffer 2. The upper panels show the raw ITC data for injecting FAD into the cell containing apo-OhyA at 25°C. The lower panels show normalized ITC data for titrations plotted against molar ratio of FAD/apo-OhyA and thermodynamic parameters derived thereof. The solid lines through the datasets represent the best fit of the data.

ITC data showed, that no realistic molar binding ratio of FAD/apo-OhyA were detected (Figure 35). Most probably, binding ratios of did unlikely reflect true conditions in solution since only a small percentage of OhyA could rebind the cofactor in the experimental set up. However, even if not ideal for immaculate characterization of the interaction between the flavin cofactor and its binding partner, the results still unambiguously revealed a beneficial interaction between the FAD cofactor and OhyA. This was demonstrated by the decrease in heat generation when approaching saturation, and by the negative values for the enthalpy

change ΔH. The values of the association constant K_a = 3.24E+05 ± 1.26E+05 M and K_a = 5.55E+05 ± 5.75E+04 M, respectively, allowed determination of a reliable K_d value in the range of 1.8 µM to 3.1 µM for FAD binding.

Enzyme activity for conversion of OA by isolated OhyA was assayed *in vitro* at pH 6.0 and standard conditions with 2 mM substrate and 0.05 mg mL^{-1} of purified enzyme. Activities were determined for OhyA and apoenzyme, both with and without incubation with a molar excess of free FAD prior to the reaction (Figure 36).

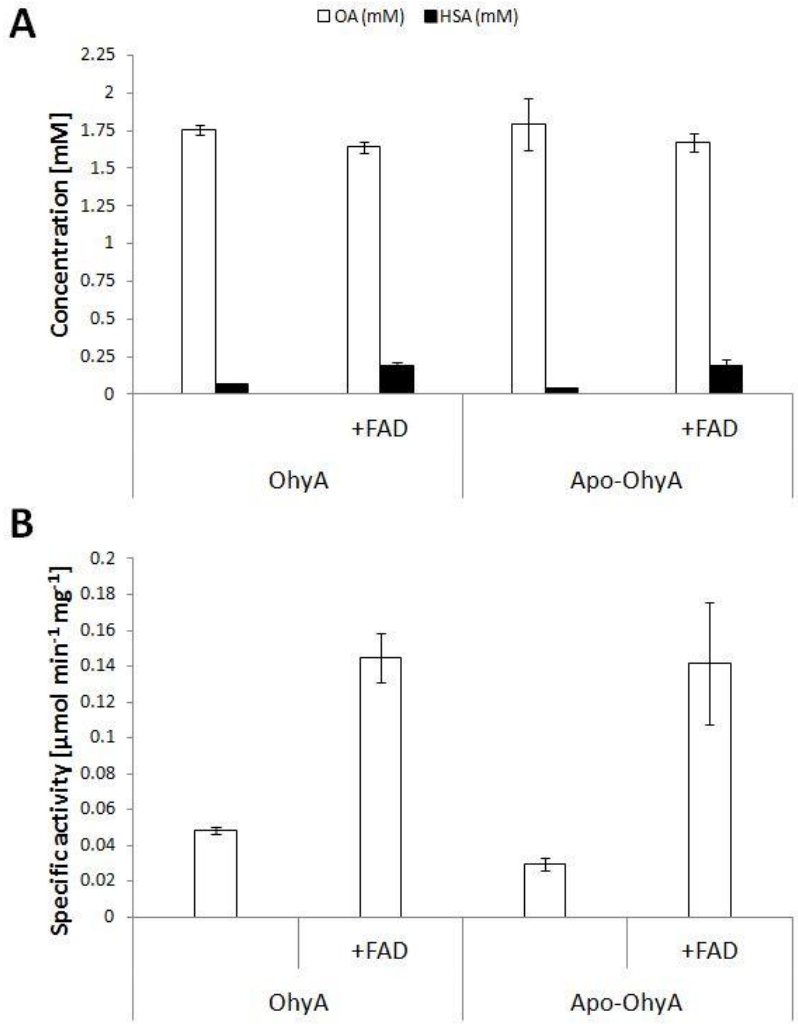

Figure 36: Effect of FAD-excess on the activity of OhyA during *in vitro* conversion of OA to 10-HSA and specific activities thereof. (A) Yield of free fatty acids using internal standards for quantitation. Substrate concentration was 2 mM and enzyme concentration was 0.05 mg mL^{-1}. Reactions were carried out at pH 6.0 and the standard conditions described in the text. (B) Specific activities of purified OhyA. Mean values and ranges of two individual experiments are given.

All enzyme preparations tested hydroxylated the cis-9 double bond of OA to produce 10-HSA (Figure 36). Although the 10-HSA titer was higher with OhyA than with the apoprotein,

addition of FAD resulted in enhanced product formation for both under the standard reaction conditions. Enzyme activities of FAD-loaded proteins could only be calculated with a certain error due to flavin absorbance at 280 nm, which resulted in overestimation of protein amounts and, thus, underestimation of the enzyme activities. Nevertheless, it was judged that the influence did not highly falsify the data, but still should be kept in mind. Specific activities of OhyA and apo-OhyA were 0.048 ± 0.002 µmol min^{-1} mg^{-1} and 0.029 ± 0.003 µmol min^{-1} mg^{-1}. Incubation of the enzyme with FAD prior to the reaction resulted in specific activities of 0.144 ± 0.013 µmol min^{-1} mg^{-1} and 0.141 ± 0.034 µmol min^{-1} mg^{-1}, implying at least a 3-fold increase due to addition of the cofactor. Compared with *in vitro* reactions carried out with CFEs, specific activities of isolated enzyme preparations were approx. one order of magnitude lower even after incubation with the cofactor, presumably because of the treatment during deflavination.

6.5 Strategies for implementation of a HTS assay for identification of oleate hydratase mutants with improved characteristics

A growth assay was considered for the development of a HTS of oleate hydratase mutant libraries for variants with improved characteristics. Two bacterial species with fundamentally different biochemical properties were evaluated regarding their sensitivity to OA. Therefore, the viability of *E. coli* and *B. subtilis* in liquid media supplied with OA was quantified. Growth of *E. coli* BL21Star™ (DE3) [pMS470-HISTEV] on a high OA concentration was recorded in LB-medium supplied with 30 mM OA in 1% Triton X-100, and a control medium. A_{600} values were recorded between 300 min and 475 min after inoculating the cultures to an A_{600} of 0.01 (Figure 37).

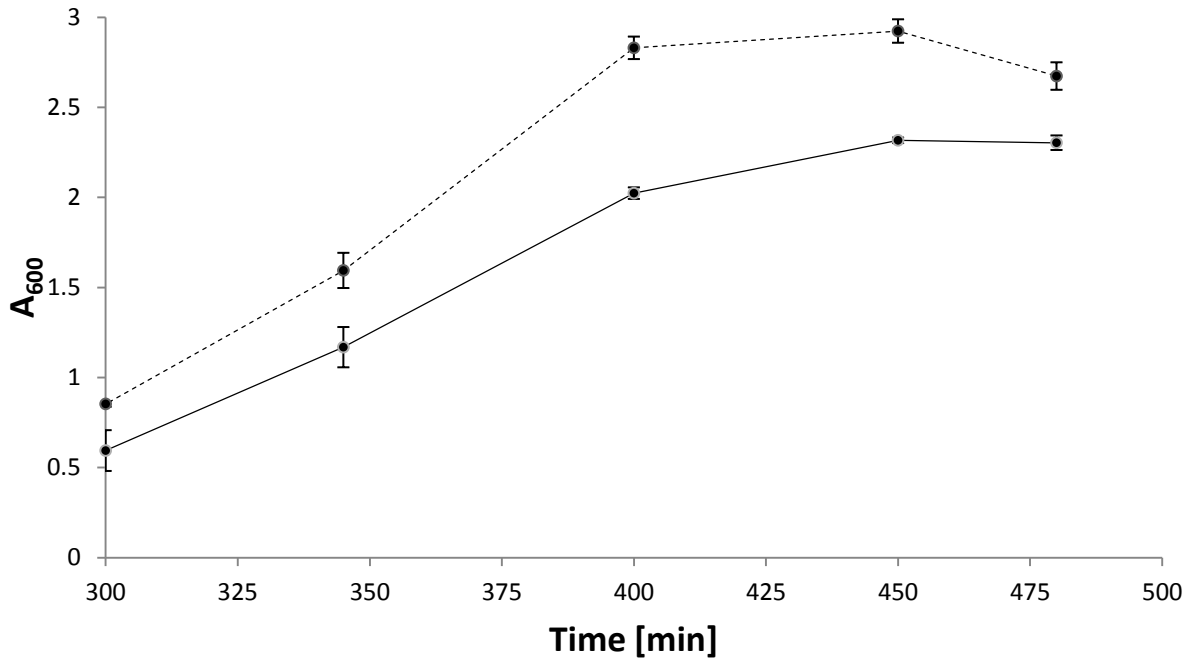

Figure 37: Effect of OA on the growth of *E. coli* BL21Star™ (DE3) [pMS470-HISTEV] in liquid medium. Solid line: LB-medium supplied with 30 mM OA and 1% Triton X-100. Dashed line: LB-medium supplied with 1% Triton X-100. Bacteria were incubated at 37°C, samples were taken at respective time points and A_{600} was measured. Mean values and standard deviations of biological triplicates are given.

The effect of OA on bacterial growth was determined in the exponential and early stationary phase (Figure 37). *E. coli* BL21Star™ (DE3) [pMS470-HISTEV] cultivated in medium with OA grew worse than the control strain over the entire time span. Despite entering the stationary phase almost concurrently, lower cell densities were obtained with the strain in medium supplemented with OA. Growth differences between *E. coli* BL21Star™ (DE3) [pMS470-HISTEV] in medium with OA and the control medium were significant. Nonetheless, discrimination between both cultures based on sensitivity to OA was not regarded as good enough for the conditions in a robust HTS system.

The inhibitory effect of OA on *B. subtilis* was determined for free unsaturated fatty acid concentrations ranging from 0 mM to 5 mM in a 96 well plate format. Cell densities were assessed 0 min, 80 min, 165 min and 300 min after inoculation of bacteria in media supplemented with OA (Figure 38).

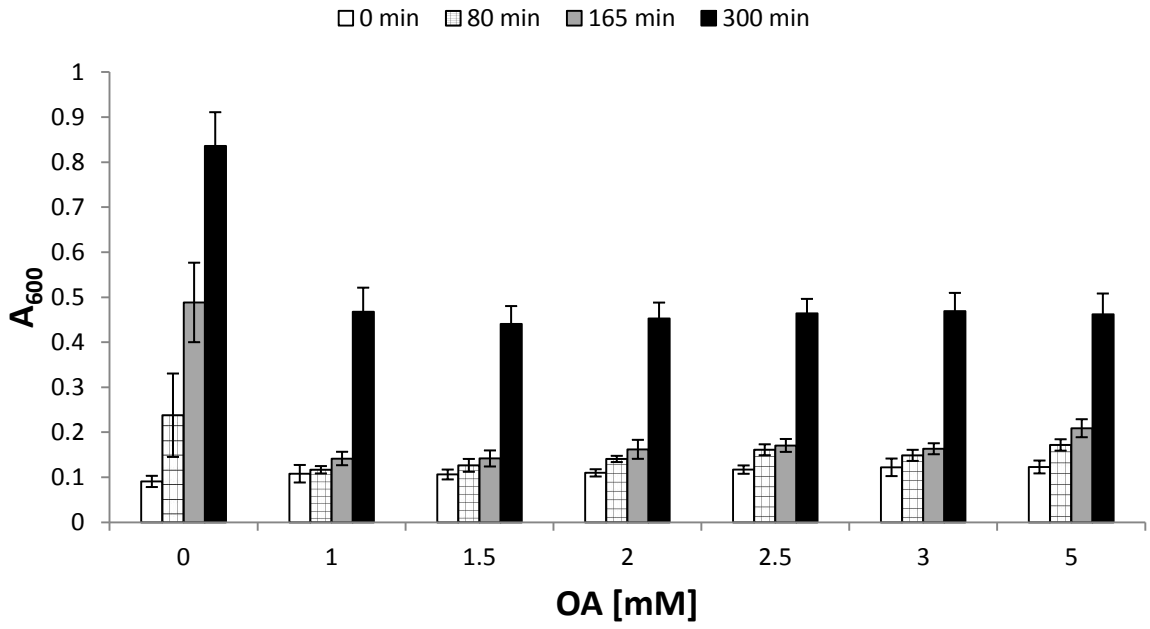

Figure 38: Effect of OA on the growth of *B. subtilis* in liquid medium. Bacteria were incubated at 37°C in 96 well plates supplied with media containing different concentrations of OA. Samples were taken at respective time points and A_{600} was measured. Mean values and standard deviations of 12 individual experiments are given.

At time points 80 min, 165 min and 300 min, considerably higher A_{600} values were measured in medium lacking OA compared to the other tested conditions, indicating a clear inhibitory effect of OA on the growth of *B. subtilis* (Figure 38). No increase of sensitivity at higher OA concentrations could be derived from the collected data. Since the A_{600} values of bacteria incubated in the presence of OA were, on average, 3-fold and 1.8-fold lower after 165 min and 300 min, respectively than under the control conditions, sensitivity of *B. subtilis* was a promising feature for application in a robust HTS system relying on growth deficiency for identification of oleate hydratase mutants with improved characteristics, e.g. turnover of OA.

In vivo production of 10-HSA with recombinant *E. coli* expressing OhyA was performed to evaluate the effect of OA conversion to abrogate the growth defect of *B. subtilis* on OA. A resting cells assay was conducted with *E. coli* BL21Star™ (DE3) [pMS470-HISTEV-OhyA] and a respective EVC handled equally during all working steps. Biotransformation was initiated by addition of 10 mM of OA to approx. 5 g L^{-1} resting cells. After incubation for 45 min at 37°C and 320 rpm, the reactions were stopped and free fatty acids were extracted from the supernatants, as well as washing fractions and cell pellets. The fatty acid content in all fractions was quantified via GC-MS (Figure 39).

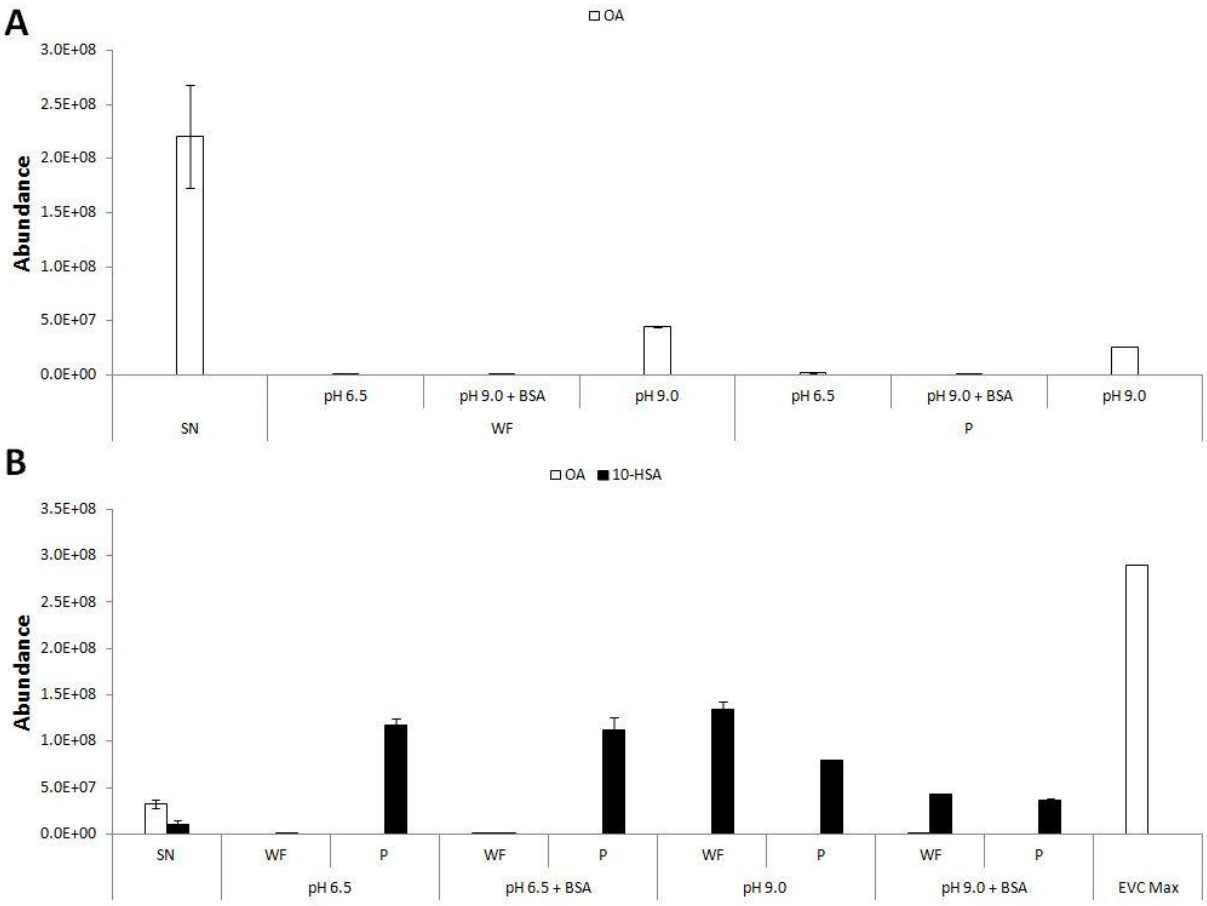

Figure 39: *In vivo* conversion of OA to 10-HSA by whole cells of recombinant *E. coli* BL21Star™ (DE3). Free fatty acid content in supernatants, washing fractions after treatment of cell pellets with solutions of different pH values and cell pellet fractions after biotransformation was quantitated via GC-MS. (A) Analysis of fractions obtained after conversion with EVC strain. (B) Analysis of fractions obtained after conversion with *E. coli* BL21Star™ (DE3) [pMS470-HISTEV-OhyA]. SN: Supernatant. WF: Washing fraction. P: Cell pellet. EVC Max: Maximum OA extracted from EVC fractions to estimate the total substrate applied.

Biotransformation of OA with the EVC strain did not result in production of 10-HSA (Figure 39). Moreover, OA was predominantly found in the supernatant after analysis of the fractions. Washing of cell pellets with solutions of pH 6.5, as well as pH 9.0 upon addition of fatty acid free BSA had no positive effect on the release of OA from cell-associated fractions. However, after treatment of cell pellets at pH 9.0 without fatty acid free BSA, substantial levels of substrate were liberated. To estimate the abundance of total substrate added for the bioconversions, maximum OA extracted after conversion with the EVC strain was used. This value was calculated by summing up the OA titer in the supernatant and cell-associated fractions after washing with the pH 9.0 solution. Evaluation of the supernatants after biotransformation with *E. coli* BL21Star™ (DE3) [pMS470-HISTEV-OhyA] only resulted in a low free fatty acid titer compared with the total substrate added. It was suspected that considerable amounts of fatty acids were cell-associated. For detection and quantitation of these fatty acids, cell pellets were washed at pH 6.5 and pH 9.0, both with and without

supplementation of fatty acid free BSA. Application of the washing solutions of pH 6.5 did not clearly improve the titer of fatty acids in the soluble fraction and they mainly remained associated with the pellets. In contrast, washing at pH 9.0 considerably increased the titer of 10-HSA in the soluble fraction. The effect was larger by washing without addition of fatty acid free BSA. Although utilization of the washing step successfully released fatty acids from the cell-associated fraction, the collective fatty acid titer in the supernatant, washing- and pellet fractions was distinctly lower than the total substrate added for all probes except for washing with the solution of pH 9.0. Interestingly, almost no OA was liberated from the cell-associated fraction due to application of any washing solution.

Summarizing, biotransformation of OA with recombinant *E. coli* expressing OhyA was easily realized. Only low titers of free fatty acids were released into the culture supernatant, whereas large quantities remained associated to the cells. Shifting the pH value from pH 6.5 to pH 9.0 effectively released 10-HSA, but not OA, into the soluble fraction.

7 Discussion

7.1 Development of an *in vitro* assay for detection of oleate hydratase activity

A GC-MS method for free fatty acid analysis was established for identification of OA and 10-HSA. Using reference compounds, unambiguous identification of the fatty acids by means of mass fragmentation patterns was accomplished. Analysis was conducted either manually by comparison of the defined cleavage products of fatty acid methyl esters, or via the NIST 08 Mass Spectral Library. For development of an *in vitro* assay method for detection of oleate hydratase activity, we referred to a protocol described by Joo et al. (2012)[7]. During assay development, the reported method was modified and optimized for our specific task. To ensure a homogeneous application of substrate in different reactions, OA was initially dissolved in ethanol (96%, v/v). OA (in ethanol) was diluted with 50 mM potassium phosphate to the desired final concentration right in the reaction vessel due to its low solubility in the ng mL^{-1} range in aqueous solution[23]. The standard *in vitro* activity assay was tested by enzymatic conversion of OA to 10-HSA using OhyA- and EVC-CFEs, respectively (Figure 5). GC-MS analysis proved hydroxylation of OA catalyzed by OhyA-CFE but not by EVC-CFE which showed applicability of the *in vitro* assay for detection of enzymatic hydration activity even in complex samples. However, several obstacles prevented quantification of the assay and, therefore, hindered determination of oleate hydratase activity with the original protocol. Even after numerous modifications, immense variations in substrate and total fatty acid titers were repeatedly observed after evaluation of the GC-MS results. Considering that preparation and addition of substrate, as well as the assay procedure itself were highly standardized in the course of assay development, it was regarded implausible that inconsistent outcomes were the result of inadequate assay handling. Preparation of the samples for GC-MS analysis after the *in vitro* assay was an additional origin for variations in the observed fatty acid titers. Especially, it had to be taken into account that it was required to extract and derivatize the prior to injection onto the chromatography column. Additionally, losses on surfaces of reaction tubes, evaporation of solvent or transfer errors added up to the expected systematic errors. To compensate for these sources of errors, internal standards were added to the substrate prior to enzymatic reactions. On the basis of their similar physical (e.g. molecular weight) and chemical (e.g. molecular structure, functional groups, polarity) characteristics to the compounds of interest, as well as their commercial availability, n-Pentadecanoic acid and 16-Hydroxypalmitic acid were selected as reference compounds for quantification of OA and 10-HSA, respectively. Internal

standard calibration plots were generated and n-Pentadecanoic acid and 16-Hydroxypalmitic acid could be unequivocally identified by analysis of mass fragmentation patterns. Subsequent *in vitro* conversion of OA using OhyA-CFE showed that application of internal standards compensated systematic errors and led to consistent results (Figure 10).

7.2 Expression of oleate hydratases in *E. coli*

After cloning and validation of correctly ligated inserts into the two His_6-tagging vectors, codon optimized oleate hydratase genes were heterologously expressed in *E. coli* BL21Star™ (DE3). Determination of CWWs of harvested strains after recombinant protein production revealed a consistently better growth of bacteria during expression from the pMS470-HISTEV vector system. Thus, this expression vector was more suitable for overexpression of oleate hydratases than pEHISTEV under the applied conditions. Since all cultures were handled equally during cultivation, the different features of both vectors, especially antibiotic selection mechanism and plasmid copy number, might be reasons for the notable differences in biomass. Furthermore, growth was affected strongest for the strains expressing heterologous protein, whereas growth of the EVC strains was only slightly impaired. Initially, the strains were cultivated at 28°C during expression of target proteins, but SDS-PAGE analysis of isolated CFEs showed, that only Oah and Cgh were sufficiently overexpressed as soluble proteins. The other oleate hydratases were only found in total lysates, hinting at formation of inclusion bodies, or in the worst cases, no protein was overexpressed at all (data not shown). To optimize expression, the cultivation temperature during IPTG induction of the pMS470-HISTEV vector system was therefore reduced to 20°C, which yielded recombinant protein in the soluble fraction of each strain as assessed via SDS-PAGE (Figure 12).

First purification attempts of His_6-tagged protein were carried out with gravity-flow purification using self-packed Ni-NTA affinity chromatography columns to find favorable conditions and buffer concentrations for isolation of the target proteins. Multiple washing steps using buffers containing 20 mM and 30 mM imidazole led to good purity of oleate hydratases, but simultaneously a substantial loss of overexpressed protein in the flow through and washing fractions was observed (Figure 13, Figure 14, Figure 15 and Figure 16). Many factors lead to poor binding of His_6-tagged protein to a column matrix, but insufficient binding capacity was most obvious in this case. The applied 1 mL columns had a dynamic binding capacity of approx. 40 mg and loading approx. 20 mL of the cell extract very likely overloaded the column matrix. After purification, all heterologously expressed proteins appeared to be yellow, and the color intensity roughly correlated with protein concentrations.

This finding indicated the presence of a flavin cofactor associated with all proteins, which was in agreement with previous identification of FAD dependent MCRA proteins from microbial origin[7,8,14].

7.3 Determination of oleate hydratase activity and characterization of reaction conditions of OhyA and Oah

Functional expression of all enzymes could be confirmed *in vitro* using purified samples (Figure 18). Since quantification was not accomplished up to that point, huge variations in total fatty acid concentrations and large error bars were noticed after evaluation of all probes. Thus, quantification of generated 10-HSA as well as enzyme activities could only be done, if feasible at all, very cautiously on the basis of this data. According to the *in vitro* assay results, conversions with purified OhyA yielded by far the highest amounts of 10-HSA, followed by Mch, Moh, Cgh, Oah, Bbh, Sah, Cah and Ckh. For reliable quantification of oleate hydratase reactions, *in vitro* reactions with internal standards and freshly prepared CFEs were performed (Figure 19). Therein, increased enzyme concentrations gave higher titers of product, but there was no linear correlation. This was possibly caused by measurement of reaction rates near substrate saturation and further addition of enzyme only slightly enhanced product formation. For reactions with Bbh and Ckh, no relevant 10-HSA titers were detected, quite contrary to earlier evidence for functional expression of all oleate hydratases. Again, improper reaction conditions might have led to the observed lack of activity if the substrate concentration of 0.15 mM was well below the K_M value of both Bbh and Cah. Unfortunately, information about kinetic parameters of the oleate hydratase reaction is scarce in literature, which makes estimations difficult. Overall, it is worth noting that for detection of enzyme activity under suitable conditions, substrate and enzyme concentrations still had to be optimized. However, since optimization for all 9 enzymes was considerably laborious, it was refrained from doing so for each protein. Enzyme activities displayed in the *in vitro* assay were characterized in CFEs for five of the enzymes that produced the largest levels of 10-HSA (Figure 20). The highest specific activity was noted for OhyA CFE (1.16 µmol min^{-1} mg^{-1}), followed by Oah (0.56 µmol min^{-1} mg^{-1}), Sah (0.32 µmol min^{-1} mg^{-1}), Cgh (0.23 µmol min^{-1} mg^{-1}) and Mch CFE (0.11 µmol min^{-1} mg^{-1}). The stated specific activities can, however, only be reckoned for the specified reaction conditions, while for accurate determination of maximal specific activities, additional characterization of reaction conditions was necessary. For OhyA, Oah, Sah and Cgh, these were the first detailed reports on enzymatic activities, whereas the specific activity of the conversion of OA by Mch and the oleate hydratases from *Stenotrophomonas maltophilia* and *Lysinibacillus fusiformis* had been reported

previously[7,10,11]. Specific activities were determined to be approx. 3.3 µmol min^{-1} mg^{-1}, 3.7 µmol min^{-1} mg^{1} and 1,580 µmol min^{-1} mg^{-1}, respectively, for Mch and the fatty acid hydratases from *S. maltophilia* and *L. fusiformis*, *in vitro* after protein purification. Reaction conditions were 25°C and pH 6.5 for Mch, 35°C and pH 6.5 for the *S. maltophilia* enzyme and 35°C and pH 6.5 for the oleate hydratase from *L. fusiformis*. The reported values were considerably higher than the ones obtained for the enzymes analyzed in this work. However, taking into account that activities were determined for the CFE, higher values are to be expected if referred only to the target proteins.

Reaction conditions were characterized only for OhyA and Oah because of the aforementioned work-intensive procedure. Maximum hydration of OA was observed at 25°C, pH 6.0, and 20°C to 25°C, pH 6.5, for OhyA and Oah, respectively (Figure 21). The maximum activities were comparable to reported values of other oleate hydratases. The reaction optimum for Mch was 25°C and pH 6.5 in 2% (v/v) ethanol[7]. Temperature and pH optima for the oleate hydratase from *L. fusiformis* were 35°C and pH 6.5[10]. For the *S. pyogenes* fatty acid hydratase, kinetic parameters were determined at 37°C and pH 6.1 upon addition of 2% (v/v) ethanol[14], and the enzymatic conversion of OA with Bbh was conducted at 25°C and pH 7.5. However, there was no explicit reference to those reaction conditions as optimal[8]. The hydration of OA by OhyA was briefly addressed by Bevers et al. in 2009[6], but only the influence of pH was recorded, and the pH optimum was at pH 6.0, which was in full accordance with the finding in this work. In general, pH optima of all studied enzymes so far were between pH 6.0 and pH 6.5, whereas temperature optima were more divergent, suggesting a higher variance in temperature- than pH-tolerance among different oleate hydratases.

7.4 Biochemical analysis of OhyA

Cell growth and recombinant protein production in *E. coli* BL21Star™ (DE3) [pMS470-HISTEV-OhyA] could be successfully optimized by incubation of the strain in AIM instead of TB-medium requiring IPTG induction. Use of AIM furthermore allowed convenient recombinant protein production without the need to monitor cell densities and add inducer. Evaluation of the protocols tested for purification of OhyA showed, that a step gradient was more suitable than a continuous gradient. An acceptable compromise between yield and purity of target protein was accomplished by removal of other proteins from the column with 25 mM imidazole (Figure 22, Figure 23, Figure 24 and Figure 25). Application of the *TALON*-protocol increased the purity of OhyA, whereas the yield was apparently not affected.

The superiority of the TALON column was somewhat surprising since only the bivalent metal ion was exchanged, although the underlying principle of both methods was the same. Repeatedly, incomplete binding of OhyA to the column matrix was recognized. During gravity-flow purification, the insufficient binding capacity was held account for elution of the target protein in the washing fractions. The low binding capacity was abrogated by application of the Äkta purifier system, yet a substantial loss of OhyA could still not be prevented. This led us to speculate on a general problem with the His_6-tag, possibly caused by non-surficial localization or other steric hindrances of His_6-tag binding. Thus, it might be beneficial to increase the binding efficiency, potentially by extending the tag to 10 His residues, or by testing the effect of N- and C-terminal tagging on column binding. However, as the amount of purified OhyA was sufficient for further quantitative analyses, it was not considered an immediate priority to perform such modifications.

The UV-Vis spectrum of the protein solution changed drastically upon gel filtration compared to the His_6-tag purified enzyme with distinct peaks emerging at 360 nm, 410 nm, 440 nm and 465 nm, representing the UV-Vis absorbance spectrum of highly pure OhyA (compare Figure 26 with Figure 28 and Figure 29 with Figure 31). Upon close observation, several interesting differences in relation to the absorbance spectrum of free flavin attracted our attention. For the free cofactor, two absorbance maxima at approx. 370 nm and 450 nm are well defined whereas in OhyA, these peaks were shifted approx. 10 nm towards a lower wavelength. Furthermore, an additional peak at 410 nm, far more predominant prior to gel filtration but still distinct afterwards, and a clear shoulder at approx. 465 nm proved to be characteristic features of the UV-Vis absorbance spectrum of OhyA. Such a split-up of flavin peaks with additional shoulders is commonly observed for a variety of different flavoproteins[24–26] and even though the precise structural reasons for a particular spectrum are often inconclusive, the protein structures surrounding the cofactor can hugely influence the obtained spectrum. In OhyA, the hydrophobic substrate cavity adjacent to the isoalloxazine moiety, as well as the bended conformation of the flavin side chain might substantially affect the detected UV-Vis absorbance spectrum.

To remove the flavin cofactor from OhyA, the protein was partially unfolded either upon immobilization on a HisTrap FF crude chromatography column or during dialysis. On-column removal did not yield sufficient apoprotein. His_6-tagged OhyA bound, as noticed previously, very inefficiently to the IMAC column, which caused poor retention of the protein. Therefore, formation of apoprotein on a preparative scale was not possible with this procedure. From the

UV-Vis absorbance spectra of OhyA aliquots after deflavination via dialysis it was concluded that the samples were indeed virtually flavin free and, thus, represented the apo-form of the protein (Figure 32). Only when using Dialysis Buffer 2, negligible residual absorbances at 440 nm and 465 nm remained, but in all cases the decoloration of the protein solutions proved efficient cofactor removal (Figure 33). Far-UV CD spectroscopy was done to monitor changes in the secondary structure as a potential consequence of deflavination with partial unfolding of OhyA (Figure 34). According to CD spectroscopy, OhyA and apo-OhyA showed very similar folds apart from small differences in the detection range for α-helical folds (208 nm and 222 nm). Consequently, no indication for a highly relevant alteration of the secondary structures upon flavin removal was found. Such alterations might have resulted in a lack of catalytic activity or inability to reconstitute the protein. Even though correct assembly of higher levels of the protein structure could not be assessed with this method, results were still considered promising for upcoming titration experiments with the flavin cofactor and activity studies. ITC measurements could, however, not detect a realistic molar binding ratio of FAD/apo-OhyA monomer, since only ratios of 1:2 and even much lower (1:50) were determined in the titrations (Figure 35). This might be explained by the fact that only a small percentage of apo-OhyA was able to reincorporate the flavin under the experimental conditions, which would imply that ITC was not a favorable method for determination of binding ratios. Nonetheless, it was possible to deduce essential information on the interaction between ligand and protein from the well correlating ITC data. Binding of FAD to OhyA clearly is an exothermic reaction and the individually determined mean values for K_d (1.8 µM and 3.1 µM) correlated well. The K_d in the low µM range indicated a somewhat, yet not very tight binding of FAD to the protein. This was in good agreement with the deflavination experiments, in which 2 M urea was sufficient to remove the cofactor during dialysis over night. *In vitro* activity assays with purified enzyme aliquots were conducted to examine the effect of FAD on catalytic activity under the previously determined temperature and pH optima. Although the real concentrations of the enzyme aliquot with bound FAD was lower than the value calculated due to the absorbance of FAD at 280 nm and, thus, specific activity was underestimated for these samples, the experimental error was disregarded. The contribution of flavin to the extinction at 280 nm ($\varepsilon_{FAD,\ 280} \approx 17{,}000\ M^{-1}\ cm^{-1}$[22]) was negligible firstly because of the 10 W residues in the amino acid chain of the OhyA monomer ($\varepsilon_{W,\ 280} \approx 5{,}500\ M^{-1}\ cm^{-1}$) and secondly, because the cofactor was not completely retained after purification. Interestingly, a substantial hydroxylation activity of approx. 60% of the activity observed prior to dialysis was detected for apo-OhyA (Figure 36). Incubation of apo-

OhyA and OhyA before dialysis with FAD increased the specific activities 5-fold and 3-fold, respectively. For apo-OhyA, the enhanced specific activity could be nicely explained by partial reincorporation of the FAD cofactor, whereas the 3-fold increase for OhyA was, at first glance, peculiar. Still, since a considerable portion of the cofactor was not retained during the extensive purification process, the protein might have likely regained capability of free FAD uptake. The considerable remaining activity of apo-OhyA might result from the fact that chemical deflavination could not remove all bound FAD. However, the clearly reduced activity of apo-OhyA is good evidence that the cofactor has a structural function for protein integrity. The results of ITC measurements would support a structural role of FAD since it was observed that reconstitution of OhyA was, at least in part, implied. Literature on the role of FAD in oleate hydratases and similar enzymes is rare. The fatty acid double bond isomerase from *P. acnes*, which is structurally similar to fatty acid double bond hydratases, uses the FAD catalytically to protonate the substrate, forming a carbo-cation intermediate and re-protonate on a different C-atom[27,28]. However, transferring the mechanistic ideas of the isomerase reaction to a hydratase reaction might be far-fetched. Joo et al. (2012) biochemically characterized Mch[7]. In this study, all catalytic activity was abolished after deflavination of the enzyme upon dialysis with 3 M urea, but stop-flow kinetic analyses did not detect a change of the redox state of FAD and a structural stabilization of the protein by the flavin cofactor was concluded. Volkov et al. (2010) on the other hand demonstrated that the fatty acid double bond hydratase from *Streptococcus pyogenes* remained active as apoenzyme, even though it was 10-50 times less active than the holoenzyme[14]. Similarly, a stop-flow kinetic analysis did not detect a reduction of the FAD cofactor during the reaction. In summary, the published studies and the present work are good evidence for a structural role of FAD in fatty acid hydration.

7.5 3D structure of OhyA

Crystallization and structural analyses of OhyA were performed by the Gruber group at University of Graz. For crystallization screens, protein was isolated via His_6-tag affinity chromatography, incubated for 1 h with FAD on ice and purified by gel filtration. Diffraction patterns of yellow protein crystals were generated via X-ray crystallography, the structure was resolved and refined (Figure 40).

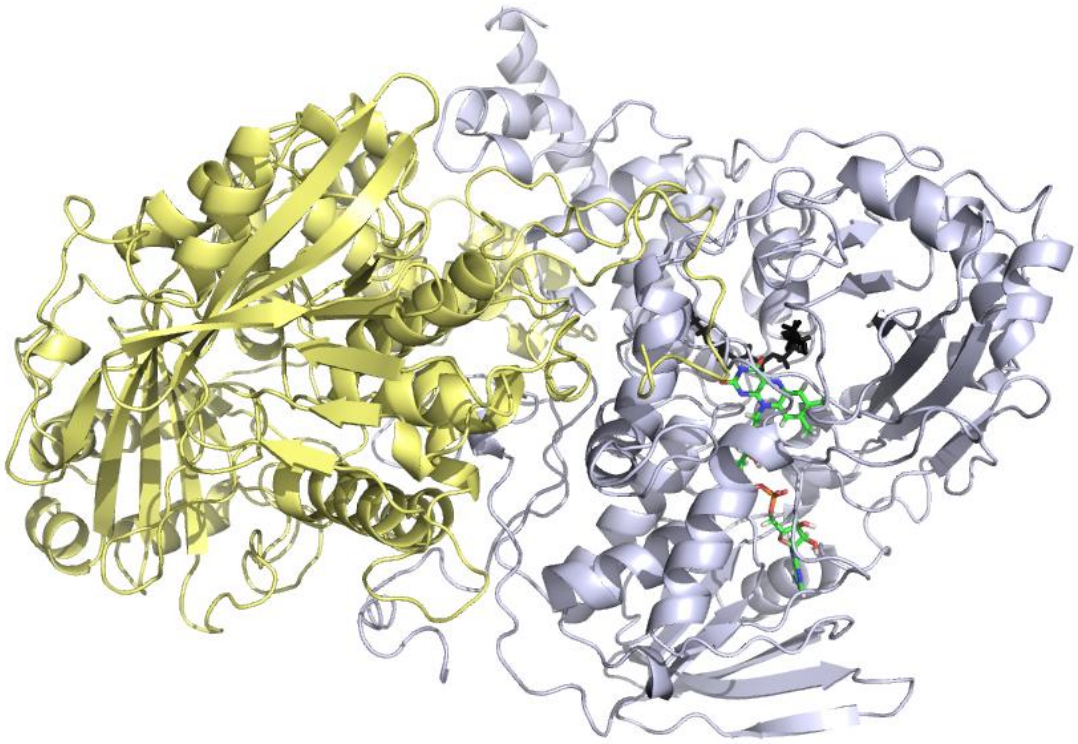

Figure 40: Structure of the OhyA Homodimer. Chain A, crystallized with the FAD cofactor, is colored in light grey and chain B is colored in yellow. The docked substrate is colored in black.

The crystal structure of OhyA was determined at a resolution of 2.34 Å. Additional information on the crystal structure is summarized in Table 9.

Table 9: Experimental details on the crystal structure determination of OhyA.

Data set	**Value**
Resolution [Å]	2.34
R-value	0.22
R-free	0.27
Space group	$P2_12_12_1$
Unit cell [Å] (a/b/c)	84.19/143.93/155.74
Unit cell [°] (α/β/γ)	90.0/90.0/90.0
Ramachandran favored [%]	92.9
Ramachandran outliers [%]	1.5

OhyA crystallized as a homodimer with two chains in the asymmetric unit. According to analysis of the 3D structure via PDBePISA, the subunits had a large surficial contact area suggesting that the interaction between the chains was not induced by crystal contacts but was presumably also retained after dissolution of the protein crystal. Both chains were crystallographically independent, but they displayed a high structural similarity at the C_α

level. Chain A crystallized with a flavin cofactor, which was identified as FAD by its electron density (Figure 41). Because of the high similarity of both OhyA protomers, it was expected to find the cofactor in both chains. Yet, a clear proof for cofactor binding could only be assigned for chain A, whereas in chain B the electron density for FAD in the analogous binding site was far less pronounced, but still sufficient to claim that each chain contained an FAD cofactor.

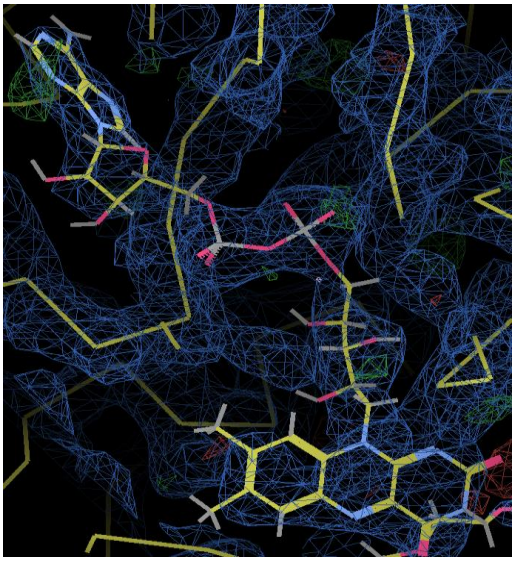

Figure 41: Electron density map of FAD and surrounding structures in chain A of the OhyA homodimer.

Comparison of biochemical analysis with the 3D structure model of OhyA showed that both were not in full accordance. Both independent studies clearly identified a non-covalently linked, oxidized flavin cofactor associated with the protein. UV-Vis absorbance spectra of OhyA cannot distinguish between FAD and FMN. However, the good affinity of FAD to its binding partner and previous findings of FAD, but not FMN, in other fatty acid hydrating enzymes suggested the presence of FAD[7–9,14]. This assumption was unconditionally verified by the electron density map during 3D structure determination (Figure 41). ITC measurements did not allow calculation of reliable molar binding ratios of FAD/apo-OhyA, but the FAD cofactor was allocated to both chains in the asymmetric unit, indicating an equimolar ratio of FAD/OhyA monomer. The ratio of FAD/OhyA in solution cannot be deduced unambiguously from the protein crystal. Although the current data indicate association of one cofactor per protomer, additional experiments would be beneficial to get supplementary evidence for this aspect of cofactor binding. For example, detection of the flavin content in the supernatant after heat denaturation of the holoenzyme can be envisioned quite easily. Furthermore, the protein was purified as a monomer after gel filtration, but the crystallization of a homodimer in the asymmetric unit suggests the stable association of OhyA

monomers in solution. It could be hypothesized that, despite dissociation due to the harsh conditions during purification, OhyA forms homodimers in solution and is biologically active as such. Nevertheless, neither biochemical analyses nor the 3D structure seem to deliver a clear solution and additional analyses would be interesting to conduct.

The predicted binding site of the flavin cofactor could be confirmed by the 3D structure, and the fatty acid substrate was docked into the binding cavity calculated via the CASoX program (Figure 42).

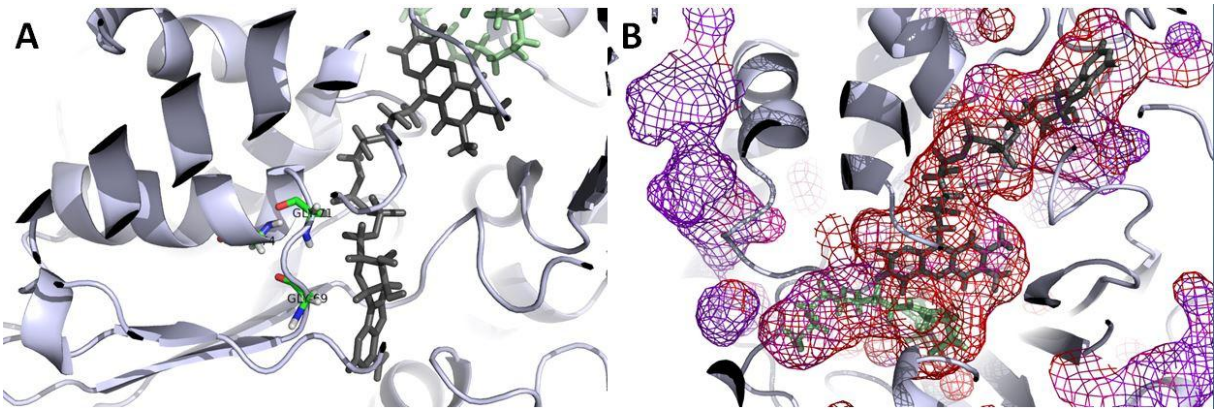

Figure 42: FAD binding site and substrate cavity in chain A of the OhyA homodimer. (A) FAD binding site. Black: Flavin cofactor. Light green: Substrate. Light grey: Protein backbone. The three characteristic glycine residues in the nucleotide binding fold are highlighted, which are essential for orientation of the protein chain for FAD binding. (B) Substrate cavity as determined via the CASoX program, indicated by the mesh around the docked substrate.

The nucleotide binding motif is part of a Rossman fold near the N-terminus of the protein chain. Whereas Rossman folds are not always involved in nucleotide binding, the sequence motif GXGXXG, where X can represent any amino acid, is usually found in those that do bind either FAD or NAD(P)[21]. The importance of the glycine residues therein is well understood: The first one (G 69) introduces a sharp turn of the main chain to adequately position the second glycine (G 71), which, for its part, makes a close contact of the main chain to the pyrophosphate moiety of FAD possible. The third glycine (G 74) on the other hand permits close packing of the α-helix with the following β-sheet[21]. Finally, a lesser conserved negatively charged residue (E 96 in OhyA) hydrogen bonds to the 2' hydroxyl group of the ribose in the adenosine moiety to non-covalently link the nucleotide cofactor to the protein. The docked substrate could be seen in close proximity to the isoalloxazine ring of FAD and a binding cavity for the fatty acid substrate was identified using the program CASoX. The cavity was almost entirely hydrophobic, except for some scattered polar residues.

The mechanism of fatty acid hydration by oleate hydratases is yet to be elucidated. The reaction itself may be considered interesting and somewhat unusual since addition of water to the non-activated double bond of a free fatty acid has to be conducted in a highly hydrophobic cavity. Nevertheless, it can be speculated about the fundamentals of a possible hydration mechanism that involves acid-base catalysis. Since the biochemical analysis of OhyA has shown that FAD is evidently not essential for the enzymatic reaction, it seems likely that polar residues might be involved in hydration of the double bond. Even though the substrate cavity is highly hydrophobic, individual charged residues are positioned near the cis-9 double bond. Notable amino acid positions are Y241, E122, Q265, H442, N438 and Y456, whereby Y241 is closest to the double bond of the substrate. Another suggestion for a residue involved in catalysis is a methionine near the cavity. In a hypothetical reaction, methionine withdraws an electron from the substrate's double bond to protonate it. In a second step, a sulfonium ion is formed by covalent binding of the substrate to the thioether group of M and finally, H_2O substitutes M and the hydroxylated fatty acid is released. However, up to that point any speculation about the mechanism of fatty acid hydration is highly vague, and detailed mutagenesis analyses have to be performed to identify residues involved in catalysis.

7.6 Strategies for implementation of a HTS assay

Generation of oleate hydratase variants with improved characteristics, such as enhanced stability or catalytic activity, and altered or extended substrate scope was considered. Because of deficiency of structural information, rational protein design was temporarily limited to OhyA and, therefore, directed evolution of other target enzymes seemed to be the method of choice. A robust, high quality screening method is the cornerstone of any random mutagenesis protein engineering approach. However, a HTS assay has to meet a variety of different criteria. The respective screens usually require adequate sensitivity, reproducibility and accuracy, as well as high throughput, robustness and, preferably, small sample volume, which makes the implementation of a HTS an even more challenging task[29]. The low solubility of the molecules of interest further increases the complexity of the specific issue in this work. Taking all these points into account, the focus here was not on establishing a definite HTS assay but, nonetheless, different principles were tested regarding their practicability in a screening method.

An *in vivo* assay for identification of oleate hydratase mutants with improved characteristics that relied on the impairing effect of OA on the growth of different bacterial species was considered. Many unsaturated free fatty acids display antibacterial activity and thus serve,

together with other lipids, as a defense mechanism against the colonization of microbes in the human skin[30,31]. While their exact mechanism of action is mostly unclear, the prime target of free unsaturated fatty acids is the bacterial cellular membrane[32]. By interacting with the cell membrane they affect processes essential for bacterial viability, for instance oxidative phosphorylation, transport across the lipid bilayer or function of membrane proteins. Other targets include nutrient uptake and inhibition of enzyme activity essential for fatty acid biosynthesis[15,33]. In general, it was shown that unsaturated free fatty acids tend to have a greater antibacterial activity than saturated free fatty acids. Medium to long chain fatty acids were more active against Gram-positive than Gram-negative bacteria. Thus, it was hypothesized previously that the hydration activity of oleate hydratases may serve as a detoxification mechanism in microorganisms harboring MCRA proteins that allow survival in free fatty acid-rich environments[14]. On that basis, the survival of one Gram-negative (*E. coli* BL21Star™ (DE3) [pMS470-HISTEV]) and one Gram-positive (*B. subtilis*) bacterium in OA rich medium was tested to subsequently evaluate the growth of a suitable organism in media after conversion of OA to 10-HSA with different oleate hydratases. OA showed antibacterial activity against *B. subtilis* and, to a much lesser extent, against *E. coli* (Figure 37). This was to some extent expected since earlier findings could detect no or only a very weak antibacterial activity of long chain unsaturated fatty acids against Gram-negative bacteria[34,35], possibly caused by the presence of a protecting lipopolysaccharide layer in these species[36]. As a consequence, *E. coli* was ruled out for application in a growth assay. For *B. subtilis*, a severe growth deficiency was determined with 1-5 mM OA in liquid medium, confirming the reported notably higher sensitivity of Gram-positive organisms (Figure 38). The bacterium therefore qualified for further consideration.

For the production of 10-HSA in a HTS system, whole cell biocatalysis seemed to be the most convenient and simple method. After *in vivo* conversion of OA, it was observed that only small amounts of free fatty acids were found in the supernatant compared with the total substrate added (Figure 39). Since hydroxylated fatty acids are able to move across lipid bilayers without any protein assistance and should therefore be exported into the supernatant, it was presumed that they remained associated with the exterior of the cells[37]. However, a large fraction of the generated 10-HSA was successfully released into the supernatant by washing with alkaline buffer at pH 9.0, fortifying the assumption that 10-HSA could effectively leave the interior of the cells but remained bound to the surface when protonated. A similar effect was encountered by Ro et al. (2006) for the release of the sesquiterpene lactone artemisinin into the culture medium after production in engineered yeast cells[38]. In

future, it might be beneficial to further develop a HTS system based on the effect of supernatants from *in vivo* conversion of OA with *E. coli* strains overexpressing oleate hydratase mutant libraries on the viability of *B. subtilis*.

Apart from the *in vivo* approach, two different *in vitro* methods for detection of the secondary alcohol formed via hydroxylation of OA were examined, but neither of them was positively evaluated. First, spectrophotometric detection of the alkyl nitrite formed upon the reaction between the hydroxyl group and nitrous acid described by Leenson (1997) was tested[39]. While characteristic differences in the absorbance spectra obtained with pure OA and 10-HSA standard solutions were observed, it was not possible to detect the nitrosation reaction of 10-HSA in a complex cell extract or whole cell sample, likely caused by the huge background signal. Secondly, the secondary alcohol was oxidized with ceric ammonium nitrate resulting in a color shift of the solution from yellow to an intense red tint. Similar to the nitrosation reaction, the background signal of cell extracts was far above the level which would allow sensitive detection and quantitation of the product. Consequently, none of the tested *in vitro* methods was positively evaluated for detection of 10-HSA.

8 Conclusions and outlook

A reliable *in vitro* assay for determination of oleate hydratase activity was developed. Nine selected oleate hydratase genes were expressed in *E. coli* and successfully purified. In subsequently performed *in vitro* assays, active expression of each protein was proven. The most active enzyme, OhyA from *E. meningoseptica*, was subjected to a biochemical analysis, which showed that the enzyme was associated with a non-covalently linked FAD that could not be assigned a direct role in catalysis. 3D structure elucidation of OhyA supported these findings and additionally suggested a homodimeric association of the soluble protein binding one FAD molecule per OhyA protomer. Strategies for implementation of a HTS assay method for screening of oleate hydratase mutant libraries for improved variants were evaluated, but neither of them are ready immediate use. Therefore, rational protein engineering based on detailed structural information, although momentarily limited to OhyA, was the most promising tool for generation of oleate hydratases with enhanced characteristics.

Based on the current project status, the focus will now shift to other areas. Starting from the acquired knowledge on the 3D structure and biochemical properties of OhyA, site-directed mutagenesis of selected amino acids in and near the substrate binding cavity will be performed to identify residues involved in catalysis and to conclude on the reaction mechanism. In addition, the 3D structure will be a crucial element in the ambitious task of enzyme engineering for generation of OhyA mutant variants with desired features such as improved stability, catalytic activity and altered product profile. Finally, based on the availability of additional protein structures, rational enzyme design will be expanded to other hydratases of interest to target utilization of the potential of these interesting biocatalysts for the production of value-added compounds.

9 References

[1] J. Jin, U. Hanefeld, *Chem. Commun.* **2011**, *47*, 2502–10.

[2] A. J. Boersma, D. Coquière, D. Geerdink, F. Rosati, B. L. Feringa, G. Roelfes, *Nat. Chem.* **2010**, *2*, 991–5.

[3] L. L. Wallen, R. G. Benedict, R. W. Jackson, *Arch. Biochem. Biophys.* **1962**, *99*, 249–253.

[4] M. J. van der Werf, W. J. van den Tweel, J. Kamphuis, S. Hartmans, J. A. de Bont, *Trends Biotechnol.* **1994**, *12*, 95–103.

[5] Y. Cao, X. Zhang, *Appl. Microbiol. Biotechnol.* **2013**, *97*, 3323–31.

[6] L. E. Bevers, M. W. H. Pinkse, P. D. E. M. Verhaert, W. R. Hagen, *J. Bacteriol.* **2009**, *191*, 5010–2.

[7] Y.-C. Joo, K.-W. Jeong, S.-J. Yeom, Y.-S. Kim, Y. Kim, D.-K. Oh, *Biochimie* **2012**, *94*, 907–15.

[8] E. Rosberg-Cody, A. Liavonchanka, C. Göbel, R. P. Ross, O. O'Sullivan, G. F. Fitzgerald, I. Feussner, C. Stanton, *BMC Biochem.* **2011**, *12*, 9.

[9] A. Volkov, S. Khoshnevis, P. Neumann, C. Herrfurth, D. Wohlwend, R. Ficner, I. Feussner, *Acta Crystallogr. D. Biol. Crystallogr.* **2013**, *69*, 648–57.

[10] B.-N. Kim, Y.-C. Joo, Y.-S. Kim, K.-R. Kim, D.-K. Oh, *Appl. Microbiol. Biotechnol.* **2012**, *95*, 929–37.

[11] Y.-C. Joo, E.-S. Seo, Y.-S. Kim, K.-R. Kim, J.-B. Park, D.-K. Oh, *J. Biotechnol.* **2012**, *158*, 17–23.

[12] B.-N. Kim, S.-J. Yeom, D.-K. Oh, *Biotechnol. Lett.* **2011**, *33*, 993–7.

[13] A. Hiseni, I. W. C. E. Arends, L. G. Otten, *ChemCatChem* **2014**.

[14] A. Volkov, A. Liavonchanka, O. Kamneva, T. Fiedler, C. Goebel, B. Kreikemeyer, I. Feussner, *J. Biol. Chem.* **2010**, *285*, 10353–61.

[15] A. P. Desbois, V. J. Smith, *Appl. Microbiol. Biotechnol.* **2010**, *85*, 1629–42.

[16] H. Lu, P. J. Tonge, *Acc. Chem. Res.* **2008**, *41*, 11–20.

[17] B. Yang, H. Chen, Y. Song, Y. Q. Chen, H. Zhang, W. Chen, *Biotechnol. Lett.* **2013**, *35*, 75–81.

[18] E. O'Reilly, V. Köhler, S. L. Flitsch, N. J. Turner, *Chem. Commun.* **2011**, *47*, 2490–501.

[19] A. El-Heliebi, Improving esterases for activity towards alternative substrates, Diploma Thesis, Graz University of Technology, **2009**.

[20] H. Liu, J. H. Naismith, *Protein Expr. Purif.* **2009**, *63*, 102–11.

[21] G. Kleiger, D. Eisenberg, *J. Mol. Biol.* **2002**, *323*, 69–76.

[22] F. Lederer, H. Ruterjans, G. Fleischmann, S. K. Chapman, in *Flavoprotein Protoc.*, **1999**.

[23] V. Oberle, Untersuchungen zum Einfluss freier Fettsäuren auf die Eigenschaften biologischer und Modellmembranen, PhD Thesis, Martin-Luther-Universität Freiburg, **1999**.

[24] J.-W. Chu, T. Kimura, *J. Biol. Chem.* **1973**, *248*, 2089–2094.

[25] H. Y. Neujahr, A. Gaal, *Eur. J. Biochem.* **1973**, *400*, 386–400.

[26] S. Weber, C. W. M. Kay, H. Mögling, K. Möbius, K. Hitomi, T. Todo, *Proc. Natl. Acad. Sci. U. S. A.* **2002**, *99*, 1319–22.

[27] A. Liavonchanka, E. Hornung, I. Feussner, M. G. Rudolph, *Proc. Natl. Acad. Sci. U. S. A.* **2006**, *103*, 2576–81.

[28] A. Liavonchanka, M. G. Rudolph, K. Tittmann, M. Hamberg, I. Feussner, *J. Biol. Chem.* **2009**, *284*, 8005–12.

[29] J.-H. Zhang, *J. Biomol. Screen.* **1999**, *4*, 67–73.

[30] J. J. Kabara, D. M. Swieczkowski, A. J. Conley, J. P. Truant, *Antimicrob. Agents Chemother.* **1972**, *2*, 23–8.

[31] D. R. Drake, K. A. Brogden, D. V. Dawson, P. W. Wertz, *J. Lipid Res.* **2008**, *49*, 4–11.

[32] D. L. Greenway, K. G. Dyke, *J. Gen. Microbiol.* **1979**, *115*, 233–45.

[33] C. J. Zheng, J.-S. Yoo, T.-G. Lee, H.-Y. Cho, Y.-H. Kim, W.-G. Kim, *FEBS Lett.* **2005**, *579*, 5157–62.

[34] J. P. Fay, R. N. Farias, *J. Gen. Microbiol.* **1975**, *91*, 233–40.

[35] M. Marounek, E. Skrivanová, V. Rada, *Folia Microbiol.* **2003**, *48*, 731–5.

[36] C. W. Sheu, E. Freese, *J. Bacteriol.* **1973**, *115*, 869–75.

[37] E. E. Pohl, A. M. Voltchenko, A. Rupprecht, *Biochim. Biophys. Acta* **2008**, *1778*, 1292–7.

[38] D.-K. Ro, E. M. Paradise, M. Ouellet, K. J. Fisher, K. L. Newman, J. M. Ndungu, K. a Ho, R. a Eachus, T. S. Ham, J. Kirby, et al., *Nature* **2006**, *440*, 940–3.

[39] I. A. Leenson, *J. Chem. Educ.* **1997**, *74*, 424.

10 Appendix

10.1 Instruments and devices

Table 10: Instruments and devices.

Task	Instrument/Device	Manufacturer
Absorbance measurement	FLUOstar Omega	BMG Labtech, Germany
	BioPhotometer Plus	Eppendorf, Germany
	Specord 210/205 dual-beam spectrophotometer	Analytik Jena, Germany
	DU® 800 UV-Visible Spectrophotometer	Bio-Rad, USA
	Microplate, 96 well, PS, U-bottom, MICROLON®	Greiner bio-one AG, Germany
	Semi-Micro-Cuvettes, PS, 10 x 10 x 45 mm	Greiner bio-one AG, Germany
Agarose gel electrophoresis	PowerPac™ Basic + Sub-Cell GT	Bio-Rad, USA
CD-spectroscopy	Jasco J-810 spectropolarimeter	Jasco, USA
Cell harvest/Centrifugation	Microcentrifuge 5415R	Eppendorf, Germany
	Tabletop centrifuge 5810R	Eppendorf, Germany
	Avanti™ centrifuge, JA-10 and JA-25.50 rotors	Beckman Coulter™, USA
Desalting/buffer exchange	HiPrep 26/10 Desalting column	GE Healthcare Life Sciences, USA
	PD-10 Desalting Columns	GE Healthcare Life Sciences, USA
Determination of DNA/protein concentration	NanoDrop 2000 UV-Vis Spectrophotometer	Thermo Scientific, USA
Electrotransformation	MicroPulser™	Bio-Rad, USA
	Electroporation Cuvettes (2 mm gap)	Life Technologies, USA
Extraction after activity assay	Vibrax VXR basic	IKA, Germany
GC-MS	Hewlett Packard 5890 Series II with a mass selective detector HP 5 MS column (Capillary 30 m x 0.25 mm x 0.25 µM film)	Agilent Technologies, Austria
Gel filtration	HiLoad 16/600 Superdex 200 pg	GE Healthcare Life Sciences, USA
Incubator (37°C)	BINDER Kühlbrutschränke	Binder GmbH, Germany
ITC-measurements	VP-ITC MicroCalorimeter	MicroCal, USA
Magnetic stirrer	IKAMAG RCT	IKA, Germany
Mixing (small volumes)	Vortex – Genie 2	Scientific Industries Inc., USA

PCR reaction	GeneAmp® PCR System 2700	Applied Biosystems, USA
pH-value measurement	inoLab WTW 720 pH meter	WTW GmbH, Germany
Plate shaker	Heidolph Titramax 1000	Fisher Scientific, USA
Protein concentration	Ultrafiltration with Amicon® Ultra-15 Centrifugal filter devices, 15 mL, 30 kDa molecular weight cutoff	Merck Millipore, Ireland
Protein electrophoresis	NuPAGE® SDS-PAGE Gel System	Life Technologies, USA
	NuPage® Novex® 4-12% Bis-Tris Mini Gels 1.0 mm, 10 or 15 wells	Life Technologies, USA
Protein purification and deflavination	Äkta purifier 10	GE Healthcare Life Sciences, USA
	HisTrap FF Crude column, 5 mL	GE Healthcare Life Sciences, USA
	HiTrap TALON® Crude column, 5 mL	GE Healthcare Life Sciences, USA
Reaction tubes for activity assay	PYREX® culture tubes	SciLabware, UK
Shaker (small volumes)	Thermomixer comfort	Eppendorf, Germany
Shaker for cell cultivation/activity assay	Multitron Standard	Infors AG, Swizerland
Sonication	Sonifier 2501	Branson, USA
Sterile work	UNIFLOW KR130 biowizard	UNIQUIP, USA
Weighing	Lab scale: SI-202	Denver Instrument, USA
	Precision scale: Kern Scale ABS 220-4	Kern &Sohn GmbH, Germany

10.2 Reagents

Table 11: Reagents and supplier.

Reagent	Supplier
10-Hydroxystearic acid	DSM Pharma Chemicals, Netherlands
16-Hydroxypalmitic acid	Sigma-Aldrich, USA
Acetic acid	Roth GmbH, Germany
Agar Agar	Roth GmbH, Germany
Agarose LE	Biozyme, Germany
Ampicillin	Sigma-Aldrich, Germany
Aqua bidest.	Fresenius Kabi GmbH, Austria
Auto Induction Medium – Terrific Broth Base including Trace Elements	Formedium, UK
Bacto™ Agar	BD, USA
Bovine Serum Albumine	Roth GmbH, Germany
Biorad Protein Assay dye reagent (5x)	Bio-Rad, USA
Dimethylsulfoxide	Roth GmbH, Germany
Enzymes and adequate buffers, various	Thermo Scientific, USA

Ethanol	Roth GmbH, Germany
Ethidium bromide	Roth GmbH, Germany
Ethyl acetate	Roth GmbH, Germany
Ethylenediamine tetraacetic acid	Roth GmbH, Germany
Ethyl oleate	Roth GmbH, Germany
Flavin adenine dinucleotide disodium salt hydrate	Sigma-Aldrich, Germany
D-Glucose	Roth GmbH, Germany
Di-potassium hydrogen phosphate	Roth GmbH, Germany
DNA Loading Dye (6x)	Thermo Scientific, USA
Glycerol	Roth GmbH, Germany
Guanidine hydrochloride	Sigma-Aldrich, Germany
HEPES	Roth GmbH, Germany
Hydrochloric acid	Roth GmbH, Germany
Imidazole	Sigma-Aldrich, Germany
Isopropyl-β-D-thiogalactopyranosid	Peqlab Biotechnologie GmbH, Germany
Kanamycin	Sigma-Aldrich, Germany
LB (Lennox)	Roth GmbH, Germany
MassRuler DNA Ladder Mix, Ready-to-Use	Thermo Scientific, USA
N,O-Bis(trimethylsilyl)trifluoroacetamide	Sigma-Aldrich, Germany
NuPage® LDS Sample Buffer (4x)	Life Technologies, USA
NuPage® MOPS SDS Running Buffer (20x)	Life Technologies, USA
NuPage® Sample Reducing Agent (10x)	Life Technologies, USA
Oleic acid	Roth GmbH, Germany
PageRuler™ Prestained Protein Ladder	Thermo Scientific, USA
Pentadecanoic acid	Sigma-Aldrich, Germany
Peptone	Roth GmbH, Germany
Phenylmethylsulfonyl fluoride	Sigma-Aldrich, Germany
Potassium bromide	AppliChem GmbH, Germany
Potassium chloride	Roth GmbH, Germany
Potassium dihydrogen phosphate	Roth GmbH, Germany
Pyridine	Roth GmbH, Germany
Sodium hydroxide	Roth GmbH, Germany
Sodium Chloride	Roth GmbH, Germany
Tris	Roth GmbH, Germany
Triton X-100	Sigma-Aldrich, Germany
Tween® 20	Roth GmbH, Germany
Urea	Sigma-Aldrich
Yeast Extract	Bacto Laboratories Pty Ltd, Australia

10.3 Kits and enzymes

Table 12: Applied kits and enzymes.

Enzyme/Kit	Supplier
FastAP™ alkaline phosphatase	Thermo Scientific, USA
FastDigest™ restriction enzymes	Thermo Scientific, USA
Gene Jet™ Plasmid Miniprep Kit	Thermo Scientific, USA
Phusion® DNA Polymerase	Sigma-Aldrich, USA
Restriction enzymes	Thermo Scientific, USA
T4 DNA Ligase	Thermo Scientific, USA

10.4 Media and buffers

Table 13: Media and buffers.

Medium/Buffer	Composition
Ampicillin stock, 100 mg/mL	100 mg/mL dissolved in ddH_2O
Binding Buffer for protein purification	50 mM HEPES, pH 7.4, 300 mM NaCl, 10 mM Imidazole
50 mM Di-potassium-hydrogen phosphate	8.71 g dissolved in 1 L ddH_2O
Desalting Buffer for protein purification	50 mM HEPES, pH 7.4, 50 mM NaCl
Dialysis Buffer 1	50 mM HEPES, pH 7.4, 4 M urea, 2 M KBr
Dialysis Buffer 2	50 mM HEPES, pH 7.4, 2 M urea, 2 M KBr
Elution Buffer for protein purification	50 mM HEPES, pH 7.4, 50 mM NaCl, 250 mM Imidazole
IPTG stock (100 mM)	1.19 g IPTG dissolved in 50 mL ddH_2O
Kanamycin stock, 40 mg/mL	40 mg dissolved in 1 mL H_2O
LB-agar	LB-Medium + 20 g/L Agar Agar
LB-medium	10 g/L tryptone, 5 g/L yeast extract, 5 g/L NaCl
MOPS SDS Running Buffer (1x)	100 mL NuPage® MOPS SDS Running Buffer (10x) dissolved in 900 mL ddH_2O
50 mM Potassium-dihydrogen phosphate	6.8 g dissolved in 1 L ddH_2O
SOC-Medium	20 g/L tryptone, 0.58 g/L NaCl, 5 g/L yeast extract, 2 g/L $MgCl_2$, 0.16 g/L KCl, 2.46 g/L $MgSO_4$, 3.46 g/L dextrose
TAE buffer, 50x	242 g L^{-1} Tris, 14.6 g L^{-1} EDTA, 57.1 mL L^{-1} acetic acid, adjusted to final volume with ddH_2O
TB-medium	12 g/L peptone, 24 g/L yeast extract, 4 mL/L glycerol to 1 L with ddH_2O, After separate autovlaving, sterile addition of 2.31 g KH_2PO_4 and 12.54 g K_2HPO_4 in 100 mL ddH_2O.
50 mM Tris-HCl, pH 9.0	6.06 g Tris diluted in 1 L ddH_2O, pH adjusted with 1 M HCl

10.5 Strains, plasmids and genes

Table 14: *E. coli* strains.

Strain	Genotype	Source
Top 10F'	F'{*lac*I^q Tn*10* (Tet^R)} *mcr*A Δ(*mrr-hsd*RMS-*mcr*BC) Φ80 *lacZ*ΔM 15 Δ*lac*X74 *rec*A1 *ara*D139 Δ(*ara-leu*)7697 *gal*U galK *rps*L *end*A1 *nup*G	Thermo Scientific, USA
BL21 Star™ (DE3)	F$^-$ *omp*T *hsd*S_B($r_B^-m_B^-$) *gal dcm rne*131 (DE3)	Thermo Scientific, USA

Table 15: Expression plasmids.

Plasmid	Features	Source
pMS470-HISTEV	N-terminal His_6-tagging expression vector with tac promoter, ampicillin resistance gene and TEV protease cleavage site for removal of His_6-tag	Constructed by Tamara Wriessnegger, ACIB
pEHISTEV	N-terminal His_6-tagging expression vector with T7 promoter kanamycin resistance gene and TEV protease cleavage site for removal of His_6-tag	[20]

Table 16: Cloned hydratase genes.

Gene	Organism	Protein size [kDa]	Accession number
OhyA	*Elizabethkingia meningoseptica*	73.5	ACT54545
mch	*Macrococcus caseolyticus*	67.3	YP_002559479
bbh	*Bifidobacterium breve*	70.5	ADY18551
ckh	*Corynebacterium kroppenstedtii*	67	YP_002907233
oah	*Ochrobactrum anthropi*	74.2	YP_001373221
moh	*Myroides odoratus*	73.5	ZP_09674164
sah	*Staphylococcus aureus*	67.8	ZP_06925789
cgh	*Chryseobacterium gleum*	73.3	ZP_07086592
cah	*Cellulophaga algicola*	73.2	YP_004165724

10.6 Primers

Table 17: List of primers used for amplification of target genes. Gray: *Nco*I restriction site. Blue: *Hin*dIII restriction site, Red: *Eco*RI restriction site.

Primer	Sequence
Fw_Eme_*Nco*I	5'- CATG **CCATGG** GC AACCCAATCACCAGCAAATTC -3'
Rv_Eme_*Hin*dIII	5'- CCC **AAGCTT** ATTAGCCACGGATACC -3'
Fw_Mch_*Nco*I	5'- CATG **CCATGG** GC TACTACAGCAACGGCAACTACG -3'
Rv_Mch_*Hin*dIII	5'- CCC **AAGCTT** ATTAGATCAGATTGGCCTC -3'
Fw_Bbh_*Nco*I	5'- CATG **CCATGG** GC TACTATTCATCAGGTAACTACGAAG -3'
Rv_Bbh_*Hin*dIII	5'- CCC **AAGCTT** ATTAGATGACATGATATTC -3'
Fw_Ckh_*Nco*I	5'- CATG **CCATGG** GT TCCATCTACCAATCTACCTATC -3'
Rv_Ckh_*Hin*dIII	5'- CCC **AAGCTT** ATTAATGGCTAGAGC -3'
Fw_Oah_*Nco*I	5'- CATG **CCATGG** GC AACGACAAAACCACGTCC -3'
Rv_Oah_*Hin*dIII	5'- CCC **AAGCTT** ATTAGTCGCGTTTG -3'
Fw_Moh_*Nco*I	5'- CATG **CCATGG** GC AAGGTAGACACGCAGAAGTTC -3'
Rv_Moh_*Hin*dIII	5'- CCC **AAGCTT** ATTAACCAATCAATTTC -3'
Fw_Sah_*Nco*I	5'- CATG **CCATGG** ACATGTACTACAGCTACG -3'
Rv_Sah_*Hin*dIII	5'- CCC **AAGCTT** ATTACAACAGTTTATGTTC -3'
Fw_Cgh_*Eco*RI	5'- CG **GAATTC** ATGAGCACGATTAACAGC -3'
Rv_Cgh_*Hin*dIII	5'- CCC **AAGCTT** ATTAGTCTTTCACGC -3'
Fw_Cah_*Nco*I	5'- CATG **CCATGG** GCAAGATCACTGAG -3'
Rv_Cah_*Hin*dIII	5'- CCC **AAGCTT** ATTAATGCGTCAGTTC -3'